GLI2 ACCELERATES CARDIAC PROGENITOR GENE EXPRESSION DURING MOUSE EMBRYONIC STEM CELL DIFFERENTIATION

By

Joel Vincent Fair

Thesis submitted to the

Faculty of Graduate and Postdoctoral Studies

in partial fulfillment of the requirements for the

MSc degree in Biochemistry

Department of Biochemistry, Microbiology, & Immunology

Faculty of Medicine

University of Ottawa

Abstract

The Hedgehog (HH) signalling pathway and its primary transducer, GLI2, regulate cardiomyogenesis *in vivo* and in differentiating P19 embryonal carcinoma (EC) cells. To further assess the role of HH signalling during mouse embryonic stem (mES) cell differentiation, we studied the effects of GLI2 overexpression during mES cell differentiation. GLI2 overexpression resulted in temporal enhancement of cardiac progenitor genes, *Mef2c* and *Nkx2-5*, along with enhancement of *Tbx5*, *Myhc6,* and *Myhc7* in day 6 differentiating mES cells. Mass spectrometric analysis of proteins that immunoprecipitate with GLI2 determined that GLI2 forms a complex with BRG1 during mES cell differentiation. Furthermore, modulation of HH signalling during P19 EC cell differentiation followed by chromatin immunoprecipitation with an anti-BRG1 antibody determined that HH signalling regulates BRG1 enrichment on *Mef2c*. Therefore, HH signalling accelerates cardiac progenitor gene expression during mES cell differentiation potentially by recruiting a chromatin remodelling factor to at least one cardiac progenitor gene.

Acknowledgements

First and foremost, I would like to thank my supervisor, Dr. Ilona Skerjanc, for her guidance and support. I would also like to thank the current and past members of Dr. Skerjanc's lab for their insight, fruitful discussions, and technical support. This includes, but is certainly not limited to, Drs. Anastassia Voronova, Ashraf Al Madhoun, and Tammy Ryan, as well as Neven Bosiljcic, Michael Shelton, Avitek Kocharyan, Abeer Zakariyah, Jennifer MacDonald, Rashida Rajgara, Erin Coyne, Donna Clary, Jun Liu, and Jacob Wong. I would especially like to thank my mentor, Dr. Anastassia Voronova who has provided an abundance of advice and support, for which I am truly grateful. I would also like to thank Dr. Alexandre Blais and Imane Chakroun for their assistance with chromatin immunoprecipitation techniques and analyses.

I am very thankful to Drs. Valerie Wallace and David Lohnes for their advice and guidance as members of my thesis advisory committee. I also owe a great amount of thanks to Drs. Alexandre Blais and Anastassia Voronova for going out of their way to help me review my thesis.

Finally, I would like to thank the University of Ottawa, the Government of Ontario, and the Canadian Institutes of Health Research for their financial support throughout my Master's degree.

Dedication

To my mom and dad.

Thank you for your endless support.

Table of Contents

List of Abbreviations

β-TrCP: β-transducin repeat-containing protein

ASCL: achaete-scute homolog 1

ASD: atrial septal defects

BAF: brahma-associated factor

bHLH: basic helix-loop-helix

BMP: bone morphogenic protein

BRG1: brahma-related gene 1/SMARCA4)

BRG1-ChIP: chromatin immunoprecipitation with an anti-BRG1 antibody

BRM: brahma/SMARCA2

ChIP: chromatin Immunoprecipitation

Chr: chromosome

Ci: cubitus interruptus

Cre: cre recombinase

Ctrl: control

DHH: desert hedgehog

DISP: dispatch

DMSO: dimethylsulphoxide

E: embryonic day

EB: embryoid body

EC: embryonal carcinoma

EnR: engrailed repression domain

ES: embryonic stem

FBS: fetal bovine serum

Fgf8: fibroblast growth factor 8

FHF: first heart field

FLAG-IP: immunprecipitation with anti-FLAG beads

FLAG: flag-tag peptide

FOXH1: forkhead box protein H1

GATA-4: GATA-binding protein 4

GLI: glioma-associated

GLI1: glioma-associated protein 1

GLI2: glioma-associated protein 2

GLI2/3: GLI2 and GLI3

GLI2A: full-length, transcriptional activator form of GLI2

GLI2R: proteolytically processed, transcriptional repressor form of GLI2

GLI3: glioma-associated protein 3

GLI3A: full-length, transcriptional activator form of GLI3

GLI3R: proteolytically processed, transcriptional repressor form of GLI3

GO: gene ontology

hES: human embryonic stem

HH: hedgehog

HH-C: carboxy-terminal peptide of hedgehog protein in hedgehog producing cell

HH-N: amino-terminal peptide of hedgehog protein in hedgehog producing cell

IF: immunofluoresence

IHH: Indian hedgehog

IP: immunoprecipitation

ISL-1: Insulin gene enhancer protein

KAAD-cyclopamine: 3-Keto-N-(aminoethyl-aminocaproyl-dihydrocinnamoyl)-cyclopamine

LIF: leukemia inhibitory factor

MEF: mouse embryonic fibroblast

MEF2C: myocyte-specific enhancer factor 2C

MEM: minimum essential medium

mES: mouse embryonic stem

mm10: *Mus musculus* genome assembly (version 10)

MyHC: myosin heavy chain

MyHC6: myosin heavy chain 6 (α-MyHC)

MyHC7: myosin heavy chain 7 (β-MyHC)

Mylc: myosin light chain

NKX2-5: NK2 homeobox 5 protein

Pax3: paired box 3

PBAF complex: polybromo-containing BAF complex

PBS: phosphate buffered saline

PDD: processing determinant domain

PTA: persistent truncus arteriosus

PTCH1: patched homolog 1

qPCR: quantitative polymerase chain reaction

RA: retinoic acid

SAG: smoothened agonist

SCUBE2: signal peptide, CUB, and EGF-like domain-containing protein 2

SEM: standard error of the mean

SHF: second heart field

SHF I: ISL-1-dependent SHF enhancer

SHF II: Nkx2-5/FoxH1-dependent SHF enhancer

SHH: sonic hedgehog

SKI: skinny hedgehog

SMO: smoothened

sPBS: Stockholm's phosphate buffered saline

SSEA-1: stage-specific embryonic antigen-1

SUFU: suppressor of fu

SWI/SNF: switch/sucrose non-fermentable

TBX5: T-box protein 5

TC: tissue culture grade

WT: wild type

YY1: Yin Yang 1

List of Figures

List of Tables

List of Appendices

1 Introduction

1.1 Heart disease

The heart is the first functional organ during mammalian development and is essential for survival *in utero* and after birth. Undoubtedly, congenital heart disease or injury to the heart during adulthood poses serious health risks. Heart disease is one of the three leading causes of death in Canada (1) and, in many cases, leads to myocardial infarction (2). If severe, myocardial infarction can lead to a loss of approximately one billion cardiomyocytes, subsequent fibrosis, major contractile dysfunction, and ultimately the risk of heart failure (3, 4).

Heart transplantation has been the primary means for treating severe heart damage (5) and, fortunately, the one-year post-transplantation survival rate has increased from ~30% in the 1970's to ~80% in the 2000's (6, 7). However, finding a compatible deceased heart donor with matching blood type, human leukocyte antigen type, and body size can be difficult. Many patients die before they can find an available matching deceased donor. Since 2000, the number of recorded heart transplants performed annually has held close to 4,000 worldwide (6). In the United States alone, there are ~2,500 adult patients on a waiting list for a heart transplant on any given day (8). Therefore, alternatives to heart transplantation, including cell-based alternatives are being investigated (7).

Recent studies have shown that a fraction of cells (between 0.45% and 22%, depending on the study) regenerate in an adult human heart, annually (9, 10). Nevertheless, these levels are insufficient for replenishing the number of cells needed to restore function in an infarcted heart in a timely manner (4). Intriguingly, murine hearts have substantial regenerative capacity prior to birth and grow primarily through hyperplasia (11, 12). This

regenerative function diminishes until it is effectively lost 7 days after birth when myocardial injury results in more fibrosis and contractile dysfunction (12, 13). If injury occurs before this critical time point, endogenous cues can rescue cardiac function within 3 weeks through global proliferation of cardiomyocytes in the heart (4). Shortly after birth, approximately 90% of the cardiomyocytes in the mouse heart become binucleated and thereafter mediate heart growth primarily through hypertrophy (12, 14). It is believed that neonatal hearts have more regenerative potential because they have mononucleated cells and less complex sarcomeres. This phenotype is similar to zebrafish cardiomyocytes, which can undergo cytokinesis more readily when required (15, 16). In both zebrafish and neonatal mice, the dominant method for regenerating injured myocardium is the proliferation of pre-existing cardiomyocytes (13, 15). Adult mouse cardiomyocytes also seem to repopulate primarily through pre-existing cardiomyocytes (16, 17). Therefore, given an insufficient supply of transplantable hearts worldwide and the limited regenerative capacity of cardiomyocytes in the mammalian adult heart, new therapies that can regenerate damaged myocardium are in high demand.

1.2 Embryonic Stem Cells

Cell-based therapies could provide an alternative to patients who have had a severe heart attack, who have lost a critical number cardiomyocytes, and who are unlikely to find a compatible heart donor. Embryonic stem (ES) cells are a cell type of interest in the field of regenerative medicine because, by providing the necessary differentiation cues *in vitro*, ES cells can theoretically be propagated and differentiated into large numbers of any specific

cell type for intended transplantation and functional integration into a damaged tissue (3, 18, 19).

By recapitulating the endogenous signals during cardiomyogenesis, many directed differentiation protocols have been able to generate large numbers of ES cell-derived cardiomyocytes *in vitro* (20, 21). Although, transplantation of human ES (hES) cell-derived cardiomyocytes into infarcted mouse hearts has not generated long-term functional improvements (16), mice have smaller and faster beating hearts, so it is possible that the hES cell-derived cardiomyocytes in these studies were unable to contribute efficiently to the mouse heart environment (16, 22). Notably, transplantation into infarcted guinea-pig hearts has proven to be more efficient (23) and more recently, hES cell-derived cardiomyocytes successfully remuscularized portions of an infarcted monkey heart (24). This regeneration in non-human primate hearts was not met without complications, as the hearts developed arrhythmias, but the successful transplantation still suggests that efficient transplantation of hES cell-derived cardiomyocytes into diseased or damaged human hearts remains promising (24). To ensure a more fluid incorporation into the host myocardium, the population of hES cell-derived cardiomyocytes could be better refined *in vitro*. By further elucidating the molecular mechanisms that influence cardiomyocyte development, it may be possible to identify additional parameters to screen for the most efficient population of hES cell-derived cardiomyocytes or hES cell-derived cardiac progenitors for transplantation.

1.3 Cardiogenesis

Cardiogenesis in mice requires a series of migratory, fusion, signalling and proliferative events to progress from a pool of cardiac precursors into the heart fields that

eventually develop into a four-chambered, functional heart (4, 25). Mouse cardiogenesis initiates at approximately embryonic day 7.5 (E7.5) and requires ~3 days to establish the basic structure of the chambers, then ~5 days to coordinate heart remodelling through valve development, chamber septation, and outflow tract septation (4). Although these stages occur over a ~3 week period in humans, the major events of mouse heart morphogenesis resemble those in human heart morphogenesis, making the mouse model a useful tool for studying cardiogenesis (22).

In the mouse model, the earliest heart precursors are found flanking the primitive streak within the mesoderm layer, shortly after gastrulation initiates, at approximately E6.0 (26). These cells express the mesoderm marker, *Brachury*, and another T-box transcription factor, *Eomesodermin* (27). These bilateral populations of cells migrate cranially from either side of the primitive streak towards the anterior of the embryo, near the extra-embryonic edge, and below the developing head fold (26, 28). At this stage the cells begin to express the early precardiac mesoderm gene, *Mesp1* (29, 30). Grafting experiments have shown that these early mesodermal cells are still plastic and only later become committed to the cardiac lineage through temporal patterning and dynamic cell migration within the destined niche (25).

At E7.5, prior to somite formation, the mesoderm layer splits at the lateral edges of the embryo to form a series of cavities that eventually join to form the pericardial coelom (31). This separation leads to splanchnic and somatic mesoderm layers on the ventral and dorsal edge of each coelom, respectively (26). The cardiac precursors remain in the splanchnic mesoderm layer (26) where they populate two morphoregulatory fields that establish the cardiac crescent (32). The first heart field (FHF) lies ventral, eventually giving

rise to the left ventricle and contributing partially to the atria. The second heart field (SHF) lies dorsal to the first heart field during the cardiac crescent stage, eventually giving rise to the right ventricle, the outflow tract, the sinus venosus, and the atria (4, 22).

In the cardiac crescent a complex transcriptional network regulates cardiac progenitor differentiation in a spatiotemporal manner through a crosstalk of inductive signals - including bone morphogenic protein (BMP), notch, Wnt/β-catenin, and hedgehog (HH) - from the surrounding tissues (4, 28, 33). The NK2 homeobox 5 protein (NKX2-5), myocyte-specific enhancer factor 2C (MEF2C), T-box protein 5 (TBX5), and GATA-binding protein 4 (GATA-4) are important transcription factors within this network, as their individual expression is essential for proper heart morphogenesis (28). *Gata-4*$^{-/-}$ mice, *Nkx2-5*$^{-/-}$ mice, *Mef2c*$^{-/-}$ mice, and mice heterozygous for both *Gata-4* and *Tbx5* all have severe heart deformities and are embryonic lethal (34-38).

Of these factors, GATA-4 is one of the first to be expressed in the mouse embryo (39) and proceeds to activate *Nkx2-5* expression (28, 40-42). These transcription factors are both common to the FHF and SHF (4). GATA-4 is also known to interact with TBX5 (43) in the FHF and, in conjunction with insulin gene enhancer protein (ISL-1) and forkhead box protein H1 (FOXH1), regulates the expression of *Mef2c* in the SHF (4, 28, 43-45). Furthermore, GATA-4 interacts with NKX2-5 and MEF2C proteins to synergistically activate downstream cardiac muscle genes (46-49).

Through additional migration, the bilateral populations of cardiac progenitor cells in the cardiac crescent move ventrally and medially, causing a fusion of endothelial cells at the midline enveloped by a layer of myocardium (4, 25). This fusion gradually progresses caudally and leads to a developing linear heart tube that is initially tethered to the embryo

along the dorsal edge of the tube through the dorsal mesocardium (4, 25). At this time, the cardiomyocytes in the myocardium begin to express myosin heavy chain (*Myhc*) and myosin light chain (*Mylc*), which encode proteins that are involved in cardiomyocyte contraction (50, 51). Both alpha and beta isoforms of *Myhc* (*Myhc6*/α-*Myhc* and *Myhc7*/β-*Myhc*, respectively) are expressed during development, however *Myhc7* is more abundant during embryogenesis and *Myhc6* becomes the predominant form after birth (52). By E8.0, the myocardium of the linear heart tube begins to beat and blood flows through its caudal inflow portion (venous pole) and out the cranial outflow tract (atrial pole) (25). The initial role of this contraction is unclear, as it precedes the need for a movement of nutrients and waste by blood circulation, but it is believed to have a role in promoting cardiomyogenesis and angiogenesis (53, 54).

The dorsal mesoderm, which is originally tethered to the linear heart tube, eventually degrades along the dorsal edge of the heart tube between the two heart poles (55). With the heart only attached at its poles, proliferation of the cells in the beating heart tube leads to a non-symmetrical bulging and sweeping of the heart to the right by E8.5 (4, 55). This stage, known as cardiac looping, moves the outflow segment of the heart ventrally and caudally, which establishes the general position of the right ventricle and the outflow tract. The inflow segment of the heart moves dorsally and cranially, causing the common atrium to rise to a position above the developing ventricles and later protrude around the outflow tract (25). The bulging junction that links these two moving segments contorts to the left of the right ventricle and establishes the position of the developing left ventricle. By E10.5, the relative positions of the four chambers are established (4).

Most of the processes after heart looping involve tissue remodelling (25). For instance, trabecular cardiomyocytes establish the inner muscular layer of the ventricles by forming organized projections in the heart lumen through trabeculation (4, 25). These projections, known as trabeculae, increase the surface area in the ventricles and provide much of the heart's contractile force (25). In addition, the chambers need to be properly partitioned to ensure unidirectional blood flow (56). The junctions between the chambers are initially positioned through the looping and proliferation of the heart tube, however efficient division of the chambers still requires a series of tightly regulated septation- and valve-developing events, including atrioventricular, outflow tract, and ventricular septation (56).

Outflow tract septation is required to divide the common outflow of blood from the ventricles into two unique arteries, the pulmonary trunk and the aorta, which eventually transport deoxygenated blood from the right ventricle to the lungs and oxygenated blood from the left ventricle to the circulatory system, respectively (56). Prior to septation, neural crest cells delaminate from the hindbrain, migrate through the pharyngeal arches, and then through the SHF to reach the distal portion of the outflow tract (57, 58). From there these cells populate mesenchymal truncal cushions that spiral down the inside of the tract on opposite edges. Eventually, the cushions from either edge protrude to the point that they fuse to form a spiral septation (56). A similar septation occurs at the proximal edge of the outflow tract with endocardium-derived mesenchyme conal cushions and connects the distal septum arteries to their respective ventricles through the pulmonary and aortic semilunar valves (59)

Heart malformations leading up to, and during, this remodelling stage account for ~30% of prenatal deaths (60). Similar congenital heart defects may have less detrimental affects during fetal development but approximately 0.4% to 5% of live births show signs of

congenital heart disease that can cause complications later in life (61). For instance, TBX5 induces *Myhc6* transcription through DNA binding (62, 63) and, like in *Tbx5*$^{+/-}$ mice (46, 64), mutations in *Myhc6* cause septation defects (63). Mutations in *Tbx5* have been shown to be the primary source of Holt-Oram syndrome in humans (65).

With many spatiotemporal events occurring throughout the elaborate development of the heart, subtle deformities can lead to major dysfunctions. Therefore, a thorough understanding of the physiological and molecular mechanisms throughout development is necessary for also identifying and treating congenital heart diseases.

1.4 *In vitro* cardiomyogenesis

The cardiac gene expression profile observed during cardiomyogenesis in differentiating mES cells is similar to that seen during cardiomyogenesis in the embryo (66). Therefore, mES cells are a useful model system for studying the gene modifications during cardiomyogenesis *in vitro*. Following aggregation of mES cells in hanging drops (67, 68), day 3 and 4 differentiating mES cells express the mesoderm marker, *Brachyury*, and the precardiac mesoderm marker, *Mesp1,* respectively (66) (Figure 1). The cardiac progenitor genes *Nkx2-5, Gata-4, Tbx5,* and *Mef2c* are expressed by day 6 of mES cell differentiation (66, 69, 70). Upon terminal differentiation, cardiomyocytes express MyHC6 and MyHC7 (71).

In addition to mES cells, P19 embryonal carcinoma (EC) cells have been used to study cardiomyogenesis *in vitro* because they express signalling pathways during differentiation that are common to those expressed during embryonic heart development (72), they are relatively easy to maintain, and their differentiation can be modulated with

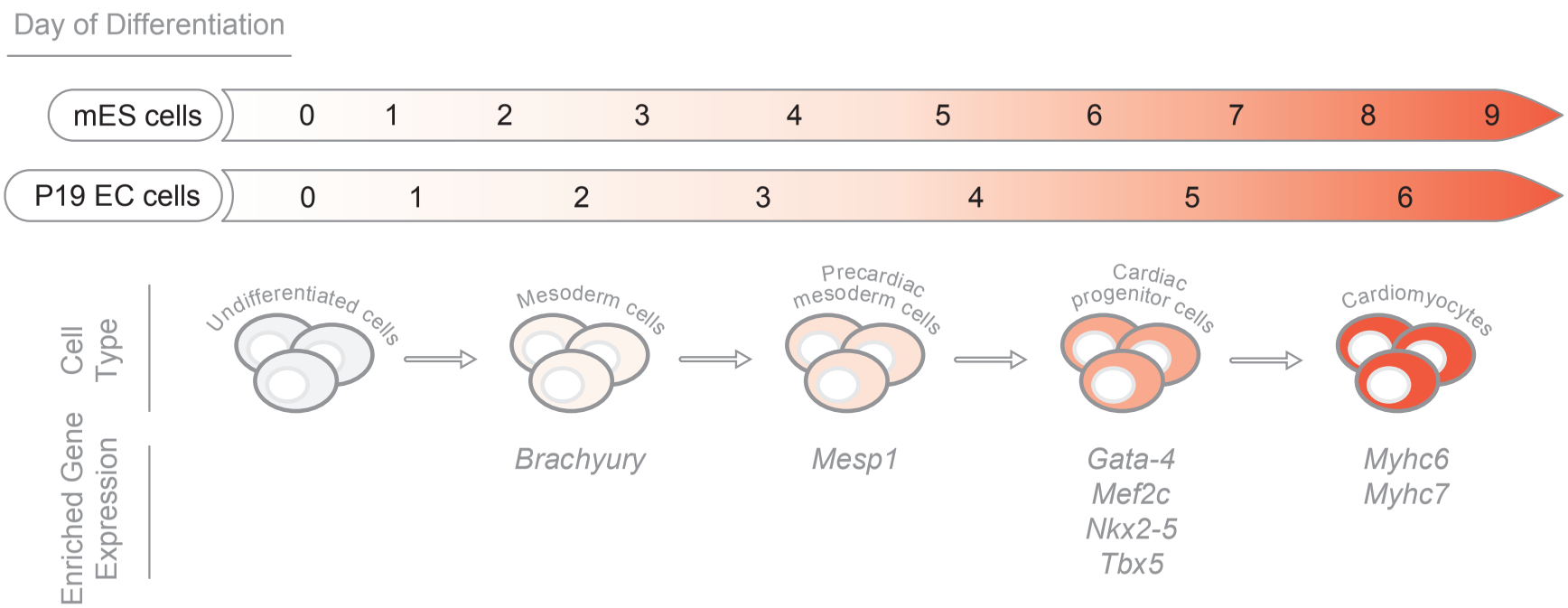
Day of Differentiation
mES cells
0 1 2 3 4 5 6 7 8 9
P19 EC cells
0 1 2 3 4 5 6
Cell Type
Enriched Gene Expression
Undifferentiated cells
Mesoderm cells
Precardiac mesoderm cells
Cardiac progenitor cells
Cardiomyocytes
Brachyury
Mesp1
Gata-4
Mef2c
Nkx2-5
Tbx5
Myhc6
Myhc7

Figure 1. *In vitro* cardiomyogenesis during mES cell and P19 EC cell differentiation. During differentiation, mES and P19 EC cell cultures give rise to cell types from the cardiac lineage. The genes enriched in these cell types are listed relative to the day when they are expressed during differentiation (66, 69-71, 73).

dimethylsulphoxide (DMSO) +/- retinoic acid (RA) to enrich for cells in the mesodermal lineage (74). P19 EC cells were first derived from teratomas in mouse testes, which were induced by grafting the testes to 7.5-day, post-copulating female mouse egg cylinders (75). The P19 EC cells were one cell type cultured directly from the tumour that had a normal 40:XY karyotype and gave rise to early mesodermal and endodermal cell types (72).

Upon DMSO treatment and aggregation, pluripotent P19 EC cells become more restricted to the mesoderm and endoderm lineages (76), express mesoderm marker *Brachyury* (77) and can differentiate into cardiomyocytes (78). P19CL6 EC cells, a derivative of P19 EC cells that have been cultured for approximately 6 months under mesoderm enhancing conditions, differentiate in a similar manner but are believed to be of a closer developmental stage to cardiomyocytes because they do not express the stage-specific embryonic antigen-1 (SSEA-1) (79-81). In addition to mesoderm-directed differentiation, P19 EC cell differentiation can be shifted towards the neuroectoderm linage with modulated RA treatment (74).

P19 EC cells can also be genetically mutated with relative ease and exemplify phenotypes displayed by similar *in vivo* genetic mutations. For instance, dominant-negative fusion protein assays with an engrailed repression domain (EnR) fused to NKX2-5 (NKX2-5/EnR) or fused to MEF2C with an *Nkx2-5* enhancer driving its expression (*Nkx2-5*-MEF2C/EnR) result in disrupted cardiomyogenesis, both *in vivo* (82, 83) and in P19 EC cells (73, 82, 84).

The HH signalling pathway has become a major developmental pathway of interest after genetic mutation analyses in developing embryos revealed that many components of the pathway are essential for proper heart tube looping and outflow tract development (85-

87). Thus, many studies have since modulated HH signalling during P19 and P19CL6 EC cell differentiation to further elucidate the molecular mechanisms behind HH-mediated cardiomyogenesis (73, 81, 88-90).

1.5 Hedgehog signalling

HH signalling is an integral component of many developmental processes including craniofacial development, retinal pigment epithelium development (91), limb digit patterning, ventral neural tube patterning (92), pancreas development (93), gut development (94, 95), erythroid differentiation (96), cardiomyogenesis (87, 89, 90), skeletal myogenesis (97-99), and hair follicle development (100). It is able to modulate these processes through a series of different functions, including pattern formation, cell proliferation, homeostasis, and tissue repair (101, 102).

The *hh* gene was discovered in *Drosophila melanogaster* and was named after the densely packed, disorganized, hair-like bristles on $hh^{-/-}$ embryos, which resembled hedgehog spines (103). A dozen years after its discovery, HH was identified as a secreted protein that patterns gene expression in adjacent cells of developing *D. melanogaster* (104-106). Further study in mammals identified three evolutionarily conserved mammalian homologues of the *D. melanogaster* protein: Indian hedgehog (IHH), shown to regulate bone and cartilage development (107, 108); desert hedgehog (DHH), shown to be essential for nerve sheath formation and germ cell development (109, 110), and sonic hedgehog (SHH), shown to regulate polarity in the notochord, floor plate, and limb buds (111-114). Once secreted, the HH ligands can travel long distances to activate HH signalling in HH-responsive cells (101).

In preparation for secretion of HH from a HH-producing cell, cholesterol is recruited to the carboxy-terminal domain of a HH protein which initiates an autoproteolytic cleavage of the carboxy-terminal peptide (HH-C) and leaves the cholesterol covalently bound to the carboxy-terminal end of the amino-terminal peptide (HH-N) (115). Further processing by skinny hedgehog (SKI) adds a palmitic acid group to the Cys residue closest to the amino-terminal end of HH-N before HH-N is presented on the surface of the HH-producing cell (101, 116). From there the protein is released via the transmembrane protein, dispatch (DISP), and signal peptide, CUB and EGF-like domain-containing protein 2 (SCUBE2) (117, 118). Alternatively, the HH-N lipoprotein may be packaged and released from the cell as a soluble multimer, a HH-N-associated lipoprotein particle, or on an exovesicle that may sequentially release the HH-N further from the cell (101). These different secretion methods are believed to mediate the varying ranges of HH signalling gradients observed in the adjacent cells of a given developing tissue (119).

In *D. melanogaster*, the zinc-finger protein, cubitus interruptus (Ci) mediates the transcriptional effects of the HH signalling pathway in the HH-responsive cells (119). This single transcriptional mediator has evolved into three separate zinc-finger, glioma-associated (GLI) proteins - GLI1, GLI2, and GLI3 - in vertebrates (120). All three GLI transcription factors have a common zinc-finger binding domain which binds to a common consensus sequence, 5'-GACCACCCA-3' (121). Once bound, these factors can mediate different transcriptional responses depending on their activator or repressor domains (119).

GLI1 has only a minor role in amplifying the transcriptional response of the HH signal through a C-terminal activator domain (122). Notably, during early embryonic development, GLI2 and GLI3 expression are essential for activating the *Gli1* promoter (119,

123). As such, GLI1 has been determined to be non-essential for ectopic HH signalling in mammalian cells (124).

The function and mechanism of GLI2 and GLI3 more closely resemble that of Ci, which each have a C-terminal activator domain, an N-terminal repressor domain, and a processing determinant domain (PDD) (119). When the proteins are full-length, they contain both an activator and a repressor domain and act primarily as transcriptional activators (GLI2A and GLI3A). After proteolytic processing, they contain only the repressor domain and act primarily as transcriptional repressors (GLI2R and GLI3R) (125, 126). The PDD in the GLI proteins is believed to support their partial cleavage in the absence of HH signalling (127) like it does for Ci (128). GLI3 has a relatively potent PDD and, thus, is often partially cleaved, while GLI2 has a less potent PDD and is more prone to complete degradation (127). GLI1, for which no truncated GLI1R has been observed, does not have a PDD (119).

Although GLI2 and GLI3 are structurally similar and can act as either activators or repressors, they predominantly have different roles. This may be in part due to the potency of their respective PDD domains (119, 127). GLI2 is primarily involved in transducing the activator response of HH signalling and GLI3 generally mediates the repressor response (119, 129, 130). Altogether, the GLI family of proteins modulates the culminated effect of the HH signalling pathway (119).

Given the pleiotropic functions of HH signalling, research efforts in many fields have sought to elucidate the mechanisms behind the signalling pathway in hopes of identifying key factors driving HH-related development and diseases (101, 119). In vertebrates, the active or repressive fate of the GLI2 and GLI3 (GLI2/3) proteins is determined within the primary cilia of cells (Figure 2). Independent of HH signalling, suppressor of fu (SUFU) can

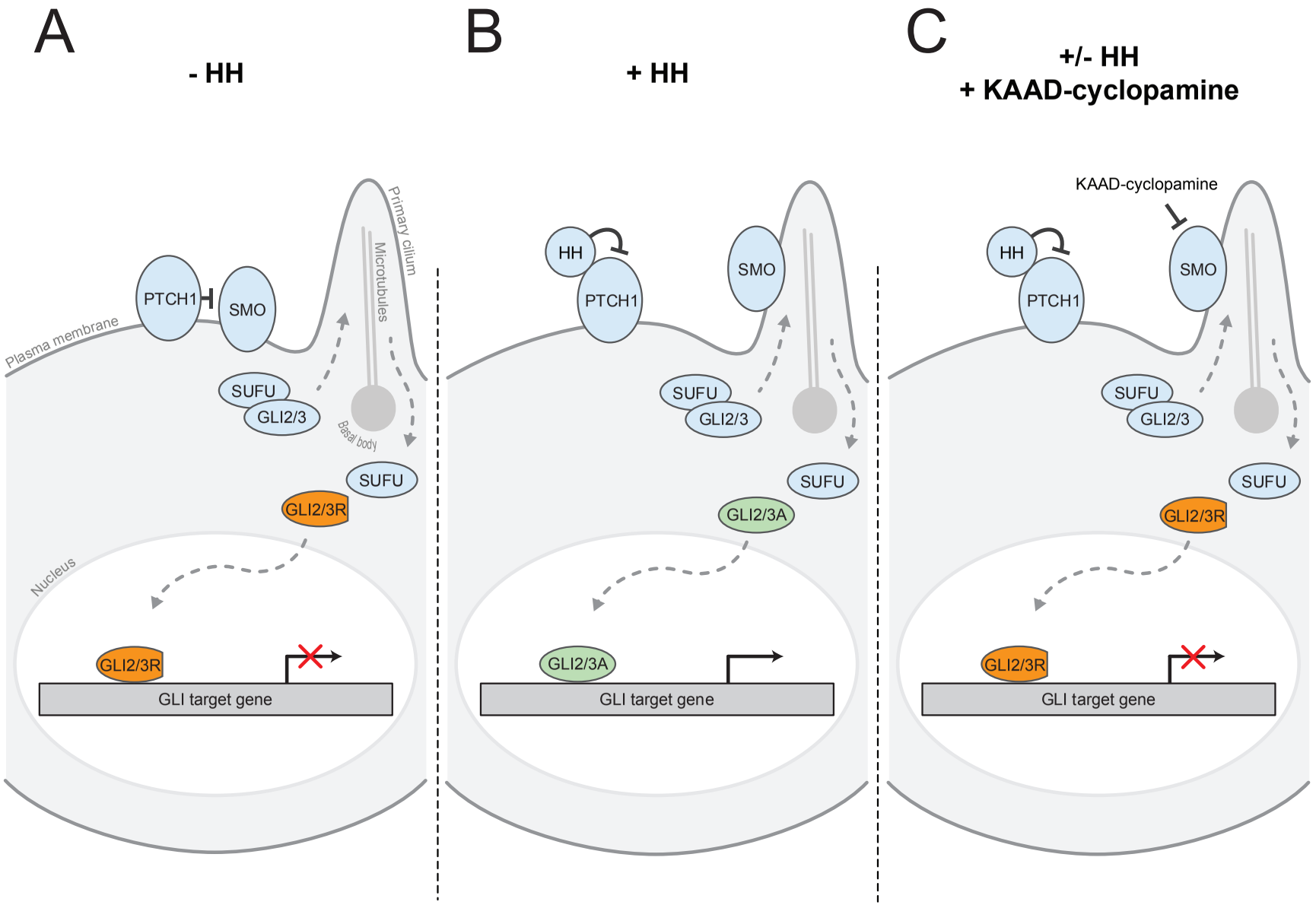
A
- HH
B
+ HH
C
+/- HH
+ KAAD-cyclopamine
Primary cilium
Microtubules
Plasma membrane
PTCH1
SMO
SUFU
GLI2/3
Basal body
SUFU
GLI2/3R
Nucleus
GLI2/3R
GLI target gene
HH
PTCH1
SMO
SUFU
GLI2/3
SUFU
GLI2/3A
GLI2/3A
GLI target gene
KAAD-cyclopamine
HH
PTCH1
SMO
SUFU
GLI2/3
SUFU
GLI2/3R
GLI2/3R
GLI target gene

Figure 2. The HH signalling pathway in the absence and presence of HH ligand. **(A)** In the absence of HH, PTCH1 inhibits SMO, which allows SUFU to transit GLI2/3 into the primary cilium and out past the basal body where kinases phosphorylate the GLI2/3 proteins. This phosphorylation triggers proteolytic cleavage of GLI2/3 to become repressor GLIs (GLI2/3R) *(orange truncated ellipses)* and enter the nucleus to repress downstream GLI target genes. (**B)** In the presence of HH, HH binds to PTCH1 allowing SMO to mediate GLI2/3's dissociation from SUFU in the primary cilium. This allows GLI2/3 to bypass phosphorylation and proteolytic cleavage, and enter the nucleus as a transcriptional activator (GLI2/3A) *(green ellipses)* (reviewed in 101, 119). **(C)** Inhibition of the HH signalling pathway can be achieved independent of HH ligand by treating cells with KAAD-cyclopamine, which binds to SMO and inhibits downstream activation of the pathway.

be found bound to GLI2 and GLI3 while moving through the primary cilium via the microtubule motor protein, KIF7 (131-134). Processing within the primary cilium has been shown to be essential for both transducing the active HH signal and maintaining an inactive HH signal (101).

In the absence of HH ligand, the transmembrane protein, patched homolog 1 (PTCH1) is enriched on the plasma membrane near the primary cilium of the HH-responsive cell and prevents another transmembrane protein, smoothened (SMO), from presenting itself on the plasma membrane of the primary cilium through a poorly characterized mechanism (Figure 2A) (101). In the absence of SMO, the SUFU-GLI2/3 complex associates with the basal body of the primary cilium where PKA, CKI, and GSK3β phosphorylate the GLI proteins (135). Another transmembrane protein, GPR161, found on the primary cilium near the basal body in the absence of HH signalling, is presumed to activate PKA through cAMP signalling (136), and thus assist in negatively regulating HH signalling. Upon phosphorylation of the GLI2/3 proteins, the E3 ubiquitin ligase β-transducin repeat-containing protein (β-TrCP) binds to the GLI2/3 proteins and mediates their proteolytic cleavage through proteasomes that are enriched near the basal body (137). This transforms the full-length GLI2/3 proteins into transcriptional repressors as they exit the cilium (101) (Figure 2A). From there they move into the nucleus where they can repress HH target genes.

The HH pathway is activated when HH ligand binds to PTCH1 (Figure 2B) (138, 139). This triggers the removal of PTCH1 from the cell's surface (140) and the removal of GPR161 from the surface of the primary cilium (136). BOC, CDO and GAS1, which each form a distinct HH-receptor complex with PTCH1, are required during this initial signal transduction step (141). With PTCH1 removed, SMO can translocate to the primary cilium

of the cell either through lateral transport on the plasma membrane or direct transport from an intracellular vesicle (142-146). SMO then accumulates around the basal body of the primary cilium through interactions with the ciliary proteins EVC and EVC2 (147, 148) which leads the SMO C-terminal tails to oligomerize (135). The mechanisms through which GLI2 and GLI3 dissociate from SUFU are still unclear, but when more SMO is near the primary cilium, the SUFU-GLI2/3 complex passes more slowly through the primary cilium and their individual protein concentrations increase especially at the cilium tip (131, 133, 149). Following dissociation from SUFU in the primary cilium (150), full length GLI2 and GLI3 bypass the proteolytic machinery into the nucleus and replace their repressor counterparts on HH target genes to enable activation (119) (Figure 2B).

As the HH ligand levels fluctuate around HH-responsive cells, the profile of active and repressive GLI transcription factors bound to HH target genes varies within the nucleus and mediates differential expression of HH target genes in a concentration dependent manner (119). This concentration-dependent response permits a gradient of HH signalling within a tissue, which influences tissue patterning (119).

In addition to unidirectional signalling, the pathway is mediated through a set of positive and negative feedback loops. *Ptch1* and *Gli1* are induced by HH signalling in all types of cells (92, 151-153) through direct binding of GLI1 and GLI2 (154, 155) in overlapping manners (156). These mechanisms further regulate the signal initiated by the initial dose of HH ligand and throttle the pathway as the concentration of the ligand fluctuates around the HH-responsive cell (119).

The stability of GLI2 was the focus of one prostate cancer research study because prostate cancer cells have higher levels of GLI2 protein than non-cancerous cells, but the

Gli2 transcript levels in both cells remained relatively similar (157). By making an *in vitro* model system with a mutant GLI2, researchers were able to recapitulate this GLI2 phenotype. The GLI2 mutant was prepared by mutating a potentially phosphorylated Ser at the 662nd residue to an Ala. As a result, the mutant GLI2^{S622A} could no longer bind β-TrCP nor be subject to β-TrCP-mediated ubiquitination (157). Therefore, without changing the level of *Gli2* expression, the amount of GLI2 protein remained high in the studied fibroblast cells due to less protein turnover.

1.6 HH signalling agonists and antagonists

To assess the effects of HH signalling on developmental processes through loss-of-function experiments many studies use the HH signalling antagonist, cyclopamine. Cyclopamine is a steroidal alkaloid common to plants of the *Veratrum* genus and was discovered after an investigation into an endemic of cyclopia in newborn lambs (158). In the 1950's, abnormal levels of fetal cyclopia in lambs from south-central Idaho caught the attention of researchers at the U.S. Department of Agriculture. This lead to the discovery of cyclopia-inducing alkaloid steroids in corn lilies, *Veratrum californicum,* on which pregnant ewes grazed at higher altitudes during droughts (159-161). The most potent of these was alkaloid V, which was subsequently named cyclopamine (162).

Decades passed before researchers elucidated the mechanism behind the cyclopic phenotype that linked cyclopamine to the HH signalling pathway (158, 163, 164). In 1998, cyclopamine and other *Veratrum* alkaloids were shown to disrupt HH dependent patterning in developing embryos, independent of cholesterol metabolism (158, 163). Later analysis showed that cyclopamine binds directly to SMO and inhibits its ability to activate GLI

proteins (165) without inhibiting its ability to translocate to the primary cilium (166) (Figure 2C).

Since the discovery of cyclopamine, other chemically synthesized derivatives have been produced. KAAD-cyclopamine, for example is roughly 10-20 times more potent than cyclopamine without being more toxic (167) and has been used to study the *in vitro* effects of HH signalling (90, 91, 168).

Smoothened agonist (SAG) is another synthetic compound that modulates HH signalling, but as its name infers, it targets Smoothened to enhance the pathway (169). This small molecule enhancer has been used to modulate HH signalling both *in vivo* and *in vitro* experiments (170, 171).

1.7 HH signalling during cardiomyogenesis

HH signalling and its primary transducer, GLI2, play an important role during cardiomyogenesis *in vivo* and *in vitro* (87, 89, 90). *Shh*$^{-/-}$ mice have considerably altered heart looping (172) and have a single outflow tract (173). The size of the embryos, including the size of the heart, is also smaller than wild type (WT) embryos. Further analysis with tissue-specific, SHF *Shh*$^{-/-}$ mouse embryos using *Nkx2-5-Cre* has revealed that HH signalling is required for mediating cardiac neural crest cells to the outflow tract cushions and is required for signalling of myocardial cells to establish proper septation (174).

Shh$^{-/-}$/*Ihh*$^{-/-}$ mouse embryos resemble *Smo*$^{-/-}$ embryos and, in addition to showing no embryonic turning, both knockout embryos have only a small linear heart tube (87). This phenotype is attributed to delayed heart tube formation that correlates with delayed *Nkx2-5* expression, compared to WT embryos (87). *Ptch1*$^{-/-}$ embryos on the other hand, which

exhibit higher levels of HH independent signalling than WT embryos, express higher levels of *Nkx2-5* in the cardiac crescent. Thus, HH signalling has a role in timely regulation of heart development.

Similar to the upstream transducers of the HH signal, the downstream transcriptional mediators are also essential for efficient heart septation. *Gli2*$^{-/-}$*Gli3*$^{+/-}$ mouse embryos have persistent truncus arteriosus (PTA) and a single outflow tract (85, 86). Together these knockout models demonstrate that functional HH signalling is essential for proper heart development in mammals.

Intriguingly, HH signalling can rescue atrial septal defects (ASD) in SHF *Tbx5*$^{+/-}$ mutant mouse embryos by potentially normalizing the proliferation of the atrial septum progenitors (175). In zebrafish, downregulation of SHH reduces *Nkx2-5* expression during embryogenesis and the number of cardiomyocytes in the developing cardiac chambers (176). Alternatively, *Shh*-injection into zebrafish embryos has the opposite effect. Another study has also shown that the number of proliferating cardiomyocytes in zebrafish treated with SAG increase by 60% (177). Meanwhile, treatment with cylcopamine, decreases proliferation by 27%. Therefore, HH signalling can modulate cardiomyocytes and atrial progenitors in vertebrates.

Members of the HH signalling pathway are expressed during cardiomyogenesis in P19 EC (73, 89, 90), P19CL6 EC (81), and mES cells (73). These HH signalling members can also regulate cardiomyogenesis induction in P19 EC cells, as overexpression of SHH or GLI2 is sufficient for inducing cardiomyogenesis through the expression of cardiac progenitor factors like *Mef2c*, *Nkx2-5*, and *Gata-4* in P19 EC cells without DMSO treatment

(89). Alternatively, inhibition of HH signalling by cyclopamine results in delayed expression of *Gata-4* (90).

Further study of GLI2's role during cardiomyogenesis *in vitro* has revealed that GLI2 and MEF2C can regulate one another's transcriptional expression during P19 EC cell differentiation, possibly by directly binding to each other's promoter regions (73). Both proteins can form a complex as well, which can synergistically activate a *luciferase* reporter gene driven by an *Nkx2-5* promoter. This multifaceted relationship between GLI2 and MEF2C *in vitro,* along with them both being essential for proper heart looping and outflow tract formation *in vivo*, suggests that HH signalling and MEF2C mediate important stages of cardiomyogenesis together, *in vivo* (37, 38).

1.8 *Mef2c*

MEF2C belongs to the myocyte enhancer factor 2 (MEF2) family of MADS-box binding transcription factors in mammals. The four factors, MEF2A-D, have redundant roles and are expressed in various cell types, but are more commonly known for their ability to regulate muscle regulatory genes (178). As seen in knockout studies, mammalian MEF2 proteins can compensate for the loss of one another (178), whereas mutations in *D. melanogaster's* single *Mef2* gene inhibits myogenesis in all muscle cell types (179). *Mef2c*$^{-/-}$ mice are able to undergo limited cardiomyogenesis in the absence of *Mef2c* likely because MEF2B is enriched 7-fold in these knockout mice and can compensate for the loss of *Mef2c* (37). Nevertheless, these mice have heart looping, right ventricle, and outflow tract defects, which culminate in embryonic lethality by E9.5. A more recent study with conditional knockout of *Mef2c*, through either *Myhc6-Cre* or *Mlc2v-Cre*, in the myocardium also show

that, although *Mef2c* is required for early heart morphogenesis, it is not required for heart morphogenesis after heart looping, as the conditional *Mef2c*$^{-/-}$ embryos live to term with no significant deficiencies (38).

Mef2c is found on chromosome 13 (Figure 3). As previously mentioned, it is expressed during cardiomyogenesis, but it is also expressed in skeletal muscle and endothelial tissue (180). The *Mef2c* gene is composed of at least 14 exons - 4 untranslated exons and 10 coding exons - which can be alternatively spliced prior to translation depending on the tissue in which it is expressed (180). Amongst these exons, it contains four known tissue-specific enhancer regions, which flank three known transcription start sites (Figure 3) (180). A skeletal muscle (SkM) specific enhancer region lies upstream of exon 1 (181) and overlaps with known MEF2C, MyoD, and E12 binding sites (182). Most of the intronic region between exons 2 and 3 is an ISL-1-dependent SHF (SHF I) enhancer region with two sets of two known binding sites for ISL-1 and GATA-4 ~1kb inwards of the 3'-end of the enhancer (44). An NKX2-5/FOXH1-dependent SHF (SHF II) enhancer region is immediately downstream of exon 3 (45), while an endothelial (Endo) specific enhancer region flanks exon 4 (183). There is a triplet of known SOX10 binding sites ~5 kb upstream of the 5' end of the endothelial enhancer (184). ETS1 and ETV2 bind to non-consensus binding domains that overlap with FOXC1, FOXC2, and FOXO1 binding sites ~7.2 kb downstream of the 3'- end of the endothelial enhancer (183, 185).

There are nine conserved GLI consensus binding motifs situated throughout the *Mef2c* gene (Figure 3) (73). GLI2 has been shown to bind to eight of them in P19 EC cells (*Mef2c* sites *B-I*) (73). One of these GLI2 binding sites is situated upstream of the open

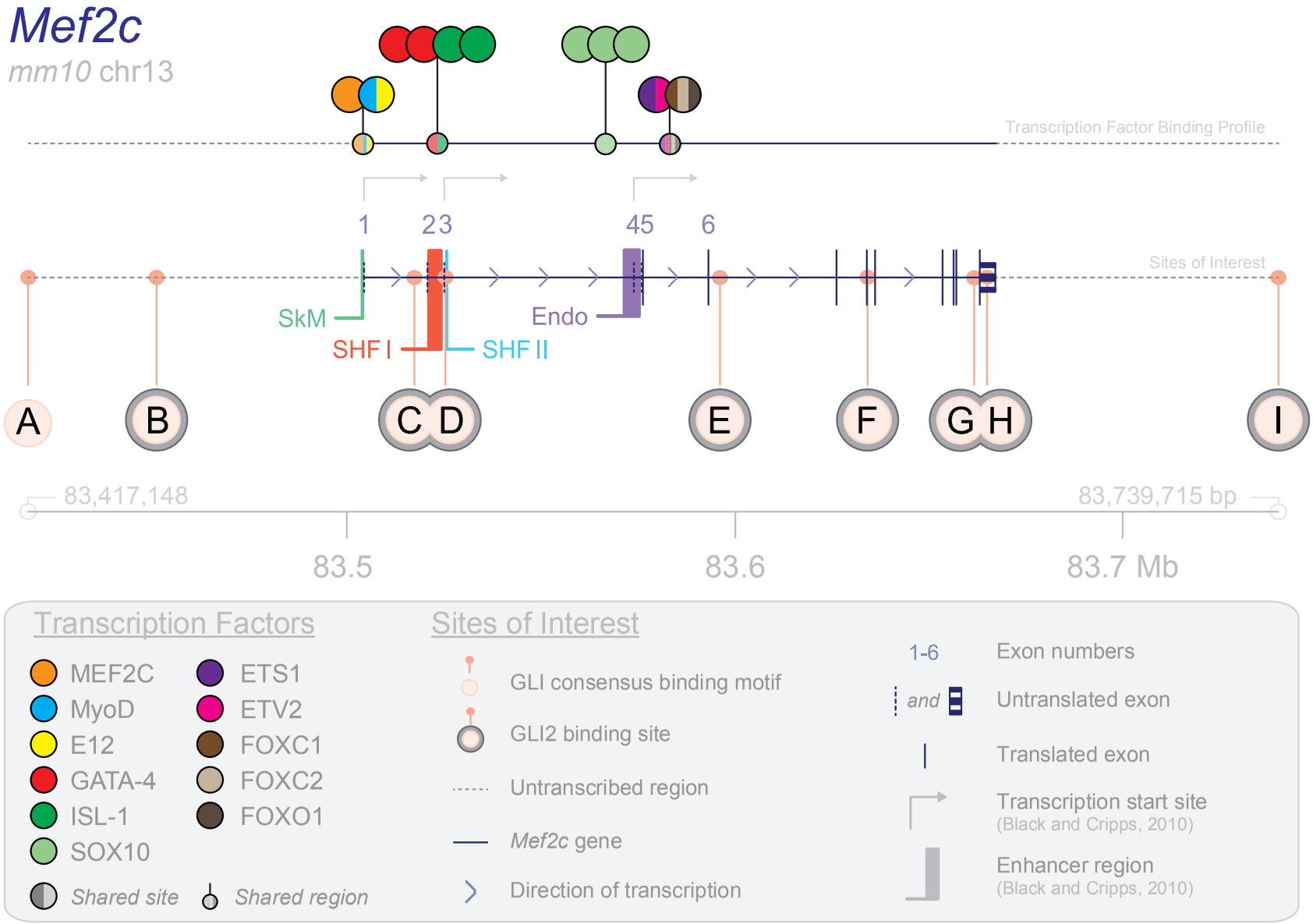
Mef2c
mm10 chr13
Transcription Factor Binding Profile
1
23
45
6
Sites of Interest
SkM
SHF I
SHF II
Endo
A
B
C D
E
F
G H
I
83,417,148
83,739,715 bp
83.5
83.6
83.7 Mb
Transcription Factors
MEF2C
MyoD
E12
GATA-4
ISL-1
SOX10
ETS1
ETV2
FOXC1
FOXC2
FOXO1
Shared site
Shared region
Sites of Interest
GLI consensus binding motif
GLI2 binding site
Untranscribed region
Mef2c gene
Direction of transcription
1-6
Exon numbers
and
Untranslated exon
Translated exon
Transcription start site
(Black and Cripps, 2010)
Enhancer region
(Black and Cripps, 2010)

Figure 3. A schematic representation of the *Mef2c* gene.
The first layer outlines the location of *Mef2c*-associating transcription factors. The second layer depicts major sites of interest in this study. The third layer marks *Mef2c*'s position in the *Mus musculus* genome (mm10 genome assembly). Sites of interest include the GLI consensus binding motifs, which were originally outlined in (73) and enhancer regions reviewed in (180). This schematic was constructed using the UCSC Genome Browser (http://genome.ucsc.edu), data collected through TRANSFAC, and data from previous publications (44, 45, 73, 180-186). A detailed description of the binding sites can be found in Appendix A. *Chr:* Chromosome. *SHF I*: ISL-1-dependent SHF enhancer. *SHF II*: NKX2-5/FOXH1-dependent SHF enhancer.

reading frame and another is downstream of it. Of the six within the *Mef2c* gene, two sites are proximal to the SHF enhancer regions. *Mef2c* site *C* is ~2.4kb upstream of the known SHF I enhancer region's 5'-end (44). *Mef2c* site *D* is roughly ~300 bp downstream of the known SHF I enhancer region's 3'-end and ~100 bp upstream of the SHF II enhancer region's 5'-end (44, 45). These many regulatory regions illustrate the complexity of *Mef2c*'s expression throughout various tissues.

1.9 SWI/SNF chromatin remodelling complexes

A combinatorial binding of transcription factors and co-activators are commonly necessary to facilitate transcriptional regulation during development (187). These combinations can be dynamic and modulate subsets of genes specific to cell lineages in a spatiotemporal manner. However, when DNA is packaged as nucleosomes around histone octamers, transcription factors have limited access to the target genes (188). Chromatin remodelling factors moderate chromatin accessibility to activate or repress genes through DNA methylation, post-translational histone modifications, or ATP-dependent translocation of nucleosomes (189-192). The switch/sucrose non-fermentable (SWI/SNF) complexes constitute one family of factors that mediate nucleosome shifting on chromatin in an ATP-dependent manner (193).

The SWI/SNF complexes belong to a family of chromatin remodelling complexes whose function is highly conserved throughout evolution (193, 194). In mammals, these complexes are commonly referred to as brahma-associated factor (BAF) complexes because brahma (BRM/SMARCA2) or its analogue, brahma-related gene 1 (BRG1/SMARCA4), are the predominant active ATPase enzymes found in mammalian SWI/SNF complexes.

ATPase enzymes associate with nucleosomes approximately 40 bp into the DNA that is wrapped around the histone octamer and then drive the DNA out from the nucleosome (194, 195). Once uncoiled from the nucleosome, the open chromatin is accessible to transcriptional machinery including RNA Polymerase II (192). A combination of the histone modification states on a given nucleosome and the selectivity of the other non-ATPase subunits determine the nucleosomes that the ATPase will associate with and displace (195).

Although similar, the functions of BRM and BRG1 are not completely redundant. *Brg1* knockout mice indicate that BRG1 is essential for early embryonic development because they die sometime during the periimplantation stage (E3.0-6.5) as a result of the mutation (196). *Brm*, however, is dispensable during development given that BRM knockout mice live to term and only display increased body mass (197). These ATPase subunits are the key enzymatic components, however BAF complexes also require additional non-ATPase subunits for proper function.

In total, the BAF complex is composed of 10-12 BAF subunits and each non-ATPase subunit has an associated number, which is defined by its molecular mass (193). Variations of these subunits in the complex enable biological specificity of the BAF complex through interactions with an assortment of transcription factors in multiple developmental lineages (193). During skeletal muscle specification, BRG1 is recruited by myogenin and MEF2D to the regulatory sequences of the skeletal myogenic genes, *MCK* and *Desmin*, and promotes terminal differentiation of skeletal myocytes (198). Similar mechanisms involving cardiac progenitor SWI/SNF complexes have been proposed to regulate cardiac progenitor differentiation as well (199).

Many conditional mutant studies outline the importance of BRG1 during cardiomyogenesis. A conditional mutation of *Brg1* in cardiac progenitor cells with *Nkx2.5-Cre;Brg1f/f* mice predominantly results in irregular ventricle morphology and embryonic lethality by E10.5 (200). Although some pups have been seen to develop to term, these pups still display severe ventricle deformities (200). Results from another study have shown, through conditional mutation of *Brg1* in the heart myocardium using *Sm22a-Cre*, that BRG1 regulates hypertrophy and *Myhc6* and *Myhc7* expression (201). This mutation results in a much thinner myocardium than normally observed on E10.5, no interventricular septation, and eventual embryonic lethality by E11.5 (201). Furthermore, when *Brg1* is conditionally knocked out of the endocardium with *Tie2-Cre*, it leads to derepression of *Adamts1,* which results in inefficient trabeculation. (202). Therefore, *Brg1* expression in the mammalian adult heart is important during many stages of cardiomyogenesis.

Given that SWI/SNF-dependent chromatin remodelling requires a complex of subunits and that their combination regulates specificity in other lineages (193), it is not surprising that a number of BAF subunits are also essential for proper heart formation. For instance, knockdown of *Baf60c* expression by RNA interference results in abnormal cardiac formation through reduced expansion of the SHF and inefficient outflow tract remodelling (42). After this observation, it was determined that BAF60C interacts with cardiac progenitor transcription factors, GATA-4, NKX2-5, and TBX5 in a dose-dependent manner to regulate cardiac genes (42). Furthermore, when ectopically expressed with GATA-4 and TBX5, BAF60C prepares target loci for GATA-4 binding and supports differentiation of non-cardiac mesoderm cells into cardiomyocytes (40).

BAF180, also known as polybromo, is another subunit expressed in the epicardium during cardiogenesis and is associated with heart chamber maturation (203). It belongs to a subset of mouse SWI/SNF complexes suitably termed the polybromo-containing BAF (PBAF) complexes. These complexes are important for proper heart development but, unlike other BAFs, are non-essential during early gastrulation (193, 203). BAF180 deletion impedes epicardium maturation and coronary development (204).

Recent studies have shown that BAF250A is a major regulatory subunit for cardiac progenitor cell proliferation and differentiation (199). *Baf250a* knockout mice are embryonic lethal by E6.5 and lack a mesoderm layer (205). Additionally, when the ES cells from this line are grown in culture, they are less pluripotent and differentiate less into mesoderm-derived cells, including cardiomyocytes. Conditional knockout of *Baf250a* in the SHF, using *Mef2c-Cre; Rosa-YFP*$^{+/-}$*; Baf250a f/f* embryos, further demonstrates the regulatory role of *Baf250a* during cardiac progenitor cell differentiation, *in vivo* and *in vitro* (199). Consistent with the expected SHF patterning, *Baf250a*$^{-/-}$ hearts have normal left ventricle growth, but have increased compact myocardium and minimal trabeculae development in the right ventricle. They also do not undergo ventricle septation (199). RNA analysis of the SHF cells in E9.5 conditional *Baf250a*$^{-/-}$ mice show that *Nkx2-5* and *Mef2c* are significantly downregulated compared to wild-type (WT) cells, while *Gata-4* and *Isl1* are not significantly different (199). Researchers further investigated these observations on a molecular level with day 6 differentiated *Baf250a*$^{-/-}$ ES cell-derived cardiac progenitor cells and determined by chromatin immunoprecipitation with an anti-BRG1 antibody (BRG1-ChIP) that less BRG1 associates with the *Mef2c* and *Nkx2-5* promoter regions than in similar WT cells (199). Furthermore, DNase I hypersensitivity assays showed that the *Nkx2-5* and

Mef2c promoters in these day 6 cultures are more resistant to DNase treatment when *Baf250a* is knocked out, suggesting that BAF20A is needed for enabling *Nkx2-5* and *Mef2c* promoter accessibility. Together, these results suggest that BAF250A recruits BRG1 and its chromatin remodelling functions to the *Nkx2-5* and *Mef2c* promoters to regulate their expression in the SHF.

1.10 Rationale

Cell-based therapies using hES cell-derived cardiomyocytes are an attractive alternative to heart transplantation, however further research is required to refine the ideal population of cardiomyocytes or cardiac progenitors needed for efficient remuscularization of infarcted hearts. Thus, additional mechanisms that regulate cardiomyogenesis *in vitro* should be investigated.

Considering the significant roles of HH signalling and its primary transducer, GLI2, during cardiomyogenesis *in vivo* and its ability to induce cardiomyogenesis in P19 EC cells *in vitro*, HH signalling likely enhances cardiomyogenesis in mES cells.

To further elucidate this enhancement, the mechanisms regulating it must also be investigated. As previously mentioned, embryos deficient for certain BAF subunits share similar heart tube looping and outflow tract deformities as embryos that are deficient for HH signalling members. Given this and the observations that BRG1 can immunoprecipitate with GLI2 protein in mouse embryonic fibroblast (MEF) cells and can associate with GLI target genes (206), HH signalling may recruit BRG1 to GLI target cardiac genes to mediate enhanced cardiomyogenesis *in vitro*.

1.11 Hypothesis

HH signalling enhances cardiomyogenesis in mES cells through its primary transducer GLI2 and mediates cardiomyogenesis *in vitro* through GLI2's recruitment of BRG1 to GLI target cardiac genes.

1.12 Objectives

To test these hypotheses the following aims were established: 1) compare the expression levels of cardiac progenitor and cardiomyocyte genes during differentiation of mES cells that overexpress GLI2 to those in control mES cells; 2) determine if GLI2 can interact with BRG1 in mES cells; and 3) determine if HH signalling regulates BRG1 association with a GLI target cardiac gene in P19 EC cells.

2 Materials and Methods

2.1 Expression vectors

A pcDNA3.1+ vector containing *Flag-Gli2*^{S662A} was graciously provided by Dr. Spiegelman and is described in detail in (157). In brief, the *Flag-Gli2*^{S662A} sequence consists of a *Flag* tag at the 5' end of a full-length mouse *Gli2* coding sequence. The *Gli2* sequence has a mutation that changes the Ser residue at site 662 in the translated protein to an Ala residue. This point mutation results in a GLI2 protein that is more stable intracellularly, due to lower susceptibility to ubiquitination and degradation (157).

A control pcDNA3.1+ vector, containing the *Flag* element alone, was constructed from the *Flag-Gli2*^{S662A} vector by excising the *Gli2*^{S662A} sequence using the EcoRI restriction enzyme (New England BioLabs). The resultant plasmid was verified by sequencing on a 3730 DNA Analyzer (Applied Biosystems).

2.2 mES cell culture

D3 mES cells (ATCC, #CRL-1934) were cultured at 37°C and 5% CO_2 on tissue culture grade (TC) adherent plates (Corning) in Dulbecco's Modified Eagle, high glucose medium (DMEM-Hi) (GIBCO) supplemented with 10% fetal bovine serum (FBS) (Wisent Inc.), 1X Minimum Essential Medium (MEM) non-essential amino acids (GIBCO), 50 μM Gentamicin (Invitrogen), 8 mg/L β-Mercaptoethanol (J.T.Baker) and 1000 U/ml leukemia inhibitory factor (LIF) (Millipore) - altogether termed mES cell medium. Cultures were fed every two days and subcultured using Trypsin-EDTA (GIBCO and Bio-Rad, respectively).

To create stable mES[FLAG-GLI2^{S662A}] cells - termed mES[GLI2] cells - $1.8x10^6$ trypsinized mES cells were electroporated with 19.2 μg of linearized FLAG-GLI2^{S662A}

construct using a single pulse of 950 μF and 250 V from a Gene Pulser Xcell Electroporation System (Bio-Rad Laboratories). To create mES[Control] cells - termed mES[Ctrl] cells - $2x10^5$ mES cells were transfected with 2 μg of circular FLAG construct using Lipofectamine as per the manufacturer's protocol (Invitrogen). Transfected colonies were selected by culturing in mES cell medium supplemented with 0.8 mg/ml Geneticin (GIBCO) two days post-transfection. After 8 to 10 days of culturing the Geneticin-resistant colonies in selection medium, clonal populations were picked. Transcription and protein expression levels of FLAG-GLI2^{S662A} were measured by quantitative PCR (qPCR) and western blot analysis, respectively.

mES cells were differentiated as previously described (207). In brief, mES cells were divided into hanging drops at $4x10^4$ cells/ml ($8x10^3$ cells per drop) and allowed to form aggregates for two days in mES cell medium without LIF. The aggregated cells, also referred to as embryoid bodies (EBs), were then pooled and left in suspension for three days on non-TC dishes (Fisher Scientific) coated with 1% w/v agarose (Mandel Scientific) before transferring to TC plates (Corning) or 0.1% gelatin-coated (Fisher Scientific) coverslips (Thermo Scientific, Fisher Scientific) to culture until day 7, 10, or 15 for the analysis of cardiomyogenesis, neurogenesis, or skeletal myogenesis, respectively. Medium was changed every two days.

2.3 P19 EC cell culture

Parental P19 EC cells (ATCC, #CRL-1825) or P19 EC cells transfected with pcDNA3-GLI2 or an empty vector control, termed P19[GLI2] and P19[Ctrl], respectively, were previously described in (208) and (73). These cells were cultured and differentiated as

per (209). Briefly, cultures were maintained at 37°C and 5% CO_2 in MEM Alpha-Medium (GIBCO) supplemented with 10% FBS (Wisent Inc.) - together termed P19 medium. For P19[GLI2] and P19[Ctrl] cell lines, puromycin (Sigma-Aldrich) was added as a selection agent at 2 g/ml.

P19 EC cell differentiation was initiated by plating $5x10^4$ cells/ml in P19 EC cell medium supplemented with 1% v/v DMSO (Sigma-Aldrich) on non-TC dishes (Fisher Scientific) pre-coated with 1% w/v Agarose (Mandel Scientific). After 4 days, the newly aggregated EBs were transferred to TC plates or 0.1% gelatin-coated (Fisher Scientific) coverslips (Thermo Scientific, Fisher Scientific) without DMSO for an additional 2 days of the 6-day protocol. Throughout the differentiation process the EB's were fed fresh medium with or without DMSO at least every two days.

To inhibit HH signalling in P19 EC cells, differentiating P19 EC cultures were treated with 5 μM KAAD-cyclopamine (Toronto Research Chemicals), as previously described (90), or with the MeOH (Fisher Scientific) vehicle alone, every second day throughout the entire 6-day protocol.

2.4 Immunoblot analysis

Total protein from differentiating mES[GLI2] and mES[Ctrl] cells was collected on days 2, 3, 4, and 5 of differentiation from a minimum of $2x10^5$ mES[GLI2] or mES[Ctrl] cells using radioimmunoprecipitation assay (RIPA) buffer (recipe in Appendix B). The lysate was clarified by centrifugation at 14,000 g for 10 min.

To analyze the presence of FLAG-GLI2^{S662A} in the stable cell lines, 300 μg of total protein extract was subjected to immunoprecipitation with 20 μl of FLAG-beads (FLAG-IP),

as per Sigma-Aldrich's protocol. Bound proteins were eluted from the beads by boiling in sample buffer for 10 min.

The resulting eluate and the original input samples were separated using a 4-12% denaturing polyacrylamide gel (NuPAGE, Invitrogen) with MOPS running buffer according to the manufacturer's protocol (Invitrogen). The resolved proteins were then transferred to a polyvinylidene fluoride (PVDF) membrane (Bio-Rad), blocked using non-fat dry milk (Carnation) reconstituted with Tris-buffered saline (TBS), and incubated with GLI2 (210) or alpha-tubulin (DM1A, Sigma-Aldrich) specific antibodies. The signal was detected using horseradish peroxidase (HRP)-conjugated secondary anti-mouse (Cell Signalling) or anti-rabbit (Santa Cruz) antibodies, followed by a chemiluminescence reaction using Pierce ECL substrate (Fisher Scientific).

Densitometry was performed on the GLI2-specific bands with the ImageJ program (National Institutes of Health, USA) (211). The densities of the GLI2 protein in the FLAG-IP samples were presented as a percentage of the highest band density. The densities of the GLI2 protein in the total protein samples were normalized to the loading control, α-tubulin, before presenting them as a percentage of the highest band density.

2.5 Quantitative PCR (qPCR) analysis

For each time-point during mES cell differentiation, a minimum of $1x10^5$ mES cells were collected for total RNA extraction using an RNeasy Micro Kit (Qiagen). Total RNA from P19 EC cells was collected from at least $5x10^5$ cells using an E.Z.N.A. Total RNA Kit (OMEGA Bio-tek). All purified extracts were reverse transcribed into cDNA using at least 500 ng of starting material and a QuantiTect Reverse Transcription Kit as per the

manufacturer's protocol (Qiagen). A negative control (no RT) was prepared alongside each experiment for every cell line to control against genomic DNA contamination. For each qPCR reaction, 1/40th of the resultant cDNA reaction product, a final concentration of 200 nM transcript-specific primers, and either a GoTaq qPCR Master Mix (Promega) or a KAPA SYBR® FAST qPCR kit (KAPA Biosystems) were used to detect transcripts of interest in a given sample with an Eppendorf realplex^2 Mastercycler. The primer sequences are listed in Table 1.

Threshold amplification cycles (Ct) values were determined for each sample, and normalized to the *β-actin* control (in parallel reactions) using the $2^{-\Delta\Delta Ct}$ method (212). The relative fold changes from each biological replicate were calculated as a percentage of the highest transcriptional expression for each respective gene (percent maximum) and presented as an average from three or more independent biological replicates, as described in (73, 99, 213). All error bars represent ± standard error of the mean (SEM). All statistical analyses were done using Student's T-tests.

2.6 Immunofluorescence

Day 7 differentiated mES cells were fixed in -20°C MeOH (Fisher), rehydrated, and washed in Stockholm's phosphate buffered saline (sPBS) (recipe in Appendix B). Pan-MyHC expression was detected by incubating monoclonal MF20 antibody supernatant (214) 1:1 with sPBS overnight at 4°C. After washing 3 times with sPBS, samples were incubated with Cy3-conjugated goat anti-mouse IgG (Jackson Immuno Research) 1:100 in sPBS for 1 hour at room temperature. Coverslips were mounted in 50 parts sPBS, 50 parts glycerol (Fisher), and 1 part Hoechst 33258 dye for staining nuclei. Indirect immunofluorescence of

Table 1. Sequences of primers used for real time qPCR analyses.

Target	Forward Primer	Reverse Primer
β-actin	AAATCGTGCGTGACATCAAA	AAGGAAGGCTGGAAAAGAGC
Ascl1	ACTTGAACTCTATGGCGGGTT	CCAGTTGGTAAAGTCCAGCAG
Brachyury	CTGGACTTCGTGACGGCTG	TGACTTTGCTGAAAGACACAGG
Brg1	CAAAGACAAGCATATCCTAGCCA	CACGTAGTGTGTGTTAAGGACC
Flag-Gli2 ^{S662A}	GGACTACAAGGACGACGATGA	CAGAGGACAGGCCTTTTTCC
Gata-4	AAAACGGAAGCCCAAGAACCT	TGCTAGTGGCATTGCTGGAG
Gli1	CCAAGCCAACTTTATGTCAGGG	TCCTAAAGAAGGGCTCATGGTA
Gli2	CAACGCCTACTCTCCCAGAC	GAGCCTTGATGTACTGTACCAC
Mef2c	TCTGTCTGGCTTCAACACTG	TGGTGGTACGGTCTCTAGGA
Mesp1	CATCGTTCCTGTACGCAGAA	TCTAGAAGAGCCAGCATGTCG
Myhc6	CAACAACCCATACGACTACGC	ACATCAAAGGGCCACTATCAGTG
Myhc7	ACTGTCAACACTAAGAGGGTCA	TTGGATGATTTGATCTTCCAGGG
Nkx2-5	AAGCAACAGCGGTACCTGTC	GCTGTCGCTTGCACTTGTAG
Pax3	TTTCACCTCAGGTAATGGGACT	GAACGTCCAAGGCTTACTTTGT
Ptch1	AAAGAACTGCGGCAAGTTTTTG	CTTCTCCTATCTTCTGACGGGT
Tbx5	CTTTCGGGGCAGTGATGAC	TTGGATGAGGTGGAGAGAGC

MyHC was visualized using a Leica DMI6000B inverted fluorescent microscope (Leica Microsystems GmbH, Germany) and captured with a Hamamatsu Orca AG camera (Hamamatsu Photonics, Germany). Pictures were processed with the Volocity 4.3.2 software (Perkin Elmer, Canada). Cells were counted based on the number of nuclei and identified as $MyHC^{+ve}$ or $MyHC^{-ve}$ using the Volocity imaging program with automated cell-identification parameters.

2.7 Mass spectrometric analysis

FLAG-IPs were performed on 5 mg of nuclear protein extracts from day 3 differentiating mES[GLI2] and mES[Ctrl] cells to identify candidate proteins that may form a complex with GLI2. A 10% fraction of the eluted proteins was retained and subjected to immunoblot analsysis using anti-GLI2 or anti-SNF2β/BRG1 (07-478, Millipore) antibodies, as outlined above. The remaining 90% fraction of the eluted proteins was resolved on a 4-12% denaturing polyacrylamide gel (NuPAGE, Invitrogen) and silver-stained. The staining identified a unique band profile in the 170-250 kDa range of the mES[GLI2] sample compared to the mES[Ctrl] sample (data not shown). Resolved proteins from both cell lines, within the 170-250 kDa range, were extracted from the gel using in-gel digestion, as per (215). The extracted samples were subjected to liquid chromatography-tandem mass spectrometry (LC-MS/MS) on a Thermo LTQ Orbitrap XL hybrid mass spectrometer with a nanospray ion source. The MS/MS ion spectra were matched against the SwissProt database (version 2013_05) using the MASCOT software (Matrix Science, UK) with a peptide mass tolerance of 10 ppm and a fragment mass tolerance of 0.6 Da (216).

2.8 Bioinformatics analysis

BRG1 genome-wide ChIP-sequencing peaks identified in undifferentiated mES cells (217) were screened for genes that contained conserved GLI consensus binding motifs, which were identified with the Multiple Sequence Local Alignment and Visualization tool (Mulan) as described in (218). Candidate genes were categorized by gene ontogolgy (GO) analysis using the Database for Annotation, Visualization, and Integrated Discovery (DAVID) bioinformatics system, as described in (219, 220).

2.9 Chromatin immunoprecipitation (ChIP) assays

ChIP assays were performed as previously described (221) using 20-25 μg of chromatin from day 4 differentiating P19[GLI2] or P19[Ctrl] cells and anti-SNF2β/BRG1 (07-478, Millipore) antibodies or normal rabbit serum (Calbiochem) at a final concentration of 1:500.

Briefly, EBs from 10 plates (15 cm) were fixed with 1% formaldehyde (BP531-500, Fisher Scientific) for 60 minutes at room temperature. The cross-linked cells were passed through a Dounce homogenizer (Bellco Glass Inc., USA) with a tight pestle for 2 sets of 30 reps and lysed with three sequential lysis buffers as described in (221). Isolated nuclei were then sonicated for 20 sets of 15 seconds at setting #10 on a Sonic Dismembrator (Model F60, Fisher Scientific) to shear chromatin to ~1,000-10,000 bp.

All immunoprecipitation (IP) steps were performed at 4°C. In preparation for each IP, 25 μg of chromatin was first pre-cleared for 2 hours with 30 μl of BSA-blocked rec-Protein G-Sepharose 4B Conjugated beads (Invitrogen). A 10% fraction was kept aside at -20°C as an input sample before incubating the remainder overnight with either antibody

listed above. The chromatin-antibody complexes were captured with 30 μl of blocked protein G beads for 2 hours. After washing the beads as described in (221), the chromatin was eluted in TE buffer containing 1%SDS and was reverse crosslinked overnight at 65°C. Contaminating RNA and proteins were removed by treatment with 20 μg of RNase A (Sigma-Aldrich) for 1 hour at 37°C and 40 μg of Proteinase K (Roche) for 2 hours at 65°C, per sample, respectively. DNA was purified using a QIAquick PCR Purification Kit (QIAGEN). To detect eluted DNA fragments, qPCR analysis was performed using 1/40th of each eluted sample, per reaction, with sequence-specific primers listed in Table 2, as mentioned above.

Chromatin from KAAD-cyclopamine- or MeOH-treated P19 EC cells was prepared as above but under different fixing and sonication conditions. Cells from 4 plates of day 4 P19 EC EBs - treated with KAAD-cyclopamine or MeOH - were fixed with 1.5 mM Ethylene glycol bis[succinimidylsuccinate] (EGS) (Thermo Scientific) for 30 min alone, then with 1% formaldehyde (Sigma-Aldrich) for an additional 30 min. Cells were passed through the Dounce homogenizer for only 1 set of 30 reps and sonicated in 1 mL, 12x12 AFA tubes (Covaris) for 30 min with an S220 Focused-ultrasonicator (Covaris) as per manufacturer's recommended operating conditions for a 200-700 bp fragment range. The IP was performed with 20 μg of chromatin. The qPCR analysis was performed, as above, but with 1/50th of each eluted sample, per reaction.

Table 2. Sequences of primers used for ChIP-qPCR analyses.

Target	Location (mm10)	Forward Primer	Reverse Primer
β-actin	Chr 5: 142,906,954 -142,907,148	GATGCTGACCCTCATCCACT	ATGAAGAGTTTTGGCGATGG
Gene Desert	Chr 15: 70,644,478 - 70,644,564	TCCTCCCCATCTGTGTCATC	GGATCCATCACCATCAATAACC
Mef2c site *A*	Chr 13: 83,417,148 - 83,417,378	TGAAAAAGGAAATATCCCACTTAGA	TTGCATGGGTTCACACCTAA
Mef2c site *B*	Chr 13: 83,450,400 - 83,450,695	AGTTGCCTGAGCCTGTTTTC	TTTTTCGGCAATGATTTTCC
Mef2c site *C*	Chr 13: 83,517,957 - 83,518,157	CTTTCGGCTGGAGAGTCTTG	TCTCCAGTTCCTGGGAAGAA
Mef2c site *D*	Chr 13: 83,524,812 - 83,524,937	ACACACGCACACTTCGTCTC	GACCCACACAGAACCTTCAAA
Mef2c site *E*	Chr 13: 83,595,419 - 83,595,594	TTCCCATTTGGACCATTACC	ACCCACGCACTGAGACTTTC
Mef2c site *F*	Chr 13: 83,633,148 - 83,633,305	AACCCCAATCTTCTGCCACT	AAGCTTTCGCTAGACGTGGA
Mef2c site *G*	Chr 13: 83,660,831 - 83,661,075	GAGCCCCCTCTCTAATGTCC	TGTGGGCAAGTGTCTTTCTG
Mef2c site *H*	Chr 13: 83,664,180 - 83,664,382	AAGTGACATTTGGGGGTCCT	CGACCGACCTGCTTTACTTG
Mef2c site *I*	Chr 13: 83,739,543 - 83,739,715	CCTAATTATTTCAGTTTGGGATGC	CCTCCCCTCTTGTCAAAGTGT

*Chr: Chromosome

3 Results

3.1 Overexpression of FLAG-GLI2^{S662A} results in increased levels of GLI2 in mES cells

mES cells were stably transfected with a *Flag-Gli2*^{S662A} vector to investigate the role of GLI2 during mES cell cardiomyogenesis. The pcDNA3.1 vector that contained the *Flag-Gli2*^{S662A} sequence also contained a neomycin resistance gene for use as a selectable marker when treated with aminoglycoside antibiotics, such as Geneticin. *Flag-Gli2*^{S662A} transcript levels were used as an initial screen for efficient exogenous *Gli2* expression within each line. The clones that survived Geneticin treatment and expressed the highest *Flag-Gli2*^{S662A} transcript levels, as determined by qPCR were subjected to western blot and qPCR analysis to assess the level of total GLI2 protein and total *Gli2* transcripts during differentiation, respectively. The cell line with the highest and most stable GLI2 expression during differentiation, from here on referred to as the mES[GLI2] cell line, was used for the following studies and compared against a control mES cell line transfected with only a *Flag* peptide tag-containing vector, from here on referred to as the mES[Ctrl] cell line.

mES[GLI2] and mES[Ctrl] cell lysates were tested for exogenous FLAG-GLI2^{S662A} protein by immunoprecipitation with anti-FLAG beads (FLAG-IP) and subsequent western blot analysis with GLI2 antibodies (Figure 4A, first row of blots). Only the mES[GLI2] cell line contained exogenous GLI2. The size of the upper band in the total protein blots (Figure 4A, second row of blots), ~180kDa, is consistent with other studies (73, 222) and equivalent to the single GLI2 band that was pulled down by FLAG-IP. The non-specific binding seen below the GLI2 band is typical of this antibody (73, 210, 222). Previous analysis of samples

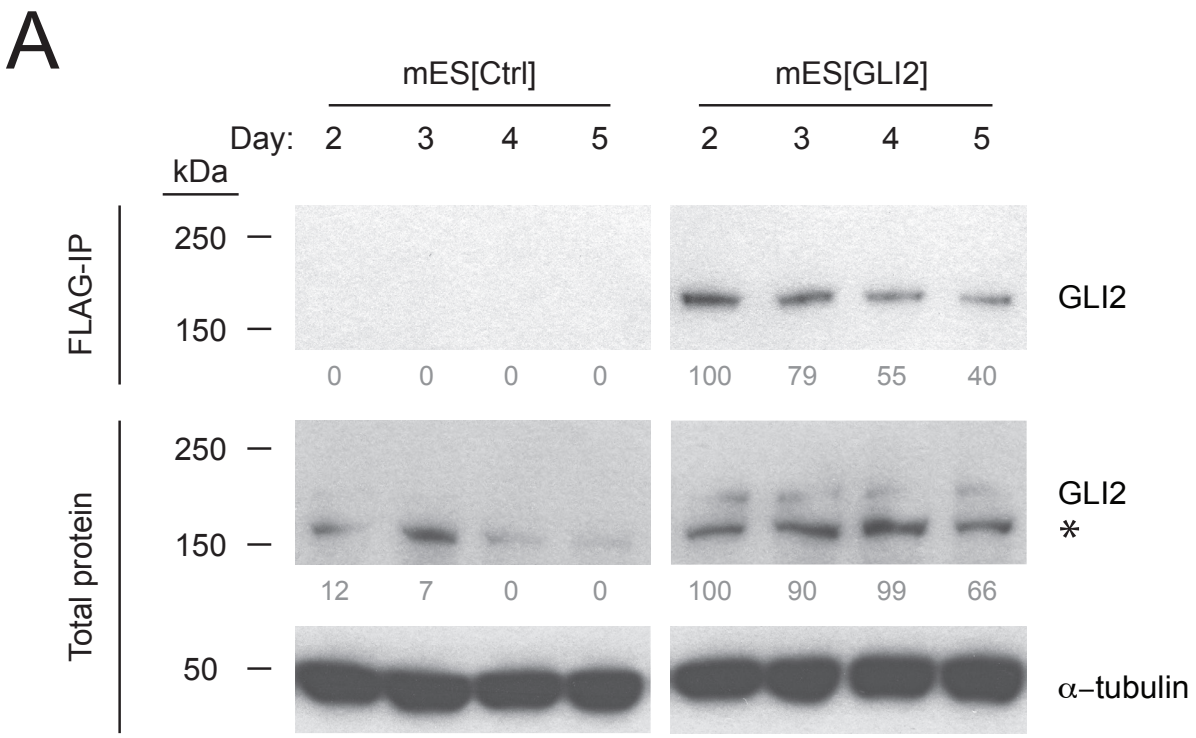
A
mES[Ctrl]
mES[GLI2]
Day: 2 3 4 5 2 3 4 5
kDa
FLAG-IP
250
150
0 0 0 0 100 79 55 40
GLI2
Total protein
250
150
12 7 0 0 100 90 99 66
GLI2
*
50
α–tubulin

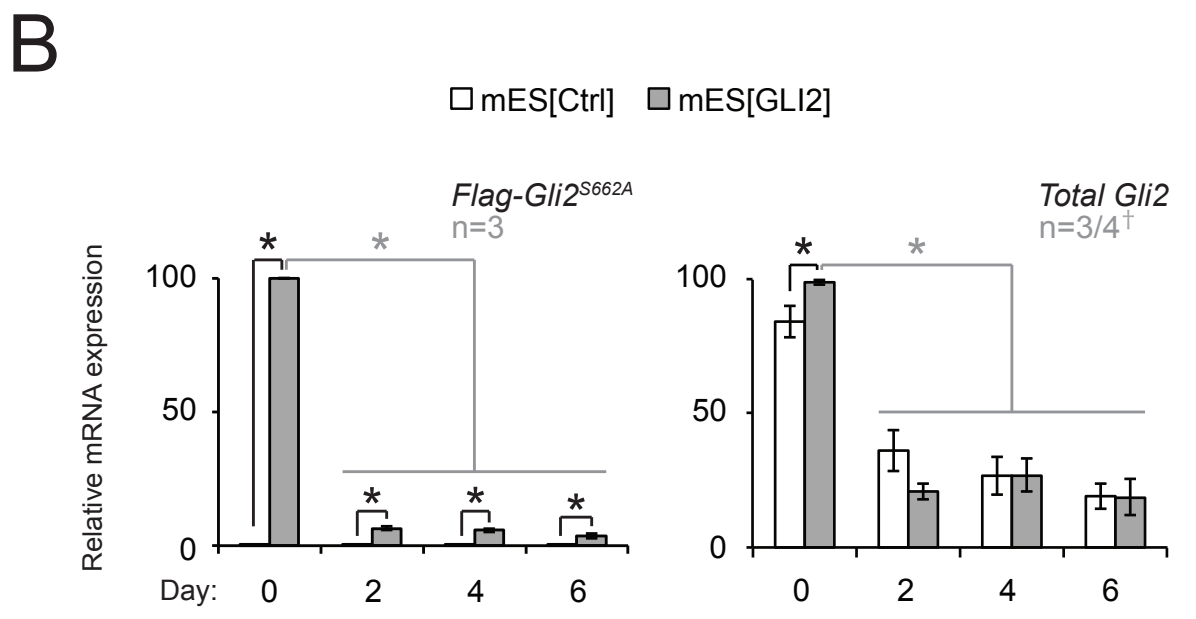
B
mES[Ctrl]
mES[GLI2]
Flag-Gli2S662A
n=3
Total Gli2
n=3/4†
Relative mRNA expression
100
50
0
Day: 0 2 4 6

Figure 4. Overexpression of GLI2 protein in mES[GLI2] cultures was maintained during differentiation.

(A) Total protein extracts from corresponding differentiating cells were analyzed by immunoblot with GLI2 antibodies, with or without prior FLAG-IP. α-tubulin was used as a loading control. *(*)* Non-specific binding of GLI2 antibody (73, 210, 222). Band densities were quantified by densitometry with ImageJ, normalized to α-tubulin and presented as a percentage of the highest expression for each set of samples. **(B)** Transcription levels of the indicated genes in differentiating cells were quantified using qPCR. Expression levels were normalized to *β-actin*, calibrated to day 0 mES[Ctrl] culture expression levels, and presented as a percentage of the highest expression level recorded, per gene. Error bars represent +/- SEM. The number of biological replicates analyzed *(*n*)* is indicated beside each graph. *(†)* n=4 for total *GLI2* days 0 and 4. One-tailed Student's T-tests were used for statistical analyses. Grey lines represent paired T-tests; black lines represent unpaired T-tests; *(*)* $p < 0.05$.

from *Gli2*$^{-/-}$ and *Gli2*$^{-/+}$ mice showed that the upper band is specific to GLI2 and the lower band is non-specific, as only the upper band is absent in the *Gli2*$^{-/-}$ sample (73).

Densitometry was performed on the GLI2-specific bands in the total protein samples to compare them quantitatively (Figure 4A, values below the second row of blots). In the mES[Ctrl] cell line, endogenous GLI2 protein was detectable on days 2 and 3 of differentiation. In the mES[GLI2] cell line, endogenous GLI2 protein levels could not be distinguished from the exogenous GLI2 protein with available antibodies. Nevertheless, it was apparent that the combined endogenous and exogenous GLI2 protein in the mES[GLI2] cultures was ~8-fold and ~13-fold higher than that of the endogenous GLI2 in the mES[Ctrl] cultures on days 2 and 3 of differentiation, respectively (Figure 4A, second row of blots). Also, total GLI2 protein was apparent in the mES[GLI2] cell line on days 4 and 5, when no GLI2 protein was detectable in the mES[Ctrl] cell line.

In addition to the total GLI2 levels observed during differentiation, both mES[Ctrl] and mES[GLI2] cell lines contained similarly higher levels of total GLI2 protein in an undifferentiated state (data not shown). The lower level of GLI2 protein upon differentiation in these cell lines has been observed in previous studies (73). Overall, these results show that the GLI2 protein was overexpressed in mES[GLI2] cells during early stages of mES cell differentiation compared to the control.

Comparable results were also observed at the transcriptional level. *Flag-Gli2*^{S662A} transcripts were only expressed in mES[GLI2] cells and were highly expressed in the mES[GLI2] undifferentiated cells (Figure 4B). Differentiation of the mES[GLI2] cells resulted in a 93.4±0.7% reduction in expression. This trend of exogenous *Gli2* levels

mirrored that of total *Gli2* transcript levels in both mES[Ctrl] and mES[GLI2] cultures during differentiation, suggesting that these two pools of transcripts could be repressed by a common post-transcriptional regulatory mechanism (Figure 4B). This downward trend of transcript levels also correlates with trends seen in other published work on differentiating mES cells (73).

Total *Gli2* transcript levels were significantly higher in the mES[GLI2] undifferentiated cultures compared to the mES[Ctrl] cultures as a result of stably transfecting the exogenous *Flag-Gli2*^{S662A} gene (Figure 4B). Nevertheless, this enhancement was not observed during differentiation. Considering that the pool of exogenous *Gli2* transcripts increased the total level of *Gli2* transcripts by 1.2±0.1 fold in undifferentiated cells, in a variable biological setting this relative difference may be less distinguishable when the expression levels are lower in differentiating cells.

For this reason, the stability of the exogenous GLI2^{S662A} protein is a key element in this model. Even though the exogenous *Gli2* transcripts were lower in their respective differentiating cultures, the exogenous GLI2^{S662A} protein was relatively stable during differentiation (Figure 4A). A GLI2^{wt} overexpression model would have likely been unable to significantly increase GLI2 during differentiation due to the regulatory mechanisms that appear to be at play at least at the post-transcriptional level. This disconnect between GLI2 protein and *Gli2* transcripts is common to prostate cancer cells, where GLI2 protein is upregulated despite relatively stable *Gli2* mRNA compared to normal prostate cells (157). Bhatia et al. were able to model this effect in 293T cells with the same GLI2^{S662A} employed in the current study (157). The downstream deregulation of β-TrCP-mediated GLI2-ubiquitination through GLI2^{S662A} provides the necessary modulation for overexpressing GLI2

in mES cells during differentiation, in light of unknown transcriptional- or translational-repressive mechanisms.

3.2 Overexpression of GLI2 results in accelerated cardiac progenitor and cardiomyocyte specific gene expression

To assess the efficacy of the GLI2 overexpression model, we monitored the expression of the GLI2 direct target gene, *Ptch1* (154). Overexpression of GLI2 resulted in a significant 2.9±0.7 fold increase of *Ptch1* transcripts in undifferentiated cells and a significant 1.4±0.2 fold increase in day 2 differentiating cells (Figure 5, panel *Ptch1*). Therefore, this implies that the overexpression of GLI2 in this mES cell system can increase GLI2 target gene expression.

During differentiation, both the mES[Ctrl] and the mES[GLI2] cell lines showed a similar transition through the mesoderm stage of differentiation, based on the levels of *Brachyury* transcripts by day 4 (Figure 5, panel *Brachyury*). On the same day, *Mesp1* levels were significantly higher in the mES[GLI2] cultures than in the control cultures, but neither of the levels in either culture were significantly higher than their respective day 0 basal levels (Figure 5, panel *Mesp1*). The *Mesp1* transcripts were only more highly expressed, as compared to day 0 values, in day 6 differentiating cultures, at which point there was no significant difference between their expressions in either line. Based on this analysis, the mesoderm and precardiac mesoderm stages of cardiomyogenesis during mES cell differentiation did not appear to be significantly regulated by GLI2 overexpression. These results are supported by previous reports, which showed that modulation of HH signalling in mouse P19 EC cells do not significantly regulate mesoderm induction (73, 89, 90).

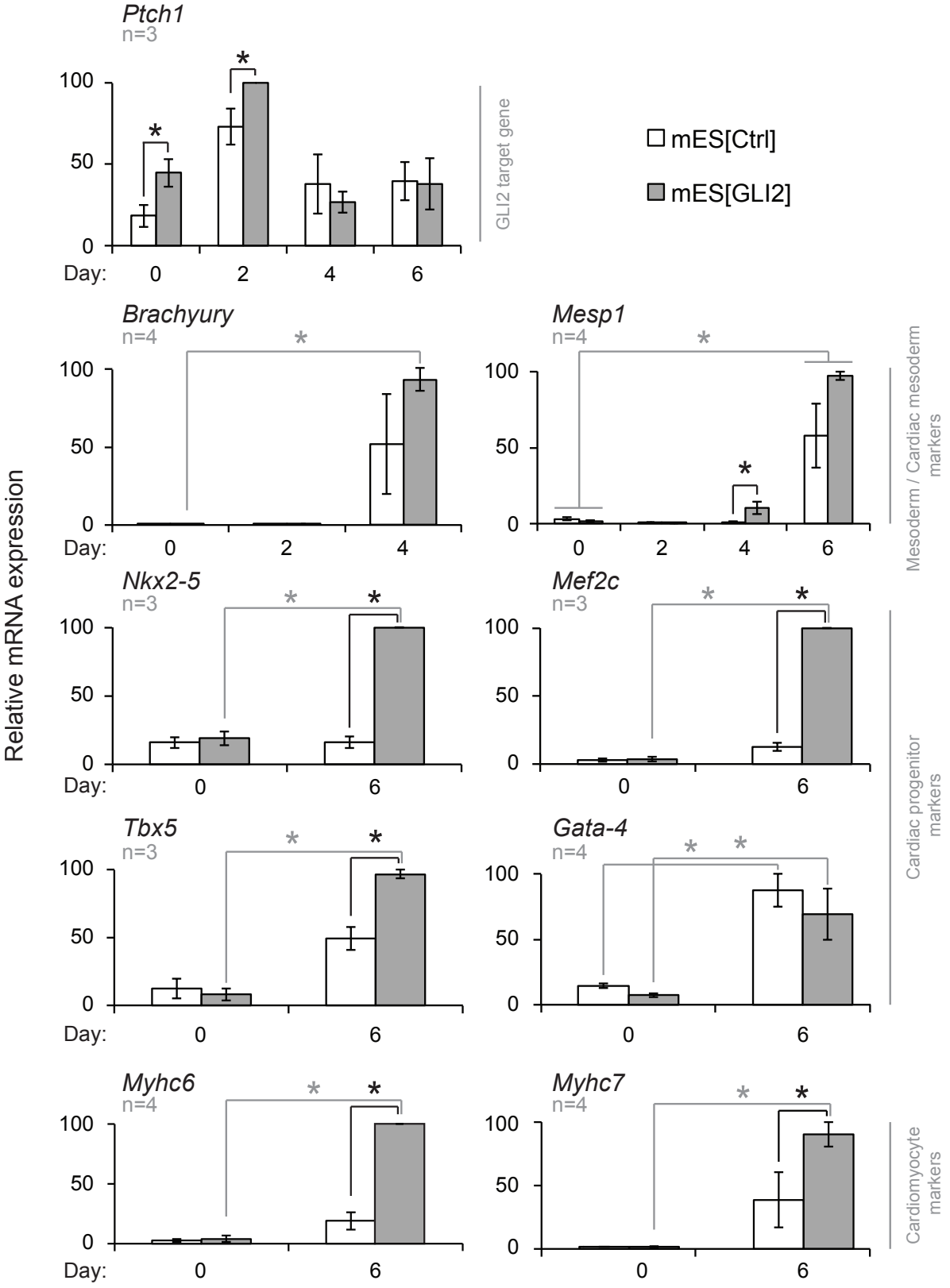
Ptch1
n=3
Brachyury
n=4
Mesp1
n=4
Nkx2-5
n=3
Mef2c
n=3
Tbx5
n=3
Gata-4
n=4
Myhc6
n=4
Myhc7
n=4
Relative mRNA expression
mES[Ctrl]
mES[GLI2]
GLI2 target gene
Mesoderm / Cardiac mesoderm markers
Cardiac progenitor markers
Cardiomyocyte markers
Day:
0
2
4
6
100
50
0

Figure 5. Overexpression of GLI2 enhances transcript expression of a GLI2 target gene and of cardiomyogenesis-specific genes.
RNA isolated from differentiating mES[GLI2] and mES[Ctrl] cultures on the days indicated was analyzed using qPCR for the expression of indicated genes known to be active in HH-responsive cells, mesoderm/cardiac mesoderm cells, cardiac progenitors, and cardiomyocytes. Expression levels were normalized to *β-actin*, calibrated to day 0 mES[Ctrl] culture expression levels, and presented as a percentage of the highest expression level recorded, per gene. Error bars represent +/- SEM. The number of biological replicates analyzed *(*n*)* is indicated on each graph. One-tailed Student's T-tests were used for statistical analyses. Grey lines represent paired T-tests; black lines represent unpaired T-tests; *(*)* $p < 0.05$.

The cardiac progenitor transcripts *Nkx2-5*, *Mef2c*, and *Tbx5* were expressed by day 6 in the mES[GLI2] cultures, when these genes are usually expressed during mES cell differentiation (66, 70, 73), and were also significantly higher than the mES[Ctrl] culture levels (Figure 5; panels *Nkx2-5*, *Mef2c*, and *Tbx5*). Since mES[Ctrl] cultures did not express these transcripts significantly over readings in the undifferentiated cultures, a new set of three independent differentiated samples was analyzed for expression of these factors once again on day 6 and additionally on day 7, to ensure that the mES[Ctrl] cell line could indeed express significant levels of cardiac progenitor genes compared to day 0 basal levels (Figure 6). Previous studies have shown that *Nkx2-5*, *Mef2c*, and other cardiac progenitor genes have yet to meet their maximum expression level by day 6 (66). Therefore, potentially higher *Nkx2-5* and *Mef2c* expression levels on day 7 were expected to provide more consistent readings of *Nkx2-5* and *Mef2c* expression levels in the mES[Ctrl] replicates.

After differentiating a new set of samples we observed that, like in the previous set of differentiated samples, *Nkx2-5* and *Mef2c* transcript levels were higher on day 6 in the mES[GLI2] cell line than the mES[Ctrl] cell line (Figure 6). However, likely due to higher *Nkx2-5* expression in the mES[Ctrl] cell line relative to that in the mES[GLI2] cell line on day 6 of differentiation, the difference in the level of the transcripts between the two lines on day 6 was not significant in these newly differentiated samples (Figure 6, panel *Nkx2-5* n=3). Notably, averaging the day 6 expression levels from all six differentiated samples indicated that, in a larger sample size, *Nkx2-5* transcript levels were significantly higher in the mES[GLI2] cultures than the mES[Ctrl] cultures on day 6 of differentiation (Figure 6, panel *Nkx2-5* n=6). Alternatively, the levels of *Mef2c* transcripts on day 6 in the mES[GLI2] cell line were still significantly higher in the new set of differentiated samples, even with

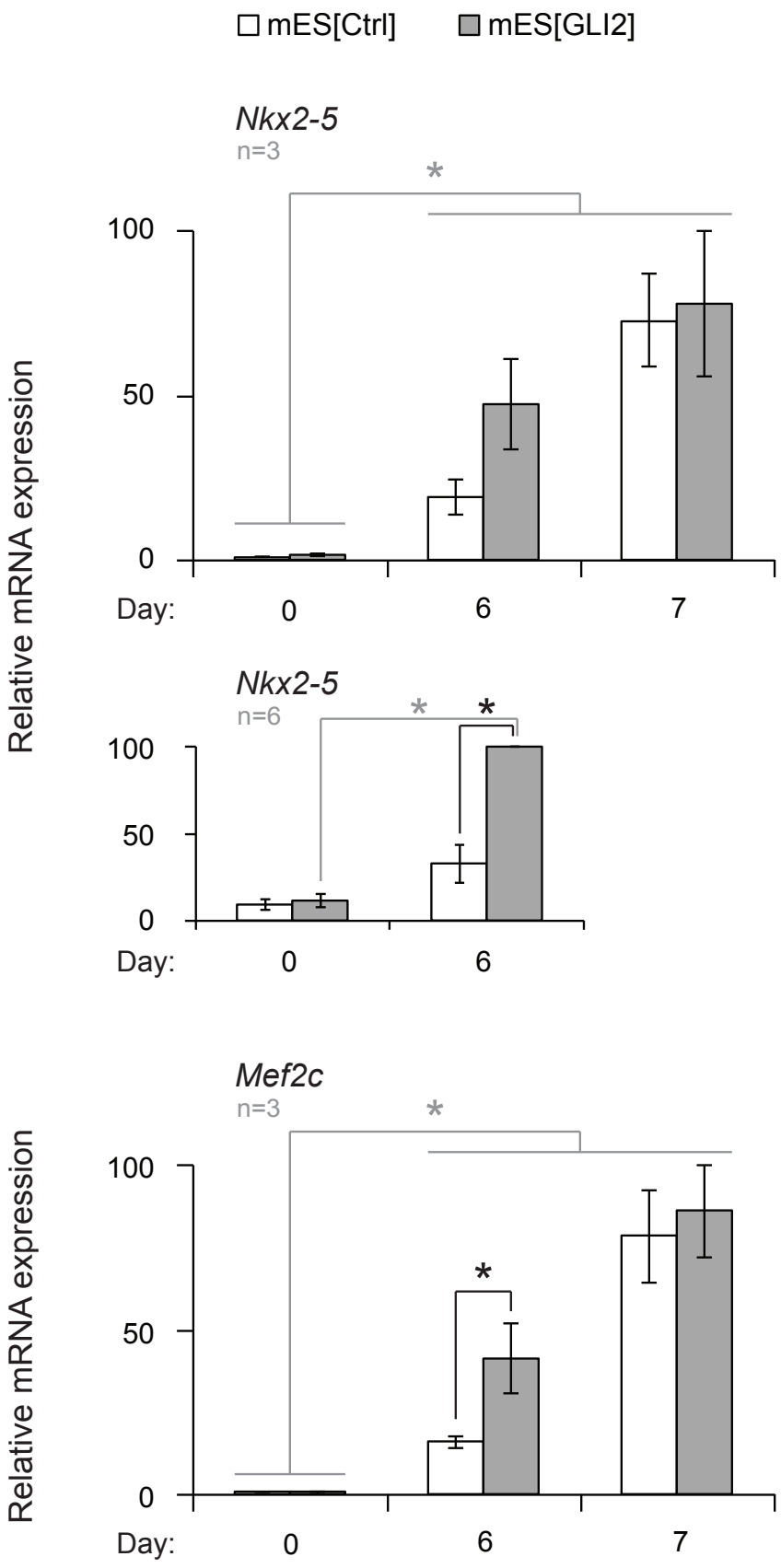
mES[Ctrl]
mES[GLI2]
Nkx2-5
n=3
*
100
50
0
Relative mRNA expression
Day:
0
6
7
Nkx2-5
n=6
*
*
100
50
0
Day:
0
6
Mef2c
n=3
*
100
50
0
Relative mRNA expression
*
Day:
0
6
7

Figure 6. Cardiac progenitor transcript levels in mES[Ctrl] cultures reach the level of those in mES[GLI2] cultures by day 7 of a 7-day differentiation protocol.
RNA was isolated from an additional set of differentiating mES[GLI2] and mES[Ctrl] cultures on the days indicated and analyzed using qPCR for the expression of indicated genes. Expression levels were normalized to *β-actin*, calibrated to day 0 mES[Ctrl] culture expression levels, and presented as a percentage of the highest expression level recorded, per gene. Error bars represent +/- SEM. The number of biological replicates analyzed (n) is indicated on each graph. One-tailed Student's T-tests were used for statistical analyses. Grey lines represent paired T-tests; black lines represent unpaired T-tests; *(*)* $p < 0.05$.

significant levels of *Mef2c* transcripts in the mES[Ctrl] cultures over the undifferentiated basal levels (Figure 6, panel *Mef2c*).

Day 7 *Nkx2-5* and *Mef2c* transcript levels were originally sought during the second set of differentiation experiments in case the respective day 6 mES[Ctrl] culture levels were still not significant over undifferentiated levels. But since the *Nkx2-5* and *Mef2c* transcript levels in the day 6 mES[Ctrl] cultures were in fact significant over the day 0 baseline, a day 7 reading was no longer necessary. Nevertheless, analysis of day 7 *Nkx2-5* and *Mef2c* transcript levels determined that, despite being lower on day 6 in the mES[Ctrl] cell line relative to the mES[GLI2] cell line, these transcript levels in the mES[Ctrl] cell line reached the same level of expression as those in the mES[GLI2] cell line by day 7 (Figure 6). This suggested that rather than continuously enhancing genes that are typical of cardiac progenitor cells, GLI2 overexpression was accelerating the expression levels of at least *Nkx2-5* and *Mef2c*.

Interestingly, overexpression of GLI2 had no visible effect on day 6 *Gata-4* transcript levels, as *Gata*-4 was significantly expressed, compared to day 0, in both lines at comparable levels on this day (Figure 5, panel *Gata-4*).

Like many of the progenitor cell markers, the expression levels of differentiated cardiomyocyte specific genes, *Myhc6* and *Myhc7*, were also higher on day 6 in mES[GLI2] cultures than in mES[Ctrl] cultures, which had only begun to express low levels of *Myhc6* and *Myhc7* transcripts (Figure 5, panels *Myhc6* and *Myhc7*). Since there were limited levels of cardiomyocyte-specific genes expressed in the day 6 mES[Ctrl] cultures, this suggested that GLI2 overexpression had also accelerated the expression of cardiomyocyte contractile protein transcripts.

To determine if the acceleration of cardiac progenitor cell and cardiomyocyte specific transcripts led to an overall enhancement of cardiomyocytes in mES[GLI2] cultures, we counted MyHC^{+ve} cells in day 7 mES[Ctrl] and mES[GLI2] cultures. On average, 8.3±2.6% and 12.4±5.9% of the total cells counted were MyHC^{+ve} in the mES[Ctrl] and mES[GLI2] cultures, respectively (Figure 7B). Similar percentages of approximately 5% mES cell-derived cardiomyocytes have been shown before by analysis of MyHC and Mlc2v on day 7 of differentiation (207) as well as MyHC and tropomyosin on day 8 of differentiation, using the hanging drop method (223). Although there was a trend towards an increase in cardiomyocytes in the mES[GLI2] cultures compared to the control, the variability between the samples across three biological replicates (Figure 7B) and another four additional replicates (data not shown) resulted in no significant difference in the percentage of MyHC^{+ve} cells on day 7.

Since the upregulation of some cardiac progenitor transcripts was only observed on day 6 in the mES[GLI2] cultures compared to the mES[Ctrl] cultures and then non-apparent by day 7, it is possible that a similar temporal acceleration of cells expressing MyHC^{+ve} cells was occurring only on day 6 and not on day 7, when MyHC^{+ve} cells were originally assessed. Immunostaining of MyHC was performed on day 6 to test this hypothesis, however very few cells extended far enough from the EBs on the coverslips to efficiently quantify the MyHC^{+ve} cells. Given these limitations, we could only confirm that GLI2 overexpression resulted in an accelerated cardiac progenitor transcriptional profile and an enhanced cardiomyocyte transcriptional profile with no apparent enrichment of MyHC^{+ve} cardiomyocytes by day 7 of differentiation.

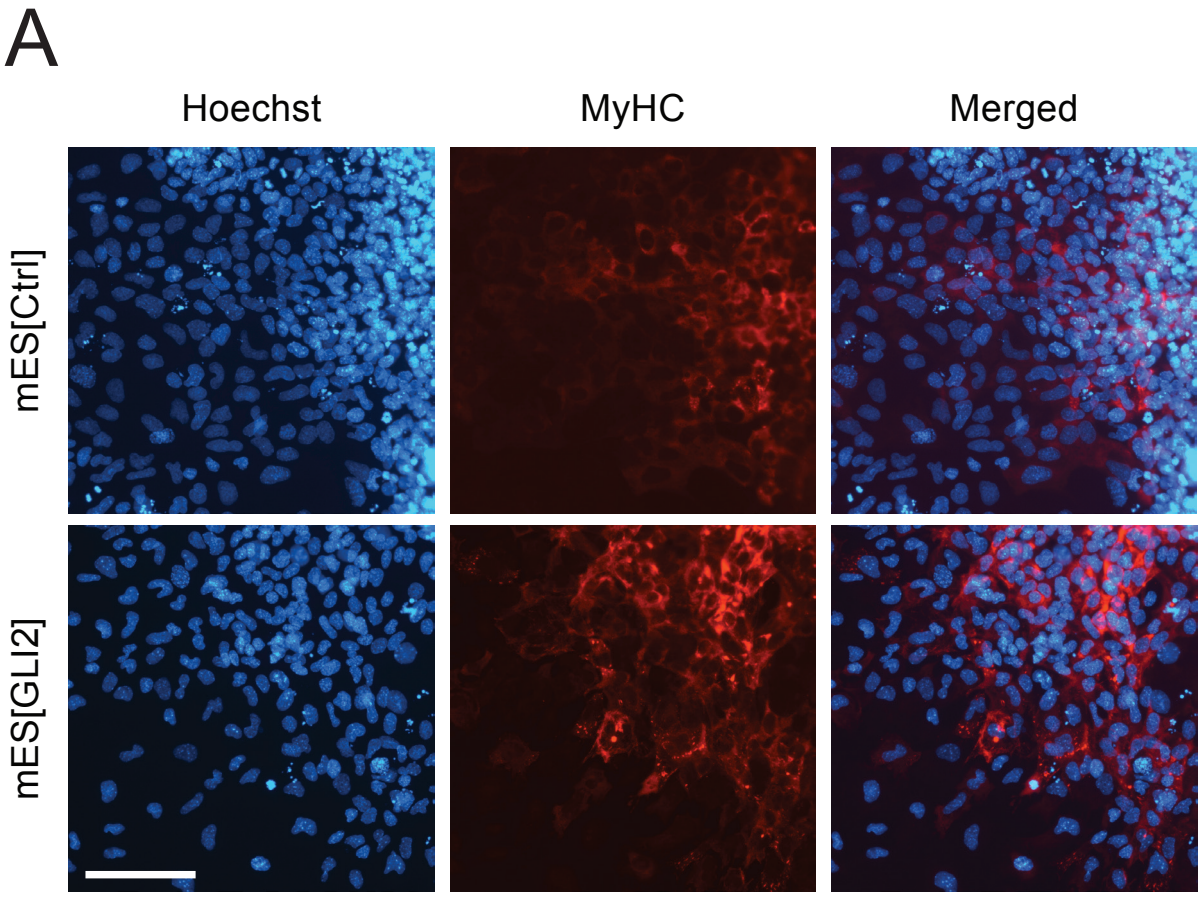
A
Hoechst
MyHC
Merged
mES[Ctrl]
mES[GLI2]

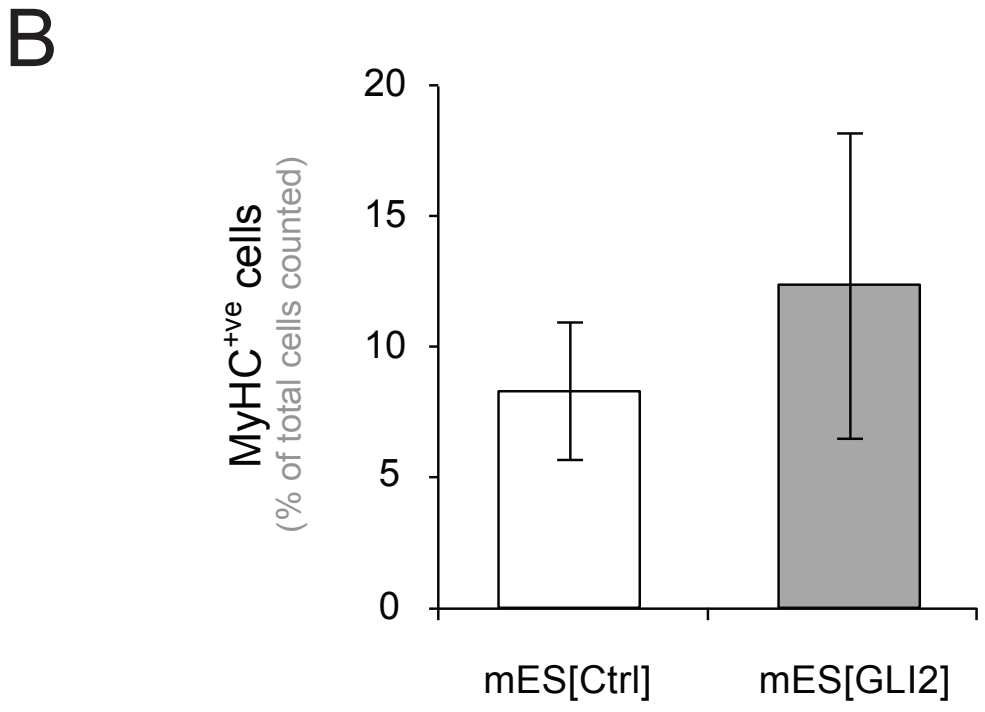
B
MyHC+ve cells
(% of total cells counted)
20
15
10
5
0
mES[Ctrl]
mES[GLI2]

Figure 7. Overexpression of GLI2 resulted in a marginal trend towards an increase in MyHC^{+ve} cells.
(A) MyHC^{+ve} cells *(red)* were visualized and **(B)** counted in corresponding day 7 differentiating cells by indirect immunofluorescence. Hoechst *(blue)* was used to visualize nuclei. Representative images of the cardiomyocyte-enriched areas on the periphery of an EB are shown. Scale bar represents 100 μm. At least 2,500 nuclei were counted across 20 random fields of view, per biological replicate; n=3. One-tailed, unpaired Student's T-tests were used for statistical analyses.

3.3 GLI2 does not significantly regulate skeletal myogenesis but may regulate neurogenesis in mES cells

In the absence of leukemia inhibitory factor (LIF), mES cells spontaneously differentiate into cells from the three germ layers (224). Therefore, considering other lineages are developing alongside cells of the cardiomyocyte lineage (68) and that HH signalling regulates many different lineages throughout development (91, 93-96, 100, 101), it is possible that the GLI2 overexpression in the mES[GLI2] cultures was modulating the expression of other genes expressed in other non-cardiomyogenic cell types. As a result of this, the development of other cell types might have been enhanced within the culture at the expense of enhancing cells in the cardiac lineage. In particular, GLI2 and HH signalling have been shown to regulate skeletal myogenesis and neurogenesis in P19 EC cells (99, 208, 222).

The paired box 3 protein (PAX3) is expressed during early embryogenesis (225) and plays a role in both skeletal myogenesis (226, 227) and neurogenesis (228). WT mES cells have been shown to express *Pax3* transcripts by day 6 of differentiation (229). Since GLI2 regulates cardiac transcript levels on this day and GLI2 can regulate skeletal myogenesis in P19 EC cells, *Pax3* transcripts were also assessed on day 6 (Figure 8, panel *Pax3*). These results showed that early expression of *Pax3* transcripts in mES cells was not significantly affected by GLI2 overexpression, as comparable levels were observed in both the mES[GLI2] and mES[Ctrl] cell lines. In addition, both lines had equivalent levels of $MyHC^{+ve}$ skeletal myocytes by day 15 of differentiation (data not shown), further suggesting that the overexpression of GLI2 did not have a significant effect on skeletal myogenesis in the mES cell system.

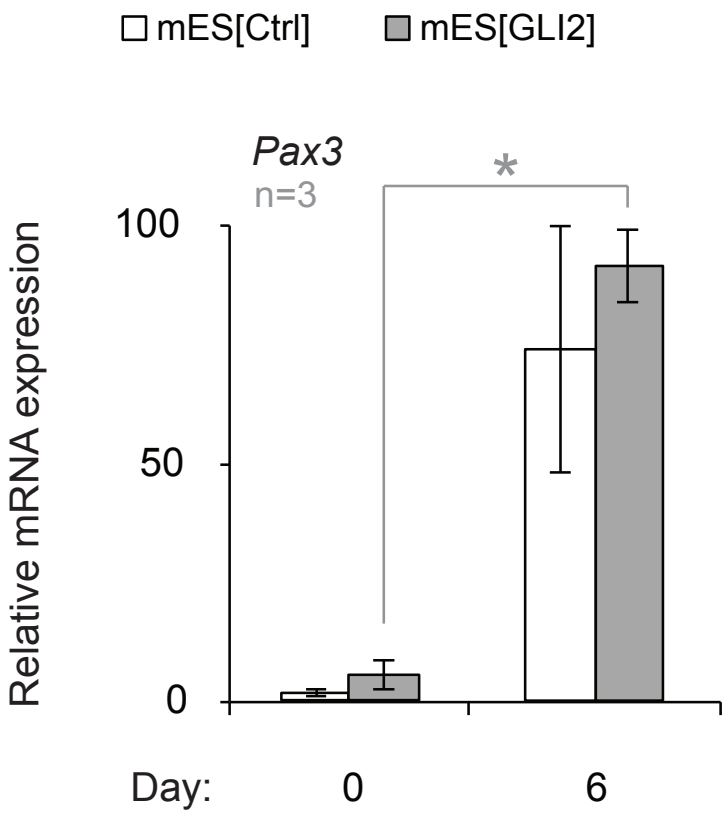
mES[Ctrl]
mES[GLI2]
Pax3
n=3
*
100
50
0
Relative mRNA expression
Day:
0
6

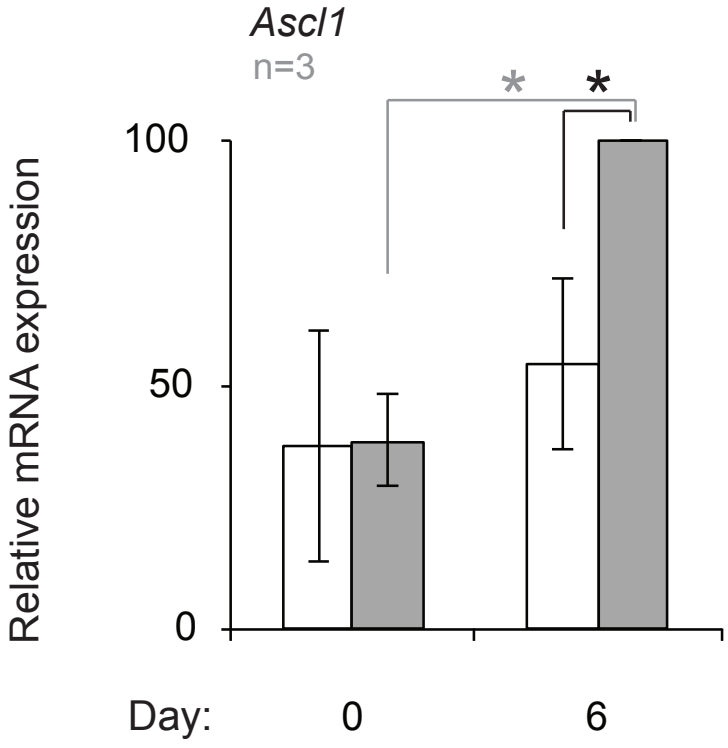
Ascl1
n=3
*
*
100
50
0
Relative mRNA expression
Day:
0
6

Figure 8. GLI2 may regulate early neurogenesis during mES cell differentiation. Total RNA was isolated from differentiating mES[GLI2] and mES[Ctrl] cultures on days indicated and analyzed using qPCR for the expression of the skeletal myogenesis and neurogenesis gene *Pax3* and neurogenesis marker *Ascl1*. Expression levels were normalized to *β-actin*, calibrated to day 0 mES[Ctrl] culture expression levels, and presented as a percentage of the highest expression level recorded, per gene. Error bars represent +/- SEM; n=3. One-tailed Student's T-tests were used for statistical analyses. Grey lines represent paired T-tests; black lines represent unpaired T-tests; *(*)* $p < 0.05$.

Previous studies have shown that achaete-scute homolog 1 (ASCL1), a basic helix-loop-helix (bHLH) transcription factor also known as MASH-1, is a major component of successful neural progenitor differentiation, both *in vitro* and *in vivo* (230-233). Studies have also determined that the *Ascl1* gene is a downstream target of HH signalling in adult neural progenitor cells (234) and a direct target of GLI2 during early neurogenesis in P19 EC cells (222).

Ascl1 transcripts in the mES[GLI2] cell line were expressed by day 6 (Figure 8, panel *Ascl1*). Meanwhile, no *Ascl1* expression was apparent in the mES[Ctrl] cell line over basal day 0 levels. The two fold increase of *Ascl1* transcripts over basal levels in the mES[GLI2] cells did not amount to an increase in neurons during the first ten days of differentiation as there were no 68kDa neurofilament (NF68/NFL)-positive cells in either culture on day 7 or day 10 (data not shown). Therefore, GLI2 may regulate *Ascl1* in mES cells, but this preliminary data suggests that there are no obvious downstream effects on neurogenesis in the first ten days of mES cell differentiation.

3.4 GLI2 interacts with BRG1 and shares a subset of target genes

Given that GLI2 overexpression regulated several cardiac progenitor transcription factors and cardiac muscle structural proteins, we sought to elucidate the mechanisms behind this enhancement. To identify potential GLI2-interacting proteins, we performed a FLAG-IP on day 3 mES[GLI2] and mES[Ctrl] cell nuclear extracts. Mass spectrometric analysis of the FLAG-IP eluates identified peptides from RNA processing proteins and filament-related proteins that were immunoprecipitated more from the mES[GLI2] nuclear extracts than the mES[Ctrl] extracts (Figure 9A).

A

Identified Proteins	Swiss-Prot Accession	Score mES[GLI2]	Score mES[Ctrl]
Myosin-10	MYH10_MOUSE	1741	3869
Myosin-9	MYH9_MOUSE	1437	4814
Probable helicase senataxin	SETX_MOUSE	**1624**	1222
Pre-mRNA-processing-splicing factor 8	PRP8_MOUSE	**1333**	823
U5 small nuclear ribonucleoprotein 200 kDa helicase	U520_MOUSE	**1009**	822
Transcription activator BRG1	SMCA4_MOUSE	**259**	138
Small subunit processome component 20 homolog	UTP20_MOUSE	**214**	56
Filamin-A	FLNA_MOUSE	**159**	131
Unconventional myosin-Va	MYO5A_MOUSE	144	208

B

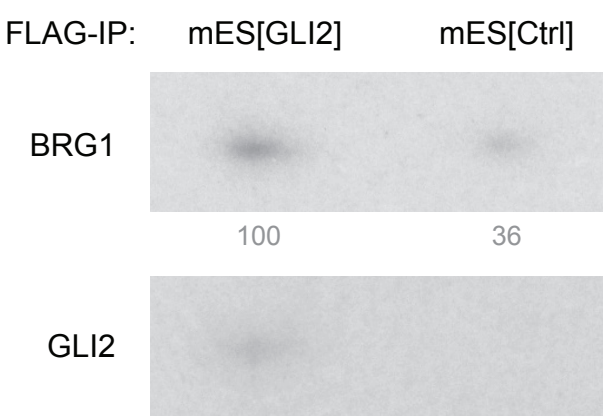

C

Category	Targets	P-value	Identified Genes
Chordate embryonic development	12	2.32E-09	*Dlc1, Smo, Hif1a, Pkd2, Hopx, Smad3, Smad2 Ttn, Tpm1, Ncor2, Myhc10, Cited2*
Embryonic development	12	2.56E-09	*Dlc1, Smo, Hif1a, Pkd2, Hopx, Smad3, Smad2 Ttn, Tpm1, Ncor2, Myhc10, Cited2*
In utero embryonic development	10	9.75E-09	*Hif1a, Pkd2, Hopx, Smad3, Smad2, Ttn, Tpm1 Ncor2, Myhc10, Cited2*
Pattern specification process	9	2.91E-07	*Foxh1, Smo, Tbx20, Pkd2, Smad3, Smad2, Ttn Rbm15, Cited2*
Cardiac muscle tissue development	6	2.36E-07	*Tbx2, Rara, Cxadr, Ttn, Tpm1, Myhc10*
Striated muscle tissue development	6	1.27E-05	*Tbx2, Rara, Cxadr, Ttn, Tpm1, Myhc10*
Muscle tissue development	6	1.77E-05	*Tbx2, Rara, Cxadr, Ttn, Tpm1, Myhc10*
Muscle organ development	6	6.09E-05	*Tbx2, Rara, Cxadr, Ttn, Tpm1, Myhc10*
Muscle cell differentiation	5	1.76E-04	*Tbx2, Rara, Cxadr, Ttn, Myhc10*
Embryonic organ development	5	2.64E-03	*Hif1a, Pkd2, Smad3, Smad2, Cited2*
Striated muscle cell differentiation	4	1.29E-03	*Rara, Cxadr, Ttn, Myhc10*
Positive reg of cell differentiation	4	8.63E-03	*Smo, Hif1a, Hopx, Smad2*
Positive reg of dev process	4	1.48E-02	*Smo, Hif1a, Hopx, Smad2*
Skeletal system development	4	3.13E-02	*Smo, Hif1a, Smad3, Smad2*
Cardiac muscle cell differentiation	3	2.08E-03	*Rara, Ttn, Myhc10*
Cardiac cell differentiation	3	2.88E-03	*Rara, Ttn, Myhc10*
Striated muscle cell development	3	7.56E-03	*Cxadr, Ttn, Myhc10*
Muscle cell development	3	9.57E-03	*Cxadr, Ttn, Myhc10*
Developmental growth	3	2.44E-02	*Smo, Smad3, Smad2*

Figure 9. BRG1 immunoprecipitates with GLI2 in day 3 differentiating mES[GLI2] cells.
(A) Mascot scores of proteins (corresponding to range 170-250 kDa) submitted to mass spectrometric analysis, following immunoprecipitation by FLAG-IP from day 3 mES[GLI2] or mES[Ctrl] nuclear extracts. Only proteins with mascot scores >100 are shown. Proteins that have higher mascot scores in the mES[GLI2] sample than the mES[Ctrl] sample are highlighted in grey and have bolded scores. **(B)** An immunoblot analysis probed with either anti-BRG1 or anti-GLI2 antibodies performed on 10% of the FLAG-IP eluates from *(A)*. Results from a BRG1-band densitometry analysis are shown as a percentage of the highest expression. **(C)** Selected gene ontology biological processes significantly enriched among genes containing BRG1-associating sites (217) and GLI consensus binding motifs in the UTR, promoter, intron, or coding sequence regions. A total of 38 potential gene targets were analyzed.

Interestingly, BRG1, an active member of the BAF chromatin remodelling complex was also identified and had a higher mascot score in the mES[GLI2] sample (Figure 9A). Sequential western blot analysis of the remaining FLAG-IP samples with anti-BRG1 and anti-GLI2 antibodies confirmed co-immunoprecipitation of BRG1 with FLAG-GLI2^{S662A} in mES[GLI2] cells as the BRG1 band in the mES[GLI2] sample was 2.8-fold over the background band in the mES[Ctrl] sample, based on densitometry analysis (Figure 9B). Like in the mass spectrometric analysis, there was similar background detected in the mES[Ctrl] sample when analyzed by western blot. Despite the background in these experiments, BRG1's ability to precipitate with GLI2 is supported by experiments in NIH 3T3 cells, where BRG1 was found to interact with HA-tagged GLI2 protein (206).

The observed co-immunoprecipitation of GLI2 and BRG1 during mES cell differentiation led to our hypothesis that GLI2 could recruit BRG1 to regulatory regions of genes to modulate their expression. This hypothesis was supported by a gene ontology (GO) analysis of genes that immunoprecipitated with BRG1 in undifferentiated mES cells (217) and had conserved GLI consensus binding motifs. In total, 38 BRG1-associated, cardiac-related gene targets that contained GLI consensus binding motifs in the UTR, promoter, intron, or coding sequence regions were identified (Figure 9C). The genes identified were significantly related to embryonic development, pattern specification, and skeletal and cardiac muscle tissue development GO biological processes.

Although this analysis included only genes that associated with BRG1 in undifferentiated mES cells (217), given the results and the known roles of BRG1 and GLI2 in heart development (85, 86, 200), we were interested in knowing if GLI2 and BRG1 could co-regulate genes of some key transcription factors implicated in cardiomyogenesis. *Mef2c*

was recently identified as a direct target of GLI2 during P19 EC cardiomyogenesis (73). In particular, MEF2 factors are critical during heart development *in vivo* and *in vitro* (37, 38, 82). The results in Figure 5 and Figure 6, which show an acceleration of *Mef2c* transcripts in differentiating mES[GLI2] cells, further support these results. Thus, we set out to determine if BRG1 associates with *Mef2c* regulatory elements in a HH dependent manner.

3.5 GLI2 overexpression results in enriched BRG1 association on *Mef2c* regulatory elements

First, we sought to determine if GLI2 regulates *Brg1* expression by analyzing *Brg1* transcripts in both the mES[GLI2] and the mES[Ctrl] cells. *Brg1* mRNA expression increased slightly upon differentiation in both mES[Ctrl] and mES[GLI2] cell lines (Figure 10A). However, it reached statistical significance ($p<0.05$) only on day 4 of mES[GLI2] cell differentiation (Figure 10A). Notably, on day 6 of mES[GLI2] cell differentiation, *Brg1* transcript levels were lower than in mES[Ctrl] differentiating cells.

Considering mES cells spontaneously differentiate into lineages of all three germ layers (224) and BRG1 is expressed in many different mammalian cell types (193), it is difficult to make definitive conclusions about its pattern of expression during mES cell cardiomyogenesis and its regulation by GLI2 during mES cell differentiation. For these reasons, we analyzed the expression of *Brg1* transcripts in P19 EC cells, which differentiate into a culture of predominantly endodermal- and mesodermal-derived cells upon aggregation and treatment with DMSO (74, 76) and express cardiomyocytes by day 6 of differentiation (235). Moreover, other studies have also shown that P19 EC cells express stable levels of BRG1 protein during aggregated differentiation (236).

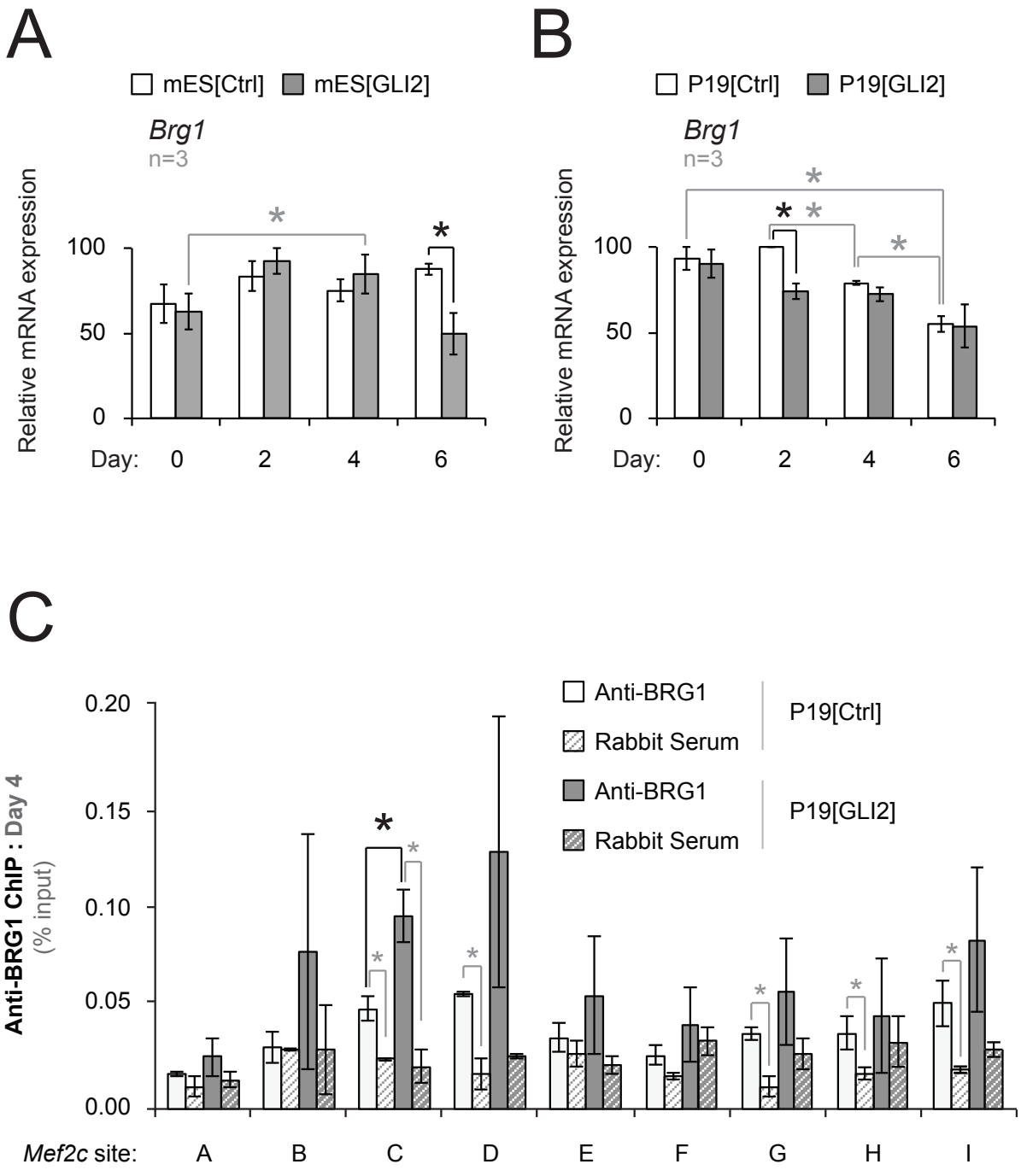
A
mES[Ctrl]
mES[GLI2]
Brg1
n=3
Relative mRNA expression
100
50
0
Day: 0 2 4 6
B
P19[Ctrl]
P19[GLI2]
Brg1
n=3
Relative mRNA expression
100
50
0
Day: 0 2 4 6
C
Anti-BRG1 ChIP : Day 4
(% input)
0.20
0.15
0.10
0.05
0.00
Anti-BRG1
Rabbit Serum
Anti-BRG1
Rabbit Serum
P19[Ctrl]
P19[GLI2]
Mef2c site: A B C D E F G H I

Figure 10. GLI2 recruits the chromatin remodelling protein, BRG1, to a GLI2 binding site in the *Mef2c* gene.
Brg1 mRNA expression levels were analyzed in **(A)** mES[GLI2] and mES[Ctrl], and **(B)** P19[GLI2] and P19[Ctrl] cultures. Expression levels were normalized to *β-actin*, calibrated to day 0 mES[Ctrl] or P19[Ctrl] culture expression levels, and presented as a percentage of the highest expression level recorded, per gene; n=3. Two-tailed Student's T-tests were used for statistical analyses. Grey lines represent paired T-tests; black lines represent unpaired T-tests; *(*)* $p < 0.05$. **(C)** An anti-BRG1 ChIP was performed on day 4 differentiating P19[GLI2] and P19[Ctrl] cultures with subsequent qPCR analyses of all nine GLI consensus binding motifs in *Mef2c (Mef2c* sites *A-I),* depicted in Figure 3; n=3. All error bars represent +/- SEM. One-tailed Student's T-tests were used for statistical analyses. *(*)* $p < 0.05$.

By day 6 of P19 EC cell DMSO-induced differentiation, ~10% of our cultures had a cardiomyocyte phenotype and the remaining cells had a fibroblast-like morphology (data not shown), as seen in previous studies (73, 78, 235). During P19 EC cell differentiation, *Brg1* transcript expression decreased slightly after day 2 of differentiation in the P19[Ctrl] cell line (Figure 10B). In the P19[GLI2] cell line, the expression of *Brg1* grossly followed the same pattern, however, there was a significant decrease in *Brg1* transcripts on day 2 in P19[GLI2] cells, as compared to levels in P19[Ctrl] cells. Importantly, there was no significant change in *Brg1* expression on day 4 in P19[GLI2] versus P19[Ctrl] cultures (Figure 10B).

Our lab has previously shown that GLI2 binds eight of the nine conserved GLI consensus binding motifs found in *Mef2c* gene on day 4 of P19[GLI2] cell differentiation *(Mef2c* sites *B-I)* (73). Given that BRG1 immunoprecipitates with GLI2, we performed an anti-BRG1 ChIP on day 4 of P19[Ctrl] and P19[GLI2] cell differentiation, to determine if BRG1 associates with *Mef2c* genomic elements during differentiation, and also if GLI2 can modulate the potential association.

Results from the BRG1-ChIP showed an association of BRG1 with *Mef2c* sites *C, D,* and *G-I* in P19[Ctrl] cells as compared to non-specific rabbit serum values (Figure 10C). Notably, although there was a similar trend in the P19[GLI2] cells, we did not observe statistical significance for sites *D* and *G-I* when compared to their respective non-specific rabbit serum values (Figure 10C). *Mef2c* site *A*, which lacked GLI2 association under the same experimental conditions (73), showed no significant signs of being bound by BRG1 in either cell line. However, the association of BRG1 with the *Mef2c* site *C* was significantly ($p<0.05$) higher in P19[GLI2] cells as compared to P19[Ctrl] cells. *Mef2c* site *C* is of significant interest as it is located proximally to the ISL-1-dependent SHF enhancer region

and upstream of a known transcription start site in the developing heart (Figure 3) (44, 180). Thus, we chose *Mef2c* site *C* to further investigate if BRG1 association is dependent on HH signalling during P19 EC cell cardiomyogenesis.

3.6 Inhibition of HH signalling results in reduced BRG1 association on *Mef2c* site *C*

Following these results from gain-of-function experiments, we proceeded to investigate the GLI2 and BRG1 relationship on *Mef2c* gene through loss-of-function experiments. For this, the HH signalling inhibitor, KAAD-cyclopamine, was used to repress the activity of downstream HH signalling transducers, such as GLI2. Our lab has previously used KAAD-cyclopamine to successfully inhibit HH signalling in a variety of cells, such as P19 EC cells, C3H10T1/2 fibroblasts, and adult skeletal muscle satellite cells (90, 99). *Gli1*, a direct target of GLI2 (155), was used as an indicator of HH inhibition, like in previous reports (99).

KAAD-cyclopamine treatment resulted in a 71.7±17.0% and 60.5±25.0% decrease in *Gli1* expression on days 4 and 6 of P19 EC cell differentiation, respectively, compared to treatment with a vehicle control (Figure 11A). Similar cyclopamine-mediated reductions of *Gli1* expression have been seen before in P19 EC cells (90), P19CL6 EC cells (81), mES cells (237), freshly isolated mouse satellite cells cultured *in vitro* (99), mouse embryonic fibroblasts (99, 206), zebrafish (238), and *Xenopus* retina (91).

By day 6, differentiating P19 EC cells treated with KAAD-cyclopamine expressed 45.9±16.7%, 74.8±12.2%, and 65.4±5.9% significantly lower *Mef2c, Gata-4,* and *Tbx5* transcript levels, respectively, compared to differentiating cells treated with the vehicle

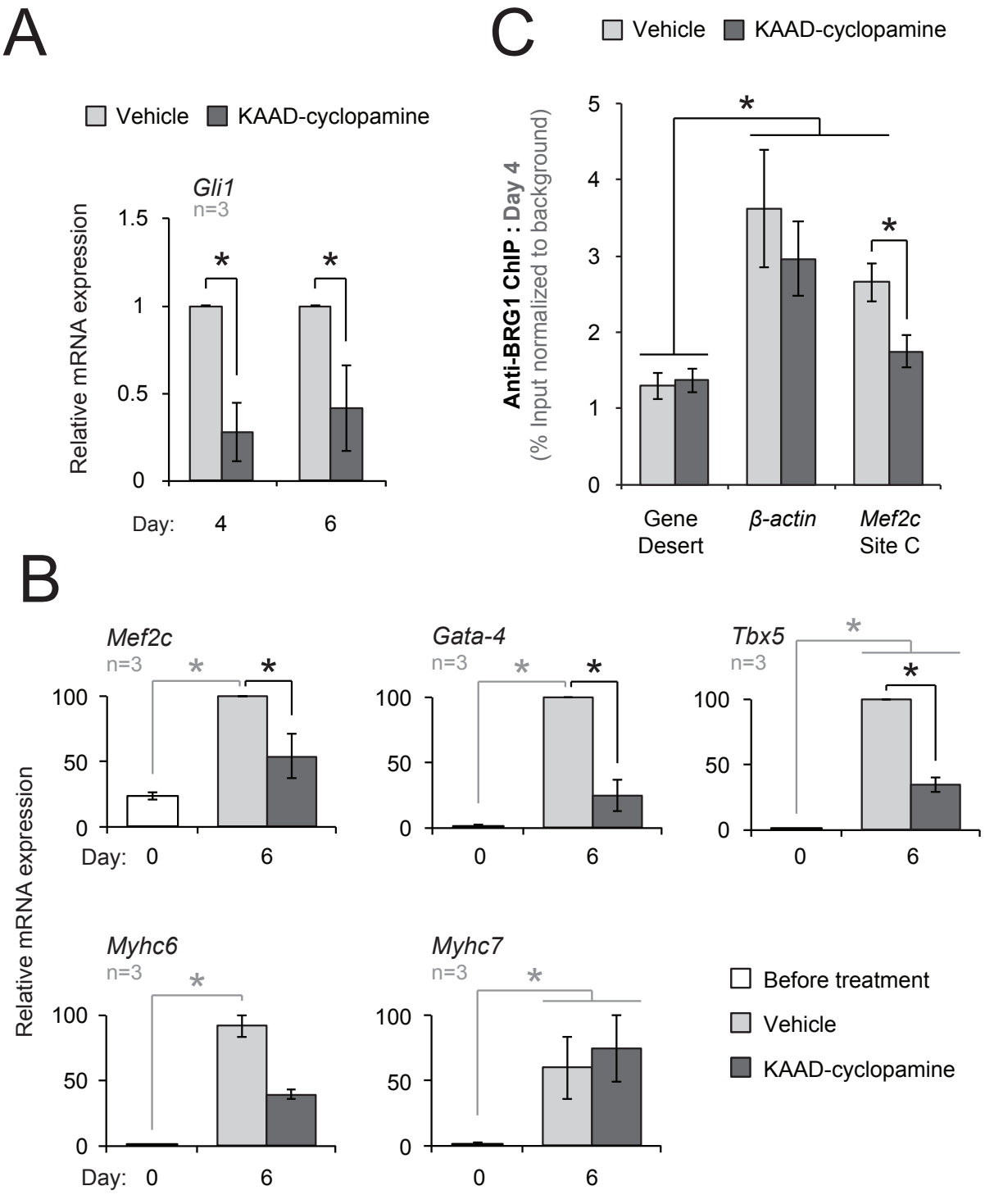
A
Vehicle
KAAD-cyclopamine
Gli1
n=3
Relative mRNA expression
1.5
1
0.5
0
*
*
Day: 4 6
C
Vehicle
KAAD-cyclopamine
Anti-BRG1 ChIP : Day 4
(% Input normalized to background)
5
4
3
2
1
0
*
*
Gene Desert
β-actin
Mef2c Site C
B
Mef2c
n=3
Gata-4
n=3
Tbx5
n=3
Myhc6
n=3
Myhc7
n=3
Relative mRNA expression
100
50
0
Day: 0 6
Before treatment
Vehicle
KAAD-cyclopamine

Figure 11. HH signalling contributes to the recruitment of BRG1 to *Mef2c*.
(A) A decrease in HH target gene expression, *Gli1*, was assessed by qPCR in differentiating P19 EC cultures, treated with MeOH vehicle or KAAD-cyclopamine. *Gli1* mRNA expression levels were normalized to *β-actin* and presented as a fold-change over MeOH-treated culture expression levels from the same day; n=3. **(B)** The effect of KAAD-cyclopamine treatment on the expression level of cardiomyogenesis-specific genes was assessed using qPCR analysis. Expression levels were normalized to *β-actin*, calibrated to day 0 untreated culture expression levels, and presented as a percentage of the highest expression level recorded, per gene; n=3. **(C)** An anti-BRG1 ChIP was performed on day 4 differentiating P19 EC cultures that were treated with either MeOH vehicle or KAAD-cyclopamine, n=3. Each ChIP was followed by qPCR analyses on a gene desert region *(negative control)*, *β-actin (positive control)*, and *Mef2C* site *C*. All error bars represent +/- SEM. Two-tailed Student's T-tests were used for statistical analyses. Grey lines represent paired T-tests; black lines represent unpaired T-tests; *(*)* $p < 0.05$.

(Figure 11B; panels *Mef2c*, *Gata-4*, and *Tbx5*). These lower levels of cardiac progenitor cell-specific transcripts were expected as P19 EC cells treated with cyclopamine show repressed *Gata-4* expression (90) and P19CL6 EC cells treated with cyclopamine show lower levels of *Gata-4* and *Nkx2-5* (81). Importantly, our data indicated that neither the level of contractile protein transcripts in the day 6 EBs (Figure 11B, panels *Myhc6* and *Myhc7*) nor the number of $MyHC^{+ve}$ cardiomyocytes (data not shown) significantly differed between KAAD-cyclopamine and vehicle treatments. This is supported by previous reports, where P19 EC cells treated with cyclopamine during differentiation did not show any difference in the number of $MyHC^{+ve}$ cardiomyocytes either (90). Thus, inhibition of HH signalling downregulated, but did not abolish, normal expression of cardiac progenitor specific transcripts and, overall, did not repress the formation of cardiomyocytes.

To test if inhibition of HH signalling attenuated the ability of BRG1 to associate with *Mef2c* site *C*, we performed a BRG1-ChIP in day 4 differentiating P19 EC cells treated with vehicle or KAAD-cyclopamine. The results indicated an association of BRG1 with *β-actin,* a known BRG1 target in mES cells (217) *(positive control)* when compared to a gene desert region located on chromosome 15, which is at least 560 kb from any known open reading frame *(negative control)* (Figure 11C). This demonstrated the specificity of the BRG1-ChIP assay. BRG1 also associated with *Mef2c* site *C* (Figure 11C), in accordance with Figure 10C.

KAAD-cyclopamine treatment had no significant effect on BRG1's association with the gene desert or *β-actin*. However, inhibition of HH signalling with KAAD-cyclopamine significantly ($p<0.05$) reduced the enrichment of BRG1 on *Mef2c* site *C*. Therefore, HH signalling is required, at least to some extent, for the efficient expression of *Mef2c* mRNA and the efficient association of BRG1 to the *Mef2c* gene.

4 Discussion

4.1 HH signalling regulates acceleration of cardiac progenitor genes during mES cell differentiation

Using a stabilized GLI2 mutant, we observed that GLI2 regulates early expression of cardiac progenitor transcripts (Figure 5). Overall, the effects of GLI2 overexpression resulted in an acceleration of cardiomyogenesis during the cardiac progenitor stage (Figure 6). This effect is not believed to be due to an increase in mesoderm formation because GLI2 overexpression did not have any significant effect on the levels of *Brachyury* or *Mesp1* compared to the levels in the control cultures on days that had significant expression over basal day 0 levels (Figure 5). Previous studies have observed similar results when HH signalling is modulated in P19 EC cells (73, 89, 90).

When GLI2 is overexpressed, *Mef2c*, *Nkx2-5*, and *Tbx5* are significantly enhanced on day 6 of differentiation in mES cells (Figure 5), similar to how GLI2 overexpression affects cardiac progenitor cell enriched genes in P19[GLI2] cultures (73). *Mef2c* and *Nkx2-5* both had accelerated expression in mES[GLI2] cultures on day 6 of differentiation relative to control cultures (Figure 6). This accelerated expression *in vitro* correlates with the HH-mediated expression of *Nkx2-5 in vivo* (4). In *Ptch1*$^{-/-}$ embryos, HH independent activation of the HH signalling pathway is present and results in enhanced *Nkx2-5* expression in the cardiac crescent. Alternatively, *Smo*$^{-/-}$ and *Shh*$^{-/-}$/*Ihh*$^{-/-}$ embryos have reduced *Nkx2-5* expression in the cardiac crescent at the 2-3 somite stage (~E7.5) and delayed heart tube formation (87), which normally occurs around E8.0 (4). In the *Smo*$^{-/-}$ embryos, the reduced *Nkx2-5* expression is only temporary as *Nkx2-5* expression returns to normal levels found in WT embryos by E9.0. These loss-of-function observations in the embryo are consistent with

our gain-of-function experiments in mES[GLI2] cells and further suggest that HH signalling regulates *Nkx2-5* expression during early cardiomyogenesis through a mechanism that is independent from the mechanism that regulates *Nkx2-5,* post-heart looping (87). Therefore, the acceleration of the cardiac progenitor transcripts in mES cells is in line with what is seen *in vivo* during heart development.

In mES[GLI2] cultures, *Tbx5* expression levels were upregulated compared to the control cultures on day 6 of differentiation (Figure 5). This follows the same general expression pattern seen in the P19[GLI2] cell model on day 6 of differentiation as well (73). When HH signalling is inhibited in P19 EC cells by KAAD-cyclopamine, day 6 expression levels of *Tbx5* are reduced compared to vehicle-treated cells (Figure 11). Furthermore, expression of a GLI/EnR fusion repressor protein during P19 EC cell differentiation reduces day 6 expression of *Tbx5* (73). Therefore, given these observations, *Tbx5* expression is regulated by HH signalling *in vitro,* during P19 EC and mES cell differentiation.

The expression of *Tbx5* in the heart has been studied throughout cardiogenesis because mutations in *Tbx5* lead to Holt-Oram syndrome (239, 240). *Tbx5* is more commonly expressed in the FHF (4) and has not been studied extensively in the SHF (175). A recent study has shown that *Tbx5* expression in the SHF, but not expression in the myocardium or the endocardium, is essential for atrial septation and mediates this process through a regulatory network with HH signalling (175). However, in this molecular network, TBX5 functions upstream and parallel to HH signalling *in vivo*. HH signalling upstream of *Tbx5* expression is less understood. Therefore, although HH signalling has been shown to regulate *Tbx5* expression in the current study, further investigation is required to elucidate the mechanisms behind its observed HH-mediated regulation.

4.2 GLI2-mediated acceleration of cardiac progenitor gene expression does not enhance the number of cardiomyocytes during mES cell cardiomyogenesis

Although GLI2 enhances many cardiac progenitor and *Myhc* gene expression levels at the onset of cardiomyogenesis (Figure 5), the system does not result in an increased percentage of cardiomyocytes by day 7 of mES cell differentiation (Figure 7). There is possibly a higher percentage of cardiomyocytes in the mES[GLI2] cultures on day 6 of mES cell differentiation when the cardiac progenitor genes are enhanced, but as mentioned before, it is difficult to quantitatively assess the number of cardiomyocytes in day 6 EBs. To circumvent this issue EBs could theoretically be dissociated into single cells and either analyzed by IF or by flow cytometry.

If there happen to be more cardiomyocytes in day 6 differentiating mES cells, this could suggest that HH signalling accelerates cardiomyocyte differentiation similar to how it accelerates the expression of cardiac progenitor genes (Figure 6). However, proper quantitative analysis would have to be performed on day 6 and day 7 differentiating mES[GLI2] and mES[Ctrl] cells to effectively confirm this. Given that *Myhc6* and *Myhc7* transcript levels are enhanced in day 6 differentiating mES[GLI2] cells compared to control cells (Figure 5), it is plausible that the number of cardiomyocytes may also be enhanced on day 6 of differentiation. By day 7 of differentiation, *Myhc6* and *Myhc7* gene expression in mES[Ctrl] cultures may also catch up to the level of expression in mES[GLI2] cultures given the trend that *Nkx2-5* and *Mef2c* show on these days (Figure 6). If the *Myhc6* and *Myhc7* gene expressions were to do this, it would align with the observation that there is no significant difference in the percentage of $MyHC^{+ve}$ cells on day 7 in the mES[GLI2] and

mES[Ctrl] cultures (Figure 7). In summary, quantification of cardiomyocytes in day 6 differentiating mES[GLI2] and mES[Ctrl] cultures and an analysis of transcriptional *Myhc* isoforms in day 7 differentiating mES[GLI2] and mES[Ctrl] cells are further required for assessing if GLI2 overexpression also results in the acceleration of cardiomyocyte formation and *Myhc* isoform expression, respectively.

Alternatively, overexpression of GLI2 may accelerate the absolute number of cardiomyocytes but not increase the actual percentage of cardiomyocytes in mES[GLI2] cells compared to control cells. HH signalling gain-of-function experiments in P19 EC cells, both induced cardiomyogenesis (89) and enhanced it (73). However, these cells may be more susceptible to differentiate into cardiomyocytes because they are more prone to differentiate into cells of the mesodermal lineage (74). mES cells, though, can give rise to cell types from each of the endoderm, mesoderm, and ectoderm germ layers that develop in parallel during mES cell differentiation (224, 241, 242). Therefore, mES cells may not have as many mesoderm cells that are susceptible to HH-mediated regulation. Since HH signalling regulates many other lineages from the endoderm and ectoderm during early development (91-95), GLI2 overexpression in mES cells may increase the number of cells from other lineages while increasing the number of cardiomyocytes, leading to similar percentages of cardiomyocytes in the mES[GLI2] and mES[Ctrl] cultures. Even if HH signalling does not enhance the number of non-cardiomyocytes, HH signalling may still enhance mechanisms in the neighbouring lineages that in turn negatively regulate cardiomyocyte differentiation and keep the percentage of cardiomyocytes in the culture at levels comparable to those in the control cultures.

HH signalling may also upregulate the level of *Nkx2-5*, *Mef2c*, and *Tbx5* transcripts per cardiac progenitor, rather than increase the cardiac progenitor pool by activating *Nkx2-5*, *Mef2c*, and *Tbx5* in precardiac mesoderm cells (243). This increase per cell, could then also lead to an increase in *Myhc6* and *Myhc7* transcript levels per cell, which could explain the enhanced transcript levels of *Myhc6* and *Myhc7* in the mES[GLI2] cultures compared to the control cultures on day 6 of differentiation (Figure 5). In this model, the number of cardiac progenitors that become cardiomyocytes would still remain the same but there would be potentially more MyHC per cell.

Still, although possible, this model seems less probable because it does not align with the observation that ectopic expression of SHH or GLI2 can induce *Nkx2-5* and *Mef2c* expression by day 6 of P19 EC cell differentiation (89). Also, HH signalling not only regulates the level of *Nkx2-5* expression in zebrafish, but it also increases the number of cardiomyocytes (176). Therefore, HH likely regulates the number of cells that once expressed these transcripts rather than the amount of transcripts per cell. If a suitable method for dissociating day 6 mES cell EBs can be realized, NKX2-5 positive cells could be quantified by indirect immunofluorescence or flow cytometry to see if this is the case.

Since HH signalling regulates both the expression of *Nkx2-5* and the number of cardiomyocytes in zebrafish (176), HH signalling may enhance the number of cardiac progenitors that express *Nkx2-5* in the mES[GLI2] cultures compared to the control, rather than the number of MyHC^{+ve} cardiomyocytes. In zebrafish and P19 EC cells, a larger pool of cardiac progenitor cells appears to lead directly to an increase in cardiomyocytes (89, 176).

An essential factor that enables this direct transition may be lacking during mES cell cardiomyogenesis. The pool of progenitor cells that are poised to become MyHC^{+ve} cardiomyocytes may accelerate on day 6 in the mES[GLI2] cultures but not immediately differentiate into cardiomyocytes thereafter. A regulatory mechanism may be in place that prevents too many poised cardiac progenitors from becoming cardiomyocytes. If this were the case, this HH independent mechanism would likely act downstream of *Myhc6* and *Myhc7* transcription because both of these transcripts are still enhanced when GLI2 is overexpressed (Figure 5).

Assuming that the cardiac progenitor transcripts reflect the size of the cardiac progenitor pool, the day 7 transcript results suggest that this initial acceleration of cardiac progenitor cell numbers in mES[GLI2] cultures is limited to early stages of cardiomyogenesis (Figure 6). Without other essential signals during mES cell differentiation, it appears that this acceleration does not amount to enhanced cardiomyogenesis overall. Nevertheless, this brief acceleration effect observed during mES cell differentiation does not diminish by any means the importance of HH signalling during *in vivo* embryogenesis. *Shh*$^{-/-}$ /*Ihh*$^{-/-}$ and *Smo*$^{-/-}$ embryos demonstrate that a delay of cardiomyogenesis, as a result of inhibited HH signalling, dramatically hinders heart looping to the point that only a linear heart tube remains (87). Therefore, these observations of accelerated cardiac progenitor transcripts in mES[GLI2] cultures provide preliminary evidence that HH signalling has a major role in establishing a pool of cardiac progenitor cells *in vitro* in a timely manner and provide further support that HH signalling is required for timely cardiomyogenesis *in vivo*.

4.3 BRG1 enrichment on *Mef2c* positively correlates with the expression of HH-mediated *Mef2c* expression *in vitro*

To gain insight into how HH signalling regulates certain cardiac progenitor genes *in vitro* but may not enhance the number of cardiomyocytes in differentiating mES[GLI2] cultures, we investigated which proteins GLI2 forms a complex with during differentiation. Results from mass spectrometry and subsequent western blotting identified BRG1 as a candidate protein (Figure 9).

Further investigation by BRG1-ChIP in differentiating P19[GLI2] EC cells (Figure 10) and P19 EC cells treated with KAAD-cyclopamine (Figure 11) demonstrated that BRG1 is recruited to *Mef2c* site *C,* ~2.4kb upstream of the SHF I enhancer (44), in a HH dependent manner on day 4 of P19 EC cell differentiation. When GLI2 is overexpressed in these cultures, BRG1 is enriched at *Mef2c* site *C* (Figure 10). Notably, in this same system, overexpression of GLI2 in P19 EC cells was previously shown to enhance *Mef2c* expression by day 4 of differentiation (73). mES[GLI2] cultures also showed a comparable enhancement of *Mef2c* expression on day 6 of differentiation (Figure 5). Alternatively, when HH signalling is inhibited by KAAD-cyclopamine during P19 EC cell differentiation, BRG1 association is reduced at *Mef2c* site *C* on day 4 of differentiation and *Mef2c* transcript levels are significantly reduced on day 6 (Figure 11). The combination of these gain-of-function and loss-of-function results provides thorough evidence that HH signalling regulates BRG1 enrichment on *Mef2c* and could indicate, with further investigation, that this mechanism has a role in regulating *Mef2c* expression.

A recent study in mES cells supports our observations that BRG1 associates with *Mef2c in vitro* and even further suggests that BRG1 enrichment on *Mef2c* could result in

increased chromatin accessibility in our P19 EC cultures. This study investigated BAF250A's ability to recruit BRG1 to the *Mef2c* promoter region in WT mES cells or in mES cells derived from SHF-specific *Baf250a*$^{-/-}$ mice (199). It demonstrated that BRG1 bound less to *Mef2c* in day 6 mES cells when *Baf250a* was not expressed. Since BRG1's association could be modulated by *Baf250a* expression, and *Baf250a*$^{-/-}$ mice have significantly less *Mef2c* expression in SHF cells on day E9.5 compared to WT mice, Lei *et al*. sought to determine if this reduction in BRG1 recruitment resulted in reduced chromatin accessibility. As hypothesized, the reduction did result in less accessible DNA on the *Mef2c* promoter that could only be fully digested by DNase I at high doses (199). This BAF250A-mediated reduction of BRG1 on *Mef2c* is comparable to the reduction observed during HH signalling inhibition (Figure 11). Therefore, it is likely that HH-mediated reduction of BRG1 on *Mef2c* site *C* in differentiating P19 EC cells could result in reduced chromatin accessibility as well.

BAF complexes require a collection of transcription factors and non-ATPase subunits to associate with specific targets and facilitate chromatin remodelling (193). For instance, transcription factors like GATA-4 and TBX5 mediate BAF complex association along with BAF60C (40, 200). Therefore, it seems feasible that GLI2 may mediate BRG1 association, along with BAF250A, during P19 EC and mES cell cardiomyogenesis. Since BAF60C is highly expressed in the cardiac crescent at E8.25 and is essential for chromatin remodelling in the heart (42), it would be worth determining if this factor is potentially involved in a GLI2-BRG1 complex that associates with *Mef2c* site *C*.

4.4 GLI2 mediates the enrichment of BRG1 on *Mef2c* site *C*

GLI2 is likely the downstream effector involved in HH-mediated BRG1 association on *Mef2c,* given its predominant role in activating downstream HH targets (119). Like BRG1, GLI2 is enriched on *Mef2c* site *C*, in day 4 differentiating P19[GLI2] cells (73). Also, FLAG-IP in mES[GLI2] cells followed by mass spectrometry and western blotting with BRG1-specific antibodies showed that GLI2 forms a complex with BRG1 in day 3 differentiating mES[GLI2] cells (Figure 9). Another source has shown that HA-tagged GLI2 immunoprecipitates with BRG1 in mouse embryonic fibroblasts by reciprocal IP with antibodies against the HA-tag or BRG1 (206). Together, the results from these analyses demonstrate that GLI2 is at least involved in the HH-mediated BRG1 association on *Mef2c*, if not the primary effector of the HH-mediated recruitment.

It is important to note that the inhibition of HH signalling by KAAD-cyclopamine showed that HH signalling regulates BRG1 association, but it does not distinguish which GLI proteins are needed for BRG1 recruitment. Although GLI2 is the primary effector of the HH signalling pathway (119), other GLI proteins could still be involved as well. GLI1 and GLI2 have been shown to have overlapping transcriptional activator roles on other HH target genes (156) and the GLI factors share a common DNA binding motif (121). Inhibition of HH signalling results in inhibition of all activator forms of GLI proteins, not GLI2A alone (193). GLI2 overexpression also upregulates GLI1 activity, through positive feedback loops (155), thus indicating that the gain-of-function experiment may not have only enhanced GLI2A activity but possibly GLI1 as well. Notably, ectopic GLI1 and GLI3A can also immunoprecipitate with BRG1 in mouse embryonic fibroblasts (206). Therefore other

activating GLI proteins, such as GLI1 or GLI3A, cannot be ruled out for being involved in recruiting BRG1 to *Mef2c* site *C*. A specific knockout or shRNA knockdown of *Gli2* would have to be conducted to determine if a loss of GLI2 alone results in reduced BRG1 recruitment. With the current results we can only say that GLI2 is involved in the process.

4.5 HH signalling may regulate BRG1 association on other cardiac progenitor genes expressed in the SHF

Previous studies have shown that BRG1 associates with other HH target genes, including *Gli1* and *Ptch1* in undifferentiated mES cells and in developing telencephalons (206, 217). Therefore, it is possible that HH signalling regulates BRG1 association with some of these other genes like it does on *Mef2c*. Nevertheless, there are many non-ATPase BAF subunits in the BAF complex that also mediate BRG1's interaction with chromatin (193). These subunits vary between tissues and are sometimes tissue-specific (193). Therefore, it is difficult to speculate how HH signalling enriches BRG1 on other BRG1- and HH-target genes, especially in varying tissues, without ChIP analyses.

Interestingly, like with *Mef2c*, BRG1 association and BRG1-mediated chromatin remodelling is also *Baf250a*-dependent on the *Nkx2-5* promoter in day 6 differentiating mES cells (199). In addition, *Baf250a*$^{-/-}$ mice have reduced *Nkx2-5* expression (199). Considering this, the ability of HH signalling to modulate *Nkx2-5* expression in day 6 differentiating mES cells (Figure 5), the ability of HH signalling to regulate *Nkx2-5* expression in P19 EC cells (73, 89), and GLI2's ability to activate the *Nkx2-5* promoter *in vitro* (73), it is likely that BRG1 association on the *Nkx2-5* promoter is dependent on HH signalling like it is dependent on *Baf250a* expression.

Given that BAF250A has been shown to regulate BRG1's association with SHF genes like *Mef2c* and *Nkx2-5* (199), HH signalling may regulate BRG1 enrichment on other cardiac HH target genes in cells from the SHF in a similar fashion. Therefore, if additional genes were to be tested to see if they too support HH-mediated BRG1 enrichment, genes expressed in the developing SHF, such as *Nkx2-5, Foxh1*, and *Tbx20* (28), would be an ideal starting point. *Foxh1* and *Tbx20* are interesting because they too were identified as a potential BRG1 and GLI2 target genes in our bioinformatics screen (Figure 9C).

4.6 *Gata-4* expression is not regulated by GLI2 overexpression in differentiating mES cells like in differentiating P19 EC cells

In this study we have been able to show that GLI2 overexpression results in an accelerated expression of key cardiac progenitor genes and that the acceleration of *Mef2c* could be in part due to BRG1 recruitment by GLI2. However, not all of the studied cardiac progenitor genes were enhanced on day 6 of mES[GLI2] cell differentiation compared to control levels. Based on our results, it appears that the HH-mediated regulation of *Gata-4* observed during P19 EC cell differentiation (73) does not occur during mES cell differentiation (Figure 5). Possible reasons for this discrepancy include: 1) *Gata-4* expression may be enhanced by HH signalling earlier than day 6 during mES cell differentiation; 2) the mechanisms that regulate *Mef2c*, *Nkx2-5*, and *Tbx5* expression are upstream of these factors but downstream of *Gata-4* expression*;* or 3) other molecular mechanisms may counter any HH-mediated enhancement of *Gata-4* expression.

Gata-4 expression in mES cells can be detected as early as day 3 and peaks in expression by day 5 (66, 69). Since HH signalling accelerates the expression of other cardiac progenitor genes early in their expression time course (Figure 6), HH signalling might do the same for *Gata-4* expression early in its time course, before it peaks on day 5 (66, 69). In the P19 EC cell system, *Gata-4* expression can be detected prior to day 5 of differentiation (90) but tends to be significantly expressed on days 5 and 6 when the other cardiac progenitor genes are also significantly expressed (73). Therefore, during mES cell differentiation there is a longer delay between the *Gata-4* expression peaks and the other cardiac progenitor gene expression peaks than during P19 EC cell differentiation (66, 69). The delay during mES cell differentiation is also consistent with the hierarchy of cardiac progenitor transcription factors *in vivo* because GATA-4 acts upstream of MEF2C, NKX2-5, and TBX5 during cardiomyogenesis (4). If the role of HH signalling involves accelerating cardiac progenitor gene expression rather than simply enhancing it, the acceleration of *Gata-4* expression would likely occur earlier than the other cardiac progenitor genes during mES cell differentiation.

Since *Gata-4* is expressed earlier during mES cell differentiation compared to the other cardiac progenitor genes and functions upstream *in vivo*, it is also possible that HH signalling regulates downstream of *Gata-4* expression during cardiomyogenesis in mES cells. Studies *in vivo* and in mES cells have shown that *Gata-4* expression is independently regulated from the expression of other cardiac transcription factor genes, which further supports this rationale. For instance, mice with conditional SHF *Baf250a*$^{-/-}$ have significantly decreased levels of *Mef2c* and *Nkx2-5* expression compared to WT mice, while *Gata-4* levels

remain unaffected (199). Also, chromatin on the *Gata-4* promoter is accessible in day 6 differentiating mES cells derived from both *Baf250a*$^{-/-}$ embryos and WT embryos alike. This indicates that chromatin accessibility on the *Gata-4* promoter is independent of *Baf250a* expression (199). As previously mentioned, chromatin accessibility on the *Mef2c* and *Nkx2-5* promoter are dependent on BAF250A's recruitment of BRG1. Thus, the chromatin remodelling on these cardiac progenitor genes is just one mechanism through which the regulation of these genes differ.

During *in vivo* avian heart development, the induction and maintenance of *Nkx2-5* and *Mef2c* were found to be dependent on signals from the neighbouring anterior endoderm (244). In a loss of function experiment, the adjacent endoderm was removed from the side of a developing avian heart, resulting in a decrease in *Nkx2-5* and *Mef2c*, but no observable change in *Gata-4* expression. The active component from the neighbouring endoderm that signals *Nkx2-5* and *Mef2c* in the precardiac mesoderm was determined to be fibroblast growth factor 8 (*Fgf8*) because ectopic *Fgf8* expression could rescue the expression of these two cardiac genes in the absence of the anterior endoderm (244). Although *Fgf8* expression may not be directly linked to HH signalling or chromatin remodelling in this context, it still provides an example of how *Gata-4* expression is regulated independently from *Nkx2-5* and *Mef2c* expression during heart development *in vivo*.

Another study observed enhanced *Nkx2-5* and *Tbx5* expression on day 6 of mES cell differentiation without significant enhancement of *Gata-4* expression. This enhancement occurred when Yin Yang 1 (YY1), a novel regulator of cardiac progenitor genes, was overexpressed through a doxycycline-inducible system *in vitro* (245). In this study, YY1 was shown to be essential for regulating cardiomyogenesis in differentiating mES cells and could

directly bind and enhance *Nkx2-5* expression in a GATA-4 dependent manner. Western blotting with antibodies against GATA-4 on protein lysates from *Yy1p*-transfected H9C2 cells showed that YY1 did not affect GATA-4 protein expression either (245). When overexpressed in mES cell-derived mesoderm cells, YY1 induced the expression of *Nkx2-5* and *Tbx5*. Furthermore, their genome wide analysis indicated that YY1 might also regulate *Mef2c* (245). Given the different modulation between *Gata-4* and other cardiac progenitor genes *in vitro* in this study as well, it is quite possible that HH signalling regulates cardiac progenitor genes downstream of *Gata-4* in mES cell-derived cardiac progenitors.

Although the above studies provide good support for differential regulation of *Gata-4* expression during mES cell differentiation, HH signalling could still initially enhance *Gata-4* expression but an opposing signal may counter the overall expression of *Gata-4*. These countering regulatory mechanisms could lead to an overall non-significant difference in *Gata-4* expression on day 6 of differentiation between mES[GLI2] and mES[Ctrl] cultures while still facilitating enhanced expression of other cardiac progenitor enriched genes (Figure 5).

The Wnt/β-catenin pathway has been shown to have a biphasic role during cardiomyogenesis in zebrafish and mES cells (246). In zebrafish, if Wnt/β-catenin signalling is induced prior to gastrulation, cardiomyogenesis is enhanced as the pathway induces mesoderm differentiation (246, 247). However, if Wnt/β-catenin signalling is induced during gastrulation, complete heart formation is inhibited (246). A similar biphasic role was observed in mES cells that were treated with Wnt-3A between days 2 and 5 of differentiation. These mES cells expressed higher levels of cardiac transcripts, but also

expressed significantly higher transcript levels of the Wnt/β-catenin signalling inhibitor, dickkopf-1 (Dkk1), than the control cells by day 5 (246). This shows that, *in vivo* and *in vitro*, Wnt/β-catenin signalling needs to be enhanced early and repressed later to ensure proper cardiomyogenesis.

There is some evidence that HH signalling can regulate Wnt signalling in neural progenitor cells (248) and canonical Wnt/β-catenin signalling can restrict cardiomyogenesis by inhibiting *Gata-4* expression (249). Given this, any HH-mediated enhancement of *Gata-4* expression may be attenuated by countering Wnt/β-catenin signalling that is also enhanced by HH signalling. To test this possibility it would be worth differentiating mES[GLI2] cells and mES[Ctrl] cells in the presence of recombinant DKK1 (69) following day 4 of differentiation to see if *Gata-4* levels would be higher when GLI2 is overexpressed and Wnt/β-catenin signalling is inhibited. At the same time, cardiomyocyte numbers on day 7 could be quantified to see if Wnt/β-catenin needs to be inhibited to observe HH-mediated enhancement of cardiomyocyte percentages in mES[GLI2] cultures, as well.

Based on the results in this study, it is hard to determine if *Gata-4* expression is independent of HH signalling throughout differentiation, but certainly GLI2 overexpression alone is not enough to enhance *Gata-4* expression in day 6 differentiating mES cells above control cell levels.

4.7 Conclusions

The results from this study in combination with observations from other *in vivo* and *in vitro* studies, demonstrate that GLI2 accelerates the expression of cardiac progenitor enriched genes during mES cell cardiomyogenesis (Figure 12A). ChIP analyses further

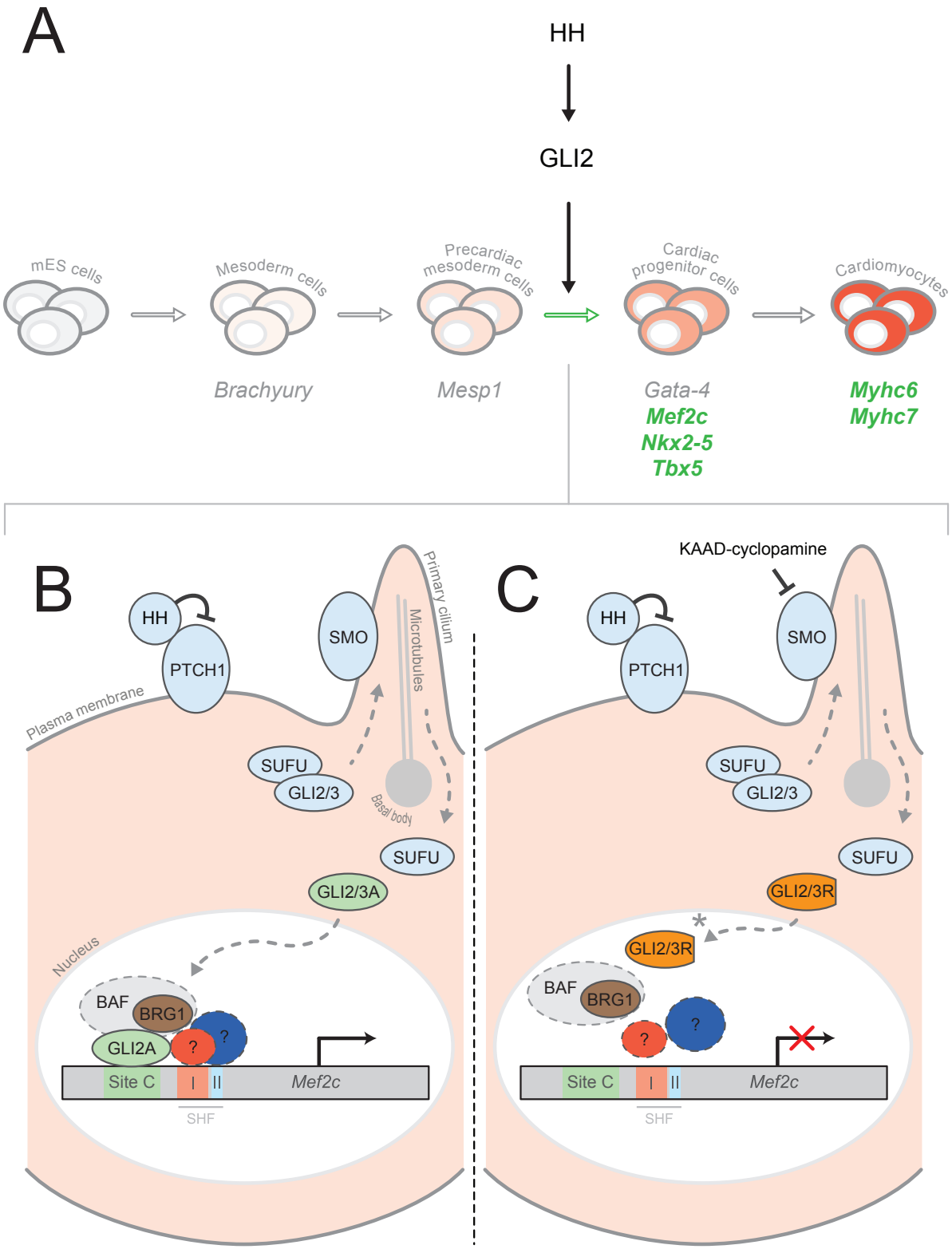
A
HH
GLI2
mES cells
Mesoderm cells
Precardiac mesoderm cells
Cardiac progenitor cells
Cardiomyocytes
Brachyury
Mesp1
Gata-4
Mef2c
Nkx2-5
Tbx5
Myhc6
Myhc7
B
HH
PTCH1
SMO
Primary cilium
Microtubules
Plasma membrane
SUFU
GLI2/3
Basal body
SUFU
GLI2/3A
Nucleus
BAF
BRG1
GLI2A
?
?
Site C
I
II
Mef2c
SHF
C
KAAD-cyclopamine
HH
PTCH1
SMO
SUFU
GLI2/3
SUFU
GLI2/3R
*
GLI2/3R
BAF
BRG1
?
?
Site C
I
II
Mef2c
SHF

Figure 12. A model summarizing the role of the HH signalling pathway and its primary transducer, GLI2, during mES cell cardiomyogenesis.
(A) In this study, GLI2 expression was observed to positively regulate cardiomyogenesis-specific transcription factors in mES cells *(highlighted in green)*. The hollow arrows indicate the transition towards a more differentiated cell type found in the cardiomyogenic lineage. The hollow green arrow marks the transition enhanced by GLI2. The solid black arrows indicate HH/GLI2's proposed direct regulation. **(B, C)** GLI2's acceleration of cardiac transcripts may be explained in part by the ability of the transcriptional activator form of GLI2 (GLI2A) *(*included in the *green ellipses, **B**)* - mediated via a functional HH signalling pathway *(light blue ellipses)* - to enrich BRG1 association at *Mef2c* site *C*. This enrichment site is proximal to known SHF enhancer regions *(I, II)*. Therefore, other cofactors *(dash-outlined ellipses)*, including the remaining BAF complex members and other unidentified SHF-related transcription factors *(?)* may support this GLI2-mediated association. When KAAD-cyclopamine inhibits HH signalling, GLI2 may be processed into GLI2R *(*included in the *orange truncated ellipses, **C**)*. Also, GLI3R (included in the *orange truncated ellipses*, ***C***) may contribute to the repression of *Mef2c* expression. The downstream binding of either GLI2R or GLI3R to *Mef2c* has yet to be assessed (*).

indicated that this acceleration, at least in the case of *Mef2c*, could be due to HH-mediated recruitment of BRG1 via GLI2 (Figure 12B, C).

Additional investigation is still required to fully understand why GLI2 overexpression does not enhance cardiomyocyte formation when the cardiac transcriptional profile is accelerated. Based on previous studies, quantification of cardiac progenitor cells on day 6 of mES[GLI2] cell differentiation should be assessed first to see if the cardiac progenitor pool is at least enriched compared to control cultures. Also, as mentioned before, the crosstalk between HH and Wnt/β-catenin signalling should be investigated to see if Wnt/β-catenin signalling is limiting the enrichment of *Gata-4* and possibly the enrichment of cardiomyocyte numbers by day 7 in mES[GLI2] cells compared to the control cells.

To extend our understanding of the molecular mechanism behind HH-mediated *Mef2c* expression, further analysis using chromatin remodelling assays and reporter assays is required. These analyses would determine if BRG1 recruitment enhances chromatin accessibility at *Mef2c* site *C* and if GLI2 and BRG1 can synergistically activate *Mef2c* by associating with a reporter construct containing the *Mef2c* site *C* and SHF enhancer regions. Given the common mechanisms that regulate *Mef2c* and *Nkx2-5* in other studies, BRG1-ChIP assays should also be performed on *Nkx2-5*. If BRG1 is also enriched at the *Nkx2-5* promoter in a HH dependent manner, then similar chromatin accessibility and reporter assays should be investigated on the *Nkx2-5* promoter as well. If successfully elucidated in P19 EC cells, the molecular mechanisms that regulate *Mef2c* and *Nkx2-5* expression should also be assessed in the mES and eventually in the hES cell model.

By elucidating the mechanisms of HH-mediated acceleration of cardiomyogenesis in mES cells and cardiomyogenesis enhancement in P19 EC cells, the intricate network of

signalling pathways driving heart development *in vitro* and *in vivo* will hopefully become clearer. Since cardiac progenitor cells have been shown to contribute in part to endogenous heart regeneration in mice (16, 17), mechanisms that enhance differentiation of ES cells into cardiac progenitor cells *in vitro* may be useful for refining current directed differentiation approaches to generate hES cell-derived cardiac progenitors that may be more efficient at remuscularizing infarcted hearts.

References

1. **Statistics Canada.** 2010. CANSIM Table 102-0529: Deaths, by cause, Chapter IX: Diseases of the circulatory system (I00 to I99), age group and sex, canada, annual (number), 2000 to 2006. Released May 4, 2010.

2. **Thygesen K, Alpert JS, White HD, Jaffe AS, Apple FS, Galvani M, Katus HA, Newby LK, Ravkilde J, Chaitman B, Clemmensen PM, Dellborg M, Hod H, Porela P, Underwood R, Bax JJ, Beller GA, Bonow R, Van der Wall EE, Bassand JP, Wijns W, Ferguson TB, Steg PG, Uretsky BF, Williams DO, Armstrong PW, Antman EM, Fox KA, Hamm CW, Ohman EM, Simoons ML, Poole-Wilson PA, Gurfinkel EP, Lopez-Sendon JL, Pais P, Mendis S, Zhu JR, Wallentin LC, Fernandez-Aviles F, Fox KM, Parkhomenko AN, Priori SG, Tendera M, Voipio-Pulkki LM, Vahanian A, Camm AJ, De Caterina R, Dean V, Dickstein K, Filippatos G, Funck-Brentano C, Hellemans I, Kristensen SD, McGregor K, Sechtem U, Silber S, Widimsky P, Zamorano JL, Morais J, Brener S, Harrington R, Morrow D, Lim M, Martinez-Rios MA, Steinhubl S, Levine GN, Gibler WB, Goff D, Tubaro M, Dudek D, Al-Attar N.** 2007. Universal definition of myocardial infarction. Circulation **116:**2634-2653.

3. **Gepstein L.** 2002. Derivation and Potential Applications of Human Embryonic Stem Cells. Circulation Research **91:**866-876.

4. **Xin M, Olson EN, Bassel-Duby R.** 2013. Mending broken hearts: cardiac development as a basis for adult heart regeneration and repair. Nature reviews. Molecular cell biology **14:**529-541.

5. **Stevenson LW.** 1994. Selection and management of patients for cardiac transplantation. Curr Opin Cardiol **9:**315-325.

6. **Stehlik J, Edwards LB, Kucheryavaya AY, Benden C, Christie JD, Dipchand AI, Dobbels F, Kirk R, Rahmel AO, Hertz MI.** 2012. The Registry of the International Society for Heart and Lung Transplantation: 29th official adult heart transplant report--2012. The Journal of heart and lung transplantation : the official publication of the International Society for Heart Transplantation **31:**1052-1064.

7. **Tonsho M, Michel S, Ahmed Z, Alessandrini A, Madsen JC.** 2014. Heart transplantation: challenges facing the field. Cold Spring Harbor perspectives in medicine **4:**a015636.

8. **Colvin-Adams M, Smith JM, Heubner BM, Skeans MA, Edwards LB, Waller C, Snyder JJ, Israni AK, Kasiske BL.** 2013. OPTN/SRTR 2011 Annual Data Report: heart. American journal of transplantation : official journal of the American Society

of Transplantation and the American Society of Transplant Surgeons **13 Suppl 1:**119-148.

9. **Bergmann O, Bhardwaj RD, Bernard S, Zdunek S, Barnabe-Heider F, Walsh S, Zupicich J, Alkass K, Buchholz BA, Druid H, Jovinge S, Frisen J.** 2009. Evidence for cardiomyocyte renewal in humans. Science **324:**98-102.

10. **Kajstura J, Urbanek K, Perl S, Hosoda T, Zheng H, Ogorek B, Ferreira-Martins J, Goichberg P, Rondon-Clavo C, Sanada F, D'Amario D, Rota M, Del Monte F, Orlic D, Tisdale J, Leri A, Anversa P.** 2010. Cardiomyogenesis in the adult human heart. Circ Res **107:**305-315.

11. **Ahuja P, Sdek P, MacLellan WR.** 2007. Cardiac myocyte cell cycle control in development, disease, and regeneration. Physiological reviews **87:**521-544.

12. **Li F, Wang X, Capasso JM, Gerdes AM.** 1996. Rapid transition of cardiac myocytes from hyperplasia to hypertrophy during postnatal development. Journal of molecular and cellular cardiology **28:**1737-1746.

13. **Porrello ER, Mahmoud AI, Simpson E, Hill JA, Richardson JA, Olson EN, Sadek HA.** 2011. Transient regenerative potential of the neonatal mouse heart. Science **331:**1078-1080.

14. **Maillet M, van Berlo JH, Molkentin JD.** 2013. Molecular basis of physiological heart growth: fundamental concepts and new players. Nat Rev Mol Cell Biol **14:**38-48.

15. **Poss KD, Wilson LG, Keating MT.** 2002. Heart regeneration in zebrafish. Science **298:**2188-2190.

16. **Laflamme MA, Murry CE.** 2011. Heart regeneration. Nature **473:**326-335.

17. **Senyo SE, Steinhauser ML, Pizzimenti CL, Yang VK, Cai L, Wang M, Wu TD, Guerquin-Kern JL, Lechene CP, Lee RT.** 2013. Mammalian heart renewal by pre-existing cardiomyocytes. Nature **493:**433-436.

18. **Riazi AM, Kwon SY, Stanford WL.** 2009. Stem cell sources for regenerative medicine. Methods in molecular biology **482:**55-90.

19. **Lerou PH, Daley GQ.** 2005. Therapeutic potential of embryonic stem cells. Blood reviews **19:**321-331.

20. **Laflamme MA, Chen KY, Naumova AV, Muskheli V, Fugate JA, Dupras SK, Reinecke H, Xu C, Hassanipour M, Police S, O'Sullivan C, Collins L, Chen Y, Minami E, Gill Ea, Ueno S, Yuan C, Gold J, Murry CE.** 2007. Cardiomyocytes

derived from human embryonic stem cells in pro-survival factors enhance function of infarcted rat hearts. Nature biotechnology **25:**1015-1024.

21. **Kattman SJ, Witty AD, Gagliardi M, Dubois NC, Niapour M, Hotta A, Ellis J, Keller G.** 2011. Stage-specific optimization of activin/nodal and BMP signaling promotes cardiac differentiation of mouse and human pluripotent stem cell lines. Cell Stem Cell **8:**228-240.

22. **Bruneau BG.** 2013. Signaling and transcriptional networks in heart development and regeneration. Cold Spring Harbor perspectives in biology **5:**a008292.

23. **Shiba Y, Fernandes S, Zhu WZ, Filice D, Muskheli V, Kim J, Palpant NJ, Gantz J, Moyes KW, Reinecke H, Van Biber B, Dardas T, Mignone JL, Izawa A, Hanna R, Viswanathan M, Gold JD, Kotlikoff MI, Sarvazyan N, Kay MW, Murry CE, Laflamme MA.** 2012. Human ES-cell-derived cardiomyocytes electrically couple and suppress arrhythmias in injured hearts. Nature **489:**322-325.

24. **Chong JJ, Yang X, Don CW, Minami E, Liu YW, Weyers JJ, Mahoney WM, Van Biber B, Cook SM, Palpant NJ, Gantz JA, Fugate JA, Muskheli V, Gough GM, Vogel KW, Astley CA, Hotchkiss CE, Baldessari A, Pabon L, Reinecke H, Gill EA, Nelson V, Kiem HP, Laflamme MA, Murry CE.** 2014. Human embryonic-stem-cell-derived cardiomyocytes regenerate non-human primate hearts. Nature **510:**273-277.

25. **Harvey RP.** 2002. Patterning the vertebrate heart. Nat Rev Genet **3:**544-556.

26. **Abu-Issa R, Kirby ML.** 2007. Heart field: from mesoderm to heart tube. Annu Rev Cell Dev Biol **23:**45-68.

27. **Costello I, Pimeisl IM, Drager S, Bikoff EK, Robertson EJ, Arnold SJ.** 2011. The T-box transcription factor Eomesodermin acts upstream of Mesp1 to specify cardiac mesoderm during mouse gastrulation. Nature cell biology **13:**1084-1091.

28. **Vincent SD, Buckingham ME.** 2010. How to make a heart: the origin and regulation of cardiac progenitor cells. Curr Top Dev Biol **90:**1-41.

29. **Saga Y, Miyagawa-Tomita S, Takagi A, Kitajima S, Miyazaki J, Inoue T.** 1999. MesP1 is expressed in the heart precursor cells and required for the formation of a single heart tube. Development **126:**3437-3447.

30. **Yoshida T, Vivatbutsiri P, Morriss-Kay G, Saga Y, Iseki S.** 2008. Cell lineage in mammalian craniofacial mesenchyme. Mech Dev **125:**797-808.

31. **Linask KK.** 1992. N-cadherin localization in early heart development and polar expression of Na+,K(+)-ATPase, and integrin during pericardial coelom formation and epithelialization of the differentiating myocardium. Dev Biol **151:**213-224.

32. **Buckingham M, Meilhac S, Zaffran S.** 2005. Building the mammalian heart from two sources of myocardial cells. Nat Rev Genet **6:**826-835.

33. **Davidson EH, Erwin DH.** 2006. Gene regulatory networks and the evolution of animal body plans. Science **311:**796-800.

34. **Lyons I, Parsons LM, Hartley L, Li R, Andrews JE, Robb L, Harvey RP.** 1995. Myogenic and morphogenetic defects in the heart tubes of murine embryos lacking the homeo box gene Nkx2-5. Genes Dev **9:**1654-1666.

35. **Kuo CT, Morrisey EE, Anandappa R, Sigrist K, Lu MM, Parmacek MS, Soudais C, Leiden JM.** 1997. GATA4 transcription factor is required for ventral morphogenesis and heart tube formation. Genes Dev **11:**1048-1060.

36. **Maitra M, Schluterman MK, Nichols HA, Richardson JA, Lo CW, Srivastava D, Garg V.** 2009. Interaction of Gata4 and Gata6 with Tbx5 is critical for normal cardiac development. Dev Biol **326:**368-377.

37. **Lin Q, Schwarz J, Bucana C, Olson EN.** 1997. Control of mouse cardiac morphogenesis and myogenesis by transcription factor MEF2C. Science **276:**1404-1407.

38. **Vong LH, Ragusa MJ, Schwarz JJ.** 2005. Generation of conditional Mef2cloxP/loxP mice for temporal- and tissue-specific analyses. Genesis **43:**43-48.

39. **Heikinheimo M, Scandrett JM, Wilson DB.** 1994. Localization of transcription factor GATA-4 to regions of the mouse embryo involved in cardiac development. Dev Biol **164:**361-373.

40. **Takeuchi JK, Bruneau BG.** 2009. Directed transdifferentiation of mouse mesoderm to heart tissue by defined factors. Nature **459:**708-711.

41. **Searcy RD, Vincent EB, Liberatore CM, Yutzey KE.** 1998. A GATA-dependent nkx-2.5 regulatory element activates early cardiac gene expression in transgenic mice. Development **125:**4461-4470.

42. **Lickert H, Takeuchi JK, Von Both I, Walls JR, McAuliffe F, Adamson SL, Henkelman RM, Wrana JL, Rossant J, Bruneau BG.** 2004. Baf60c is essential for function of BAF chromatin remodelling complexes in heart development. Nature **432:**107-112.

43. **Garg V, Kathiriya IS, Barnes R, Schluterman MK, King IN, Butler CA, Rothrock CR, Eapen RS, Hirayama-Yamada K, Joo K, Matsuoka R, Cohen JC, Srivastava D.** 2003. GATA4 mutations cause human congenital heart defects and reveal an interaction with TBX5. Nature **424:**443-447.

44. **Dodou E, Verzi MP, Anderson JP, Xu SM, Black BL.** 2004. Mef2c is a direct transcriptional target of ISL1 and GATA factors in the anterior heart field during mouse embryonic development. Development **131:**3931-3942.

45. **von Both I, Silvestri C, Erdemir T, Lickert H, Walls JR, Henkelman RM, Rossant J, Harvey RP, Attisano L, Wrana JL.** 2004. Foxh1 is essential for development of the anterior heart field. Developmental cell **7:**331-345.

46. **Bruneau BG, Nemer G, Schmitt JP, Charron F, Robitaille L, Caron S, Conner DA, Gessler M, Nemer M, Seidman CE, Seidman JG.** 2001. A murine model of Holt-Oram syndrome defines roles of the T-box transcription factor Tbx5 in cardiogenesis and disease. Cell **106:**709-721.

47. **Durocher D, Charron F, Warren R, Schwartz RJ, Nemer M.** 1997. The cardiac transcription factors Nkx2-5 and GATA-4 are mutual cofactors. EMBO J **16:**5687-5696.

48. **Morin S, Charron F, Robitaille L, Nemer M.** 2000. GATA-dependent recruitment of MEF2 proteins to target promoters. EMBO J **19:**2046-2055.

49. **Lee Y, Shioi T, Kasahara H, Jobe SM, Wiese RJ, Markham BE, Izumo S.** 1998. The cardiac tissue-restricted homeobox protein Csx/Nkx2.5 physically associates with the zinc finger protein GATA4 and cooperatively activates atrial natriuretic factor gene expression. Mol Cell Biol **18:**3120-3129.

50. **Lyons GE, Schiaffino S, Sassoon D, Barton P, Buckingham M.** 1990. Developmental regulation of myosin gene expression in mouse cardiac muscle. J Cell Biol **111:**2427-2436.

51. **Sassoon DA, Garner I, Buckingham M.** 1988. Transcripts of alpha-cardiac and alpha-skeletal actins are early markers for myogenesis in the mouse embryo. Development **104:**155-164.

52. **Ng Wa, Grupp IL, Subramaniam a, Robbins J.** 1991. Cardiac myosin heavy chain mRNA expression and myocardial function in the mouse heart. Circulation Research **68:**1742-1750.

53. **Granados-Riveron JT, Brook JD.** 2012. The impact of mechanical forces in heart morphogenesis. Circulation. Cardiovascular genetics **5:**132-142.

54. **Burggren WW, Warburton SJ, Slivkoff MD.** 2000. Interruption of cardiac output does not affect short-term growth and metabolic rate in day 3 and 4 chick embryos. The Journal of experimental biology **203:**3831-3838.

55. **Evans SM, Yelon D, Conlon FL, Kirby ML.** 2010. Myocardial lineage development. Circ Res **107:**1428-1444.

56. **Lin CJ, Lin CY, Chen CH, Zhou B, Chang CP.** 2012. Partitioning the heart: mechanisms of cardiac septation and valve development. Development **139:**3277-3299.

57. **Kirby ML, Gale TF, Stewart DE.** 1983. Neural crest cells contribute to normal aorticopulmonary septation. Science **220:**1059-1061.

58. **Jiang X, Rowitch DH, Soriano P, McMahon AP, Sucov HM.** 2000. Fate of the mammalian cardiac neural crest. Development **127:**1607-1616.

59. **Okamoto N, Akimoto N, Hidaka N, Shoji S, Sumida H.** 2010. Formal genesis of the outflow tracts of the heart revisited: previous works in the light of recent observations. Congenital anomalies **50:**141-158.

60. **Hoffman JI.** 1995. Incidence of congenital heart disease: II. Prenatal incidence. Pediatric cardiology **16:**155-165.

61. **Hoffman JI, Kaplan S.** 2002. The incidence of congenital heart disease. Journal of the American College of Cardiology **39:**1890-1900.

62. **Ghosh TK, Packham EA, Bonser AJ, Robinson TE, Cross SJ, Brook JD.** 2001. Characterization of the TBX5 binding site and analysis of mutations that cause Holt-Oram syndrome. Hum Mol Genet **10:**1983-1994.

63. **Ching YH, Ghosh TK, Cross SJ, Packham EA, Honeyman L, Loughna S, Robinson TE, Dearlove AM, Ribas G, Bonser AJ, Thomas NR, Scotter AJ, Caves LS, Tyrrell GP, Newbury-Ecob RA, Munnich A, Bonnet D, Brook JD.** 2005. Mutation in myosin heavy chain 6 causes atrial septal defect. Nat Genet **37:**423-428.

64. **Bruneau BG.** 2008. The developmental genetics of congenital heart disease. Nature **451:**943-948.

65. **Takano H, Qin Y, Hasegawa H, Ueda K, Niitsuma Y, Ohtsuka M, Komuro I.** 2006. Effects of G-CSF on left ventricular remodeling and heart failure after acute myocardial infarction. J Mol Med **84:**185-193.

66. **Bondue A, Lapouge G, Paulissen C, Semeraro C, Iacovino M, Kyba M, Blanpain C.** 2008. Mesp1 acts as a master regulator of multipotent cardiovascular progenitor specification. Cell Stem Cell **3:**69-84.

67. **Wobus AM, Wallukat G, Hescheler J.** 1991. Pluripotent mouse embryonic stem cells are able to differentiate into cardiomyocytes expressing chronotropic responses to adrenergic and cholinergic agents and Ca2+ channel blockers. Differentiation **48:**173-182.

68. **Keller GM.** 1995. In vitro differentiation of embryonic stem cells. Current opinion in cell biology **7:**862-869.

69. **Christoforou N, Miller RA, Hill CM, Jie CC, McCallion AS, Gearhart JD.** 2008. Mouse ES cell-derived cardiac precursor cells are multipotent and facilitate identification of novel cardiac genes. J Clin Invest **118:**894-903.

70. **Wu J, Kubota J, Hirayama J, Nagai Y, Nishina S, Yokoi T, Asaoka Y, Seo J, Shimizu N, Kajiho H, Watanabe T, Azuma N, Katada T, Nishina H.** 2010. p38 Mitogen-activated protein kinase controls a switch between cardiomyocyte and neuronal commitment of murine embryonic stem cells by activating myocyte enhancer factor 2C-dependent bone morphogenetic protein 2 transcription. Stem Cells Dev **19:**1723-1734.

71. **Metzger JM, Lin WI, Johnston RA, Westfall MV, Samuelson LC.** 1995. Myosin heavy chain expression in contracting myocytes isolated during embryonic stem cell cardiogenesis. Circ Res **76:**710-719.

72. **van der Heyden MA, Defize LH.** 2003. Twenty one years of P19 cells: what an embryonal carcinoma cell line taught us about cardiomyocyte differentiation. Cardiovascular Research **58:**292-302.

73. **Voronova A, Al Madhoun A, Fischer A, Shelton M, Karamboulas C, Skerjanc IS.** 2012. Gli2 and MEF2C activate each other's expression and function synergistically during cardiomyogenesis in vitro. Nucleic Acids Res **40:**3329-3347.

74. **McBurney MW.** 1993. P19 embryonal carcinoma cells. Int J Dev Biol **37:**135-140.

75. **McBurney MW, Rogers BJ.** 1982. Isolation of male embryonal carcinoma cells and their chromosome replication patterns. Developmental biology **89:**503-508.

76. **Rudnicki MA, Reuhl KR, McBurney MW.** 1989. Cell lines with developmental potential restricted to mesodermal lineages isolated from differentiating cultures of pluripotential P19 embryonal carcinoma cells. Development **107:**361-372.

77. **Vidricaire G, Jardine K, McBurney MW.** 1994. Expression of the Brachyury gene during mesoderm development in differentiating embryonal carcinoma cell cultures. Development **120:**115-122.

78. **Skerjanc IS.** 1999. Cardiac and skeletal muscle development in P19 embryonal carcinoma cells. Trends in cardiovascular medicine **9:**139-143.

79. **Habara-Ohkubo A.** 1996. Differentiation of beating cardiac muscle cells from a derivative of P19 embryonal carcinoma cells. Cell structure and function **21:**101-110.

80. **Peng CF, Wei Y, Levsky JM, McDonald TV, Childs G, Kitsis RN.** 2002. Microarray analysis of global changes in gene expression during cardiac myocyte differentiation. Physiological genomics **9:**145-155.

81. **Clement CA, Kristensen SG, Mollgard K, Pazour GJ, Yoder BK, Larsen LA, Christensen ST.** 2009. The primary cilium coordinates early cardiogenesis and hedgehog signaling in cardiomyocyte differentiation. J Cell Sci **122:**3070-3082.

82. **Karamboulas C, Dakubo GD, Liu J, De Repentigny Y, Yutzey K, Wallace VA, Kothary R, Skerjanc IS.** 2006. Disruption of MEF2 activity in cardiomyoblasts inhibits cardiomyogenesis. J Cell Sci **119:**4315-4321.

83. **Fu Y, Yan W, Mohun TJ, Evans SM.** 1998. Vertebrate tinman homologues XNkx2-3 and XNkx2-5 are required for heart formation in a functionally redundant manner. Development **125:**4439-4449.

84. **Jamali M, Rogerson PJ, Wilton S, Skerjanc IS.** 2001. Nkx2-5 activity is essential for cardiomyogenesis. J Biol Chem **276:**42252-42258.

85. **Kim PC, Mo R, Hui Cc C.** 2001. Murine models of VACTERL syndrome: Role of sonic hedgehog signaling pathway. Journal of pediatric surgery **36:**381-384.

86. **Kim J, Kim P, Hui CC.** 2001. The VACTERL association: lessons from the Sonic hedgehog pathway. Clinical genetics **59:**306-315.

87. **Zhang XM, Ramalho-Santos M, McMahon AP.** 2001. Smoothened mutants reveal redundant roles for Shh and Ihh signaling including regulation of L/R symmetry by the mouse node. Cell **106:**781-792.

88. **Clement CA, Larsen LA, Christensen ST.** 2009. Using nucleofection of siRNA constructs for knockdown of primary cilia in P19.CL6 cancer stem cell differentiation into cardiomyocytes. Methods in cell biology **94:**181-197.

89. **Gianakopoulos PJ, Skerjanc IS.** 2005. Hedgehog signaling induces cardiomyogenesis in P19 cells. The Journal of biological chemistry **280:**21022-21028.

90. **Gianakopoulos PJ, Skerjanc IS.** 2009. Cross talk between hedgehog and bone morphogenetic proteins occurs during cardiomyogenesis in P19 cells. In Vitro Cellular & Developmental Biology - Animal **45:**566-572.

91. **Perron M, Boy S, Amato MA, Viczian A, Koebernick K, Pieler T, Harris WA.** 2003. A novel function for Hedgehog signalling in retinal pigment epithelium differentiation. Development **130:**1565-1577.

92. **Lee J, Platt KA, Censullo P, Ruiz i Altaba A.** 1997. Gli1 is a target of Sonic hedgehog that induces ventral neural tube development. Development **124:**2537-2552.

93. **Kim SK, Melton DA.** 1998. Pancreas development is promoted by cyclopamine, a hedgehog signaling inhibitor. Proc Natl Acad Sci U S A **95:**13036-13041.

94. **Sukegawa A, Narita T, Kameda T, Saitoh K, Nohno T, Iba H, Yasugi S, Fukuda K.** 2000. The concentric structure of the developing gut is regulated by Sonic hedgehog derived from endodermal epithelium. Development **127:**1971-1980.

95. **Litingtung Y, Lei L, Westphal H, Chiang C.** 1998. Sonic hedgehog is essential to foregut development. Nat Genet **20:**58-61.

96. **Detmer K, Walker AN, Jenkins TM, Steele TA, Dannawi H.** 2000. Erythroid differentiation in vitro is blocked by cyclopamine, an inhibitor of hedgehog signaling. Blood cells, molecules & diseases **26:**360-372.

97. **Mo R, Freer AM, Zinyk DL, Crackower MA, Michaud J, Heng HH, Chik KW, Shi XM, Tsui LC, Cheng SH, Joyner AL, Hui C.** 1997. Specific and redundant functions of Gli2 and Gli3 zinc finger genes in skeletal patterning and development. Development **124:**113-123.

98. **Borycki AG, Brunk B, Tajbakhsh S, Buckingham M, Chiang C, Emerson CP, Jr.** 1999. Sonic hedgehog controls epaxial muscle determination through Myf5 activation. Development **126:**4053-4063.

99. **Voronova A, Coyne E, Al Madhoun A, Fair JV, Bosiljcic N, St-Louis C, Li G, Thurig S, Wallace Va, Wiper-Bergeron N, Skerjanc IS.** 2013. Hedgehog Signaling Regulates MyoD Expression and Activity. The Journal of biological chemistry **288:**4389-4404.

100. **Chiang C, Swan RZ, Grachtchouk M, Bolinger M, Litingtung Y, Robertson EK, Cooper MK, Gaffield W, Westphal H, Beachy PA, Dlugosz AA.** 1999. Essential role for Sonic hedgehog during hair follicle morphogenesis. Dev Biol **205:**1-9.

101. **Briscoe J, Thérond PP.** 2013. The mechanisms of Hedgehog signalling and its roles in development and disease. Nature reviews. Molecular cell biology **14:**416-429.

102. **Beachy PA, Karhadkar SS, Berman DM.** 2004. Tissue repair and stem cell renewal in carcinogenesis. Nature **432:**324-331.

103. **Nusslein-Volhard C, Wieschaus E.** 1980. Mutations affecting segment number and polarity in Drosophila. Nature **287:**795-801.

104. **Lee JJ, von Kessler DP, Parks S, Beachy PA.** 1992. Secretion and localized transcription suggest a role in positional signaling for products of the segmentation gene hedgehog. Cell **71:**33-50.

105. **Mohler J, Vani K.** 1992. Molecular organization and embryonic expression of the hedgehog gene involved in cell-cell communication in segmental patterning of Drosophila. Development **115:**957-971.

106. **Tabata T, Eaton S, Kornberg TB.** 1992. The Drosophila hedgehog gene is expressed specifically in posterior compartment cells and is a target of engrailed regulation. Genes Dev **6:**2635-2645.

107. **St-Jacques B, Hammerschmidt M, McMahon AP.** 1999. Indian hedgehog signaling regulates proliferation and differentiation of chondrocytes and is essential for bone formation. Genes Dev **13:**2072-2086.

108. **Vortkamp A, Lee K, Lanske B, Segre GV, Kronenberg HM, Tabin CJ.** 1996. Regulation of rate of cartilage differentiation by Indian hedgehog and PTH-related protein. Science **273:**613-622.

109. **Parmantier E, Lynn B, Lawson D, Turmaine M, Namini SS, Chakrabarti L, McMahon AP, Jessen KR, Mirsky R.** 1999. Schwann cell-derived Desert hedgehog controls the development of peripheral nerve sheaths. Neuron **23:**713-724.

110. **Bitgood MJ, Shen L, McMahon AP.** 1996. Sertoli cell signaling by Desert hedgehog regulates the male germline. Current biology : CB **6:**298-304.

111. **Riddle RD, Johnson RL, Laufer E, Tabin C.** 1993. Sonic hedgehog mediates the polarizing activity of the ZPA. Cell **75:**1401-1416.

112. **Echelard Y, Epstein DJ, St-Jacques B, Shen L, Mohler J, McMahon JA, McMahon AP.** 1993. Sonic hedgehog, a member of a family of putative signaling molecules, is implicated in the regulation of CNS polarity. Cell **75:**1417-1430.

113. **Roelink H, Augsburger A, Heemskerk J, Korzh V, Norlin S, Ruiz i Altaba A, Tanabe Y, Placzek M, Edlund T, Jessell TM, et al.** 1994. Floor plate and motor neuron induction by vhh-1, a vertebrate homolog of hedgehog expressed by the notochord. Cell **76:**761-775.

114. **Chang DT, Lopez A, von Kessler DP, Chiang C, Simandl BK, Zhao R, Seldin MF, Fallon JF, Beachy PA.** 1994. Products, genetic linkage and limb patterning activity of a murine hedgehog gene. Development **120:**3339-3353.

115. **Perler FB.** 1998. Protein splicing of inteins and hedgehog autoproteolysis: structure, function, and evolution. Cell **92:**1-4.

116. **Pepinsky RB, Zeng C, Wen D, Rayhorn P, Baker DP, Williams KP, Bixler SA, Ambrose CM, Garber EA, Miatkowski K, Taylor FR, Wang EA, Galdes A.** 1998. Identification of a palmitic acid-modified form of human Sonic hedgehog. J Biol Chem **273:**14037-14045.

117. **Tukachinsky H, Kuzmickas RP, Jao CY, Liu J, Salic A.** 2012. Dispatched and scube mediate the efficient secretion of the cholesterol-modified hedgehog ligand. Cell reports **2:**308-320.

118. **Creanga A, Glenn TD, Mann RK, Saunders AM, Talbot WS, Beachy PA.** 2012. Scube/You activity mediates release of dually lipid-modified Hedgehog signal in soluble form. Genes Dev **26:**1312-1325.

119. **Hui CC, Angers S.** 2011. Gli proteins in development and disease. Annu Rev Cell Dev Biol **27:**513-537.

120. **Kinzler K, Ruppert J, Bigner S, Vogelstein B.** 1988. The GLI gene is a member of the Kruppel family of zinc finger proteins. Nature **332:**371-374.

121. **Kinzler K, Vogelstein B.** 1990. The GLI Gene Encodes a Nuclear Protein Which Binds Specific Sequences in the Human Genome. Molecular and cellular biology **10**.

122. **Park HL, Bai C, Platt KA, Matise MP, Beeghly A, Hui CC, Nakashima M, Joyner AL.** 2000. Mouse Gli1 mutants are viable but have defects in SHH signaling in combination with a Gli2 mutation. Development **127:**1593-1605.

123. **Bai CB, Stephen D, Joyner AL.** 2004. All mouse ventral spinal cord patterning by hedgehog is Gli dependent and involves an activator function of Gli3. Developmental cell **6:**103-115.

124. **Bai CB, Auerbach W, Lee JS, Stephen D, Joyner AL.** 2002. Gli2, but not Gli1, is required for initial Shh signaling and ectopic activation of the Shh pathway. Development **129:**4753-4761.

125. **Sasaki H, Nishizaki Y, Hui C, Nakafuku M, Kondoh H.** 1999. Regulation of Gli2 and Gli3 activities by an amino-terminal repression domain: implication of Gli2 and Gli3 as primary mediators of Shh signaling. Development **126:**3915-3924.

126. **Dai P, Akimaru H, Tanaka Y, Maekawa T, Nakafuku M, Ishii S.** 1999. Sonic Hedgehog-induced activation of the Gli1 promoter is mediated by GLI3. The Journal of biological chemistry **274:**8143-8152.

127. **Pan Y, Wang B.** 2007. A novel protein-processing domain in Gli2 and Gli3 differentially blocks complete protein degradation by the proteasome. J Biol Chem **282:**10846-10852.

128. **Tian L, Holmgren RA, Matouschek A.** 2005. A conserved processing mechanism regulates the activity of transcription factors Cubitus interruptus and NF-kappaB. Nature structural & molecular biology **12:**1045-1053.

129. **Matise MP, Epstein DJ, Park HL, Platt KA, Joyner AL.** 1998. Gli2 is required for induction of floor plate and adjacent cells, but not most ventral neurons in the mouse central nervous system. Development **125:**2759-2770.

130. **Litingtung Y, Chiang C.** 2000. Specification of ventral neuron types is mediated by an antagonistic interaction between Shh and Gli3. Nature neuroscience **3:**979-985.

131. **Wen X, Lai CK, Evangelista M, Hongo JA, de Sauvage FJ, Scales SJ.** 2010. Kinetics of hedgehog-dependent full-length Gli3 accumulation in primary cilia and subsequent degradation. Mol Cell Biol **30:**1910-1922.

132. **Tukachinsky H, Lopez LV, Salic A.** 2010. A mechanism for vertebrate Hedgehog signaling: recruitment to cilia and dissociation of SuFu-Gli protein complexes. J Cell Biol **191:**415-428.

133. **Kim J, Kato M, Beachy PA.** 2009. Gli2 trafficking links Hedgehog-dependent activation of Smoothened in the primary cilium to transcriptional activation in the nucleus. Proc Natl Acad Sci U S A **106:**21666-21671.

134. **Humke EW, Dorn KV, Milenkovic L, Scott MP, Rohatgi R.** 2010. The output of Hedgehog signaling is controlled by the dynamic association between Suppressor of Fused and the Gli proteins. Genes Dev **24:**670-682.

135. **Jiang J, Hui CC.** 2008. Hedgehog signaling in development and cancer. Developmental cell **15:**801-812.

136. **Mukhopadhyay S, Wen X, Ratti N, Loktev A, Rangell L, Scales SJ, Jackson PK.** 2013. The Ciliary G-Protein-Coupled Receptor Gpr161 Negatively Regulates the Sonic Hedgehog Pathway via cAMP Signaling. Cell **152:**210-223.

137. **Wigley WC, Fabunmi RP, Lee MG, Marino CR, Muallem S, DeMartino GN, Thomas PJ.** 1999. Dynamic association of proteasomal machinery with the centrosome. J Cell Biol **145:**481-490.

138. **Marigo V, Davey RA, Zuo Y, Cunningham JM, Tabin CJ.** 1996. Biochemical evidence that patched is the Hedgehog receptor. Nature **384:**176-179.

139. **Stone DM, Hynes M, Armanini M, Swanson TA, Gu Q, Johnson RL, Scott MP, Pennica D, Goddard A, Phillips H, Noll M, Hooper JE, de Sauvage F, Rosenthal A.** 1996. The tumour-suppressor gene patched encodes a candidate receptor for Sonic hedgehog. Nature **384:**129-134.

140. **Denef N, Neubuser D, Perez L, Cohen SM.** 2000. Hedgehog induces opposite changes in turnover and subcellular localization of patched and smoothened. Cell **102:**521-531.

141. **Izzi L, Lévesque M, Morin S, Laniel D, Wilkes BC, Mille F, Krauss RS, McMahon AP, Allen BL, Charron F.** 2011. Boc and Gas1 each form distinct Shh receptor complexes with Ptch1 and are required for Shh-mediated cell proliferation. Developmental cell **20:**788-801.

142. **Murdoch JN, Copp AJ.** 2010. The relationship between sonic Hedgehog signaling, cilia, and neural tube defects. Birth Defects Res A Clin Mol Teratol **88:**633-652.

143. **Ruiz i Altaba A, Palma V, Dahmane N.** 2002. Hedgehog-Gli signalling and the growth of the brain. Nat Rev Neurosci **3:**24-33.

144. **Rohatgi R, Milenkovic L, Scott MP.** 2007. Patched1 regulates hedgehog signaling at the primary cilium. Science **317:**372-376.

145. **Milenkovic L, Scott MP, Rohatgi R.** 2009. Lateral transport of Smoothened from the plasma membrane to the membrane of the cilium. J Cell Biol **187:**365-374.

146. **Wang Y, Zhou Z, Walsh CT, McMahon AP.** 2009. Selective translocation of intracellular Smoothened to the primary cilium in response to Hedgehog pathway modulation. Proc Natl Acad Sci U S A **106:**2623-2628.

147. **Dorn KV, Hughes CE, Rohatgi R.** 2012. A Smoothened-Evc2 complex transduces the Hedgehog signal at primary cilia. Developmental cell **23:**823-835.

148. **Yang C, Chen W, Chen Y, Jiang J.** 2012. Smoothened transduces Hedgehog signal by forming a complex with Evc/Evc2. Cell research **22:**1593-1604.

149. **Chen MH, Wilson CW, Li YJ, Law KK, Lu CS, Gacayan R, Zhang X, Hui CC, Chuang PT.** 2009. Cilium-independent regulation of Gli protein function by Sufu in Hedgehog signaling is evolutionarily conserved. Genes Dev **23:**1910-1928.

150. **Tukachinsky H, Lopez LV, Salic A.** 2010. A mechanism for vertebrate Hedgehog signaling: recruitment to cilia and dissociation of SuFu-Gli protein complexes. J Cell Biol **191:**415-428.

151. **Marigo V, Johnson RL, Vortkamp A, Tabin CJ.** 1996. Sonic hedgehog differentially regulates expression of GLI and GLI3 during limb development. Dev Biol **180:**273-283.

152. **Marigo V, Scott MP, Johnson RL, Goodrich LV, Tabin CJ.** 1996. Conservation in hedgehog signaling: induction of a chicken patched homolog by Sonic hedgehog in the developing limb. Development **122:**1225-1233.

153. **Marigo V, Tabin CJ.** 1996. Regulation of patched by sonic hedgehog in the developing neural tube. Proc Natl Acad Sci U S A **93:**9346-9351.

154. **Agren M, Kogerman P, Kleman MI, Wessling M, Toftgard R.** 2004. Expression of the PTCH1 tumor suppressor gene is regulated by alternative promoters and a single functional Gli-binding site. Gene **330:**101-114.

155. **Ikram MS, Neill GW, Regl G, Eichberger T, Frischauf AM, Aberger F, Quinn A, Philpott M.** 2004. GLI2 is expressed in normal human epidermis and BCC and induces GLI1 expression by binding to its promoter. The Journal of investigative dermatology **122:**1503-1509.

156. **Eichberger T, Sander V, Schnidar H, Regl G, Kasper M, Schmid C, Plamberger S, Kaser A, Aberger F, Frischauf AM.** 2006. Overlapping and distinct transcriptional regulator properties of the GLI1 and GLI2 oncogenes. Genomics **87:**616-632.

157. **Bhatia N, Thiyagarajan S, Elcheva I, Saleem M, Dlugosz A, Mukhtar H, Spiegelman VS.** 2006. Gli2 is targeted for ubiquitination and degradation by beta-TrCP ubiquitin ligase. J Biol Chem **281:**19320-19326.

158. **Cooper MK.** 1998. Teratogen-Mediated Inhibition of Target Tissue Response to Shh Signaling. Science **280:**1603-1607.

159. **Binns W, James LF, Shupe JL, Thacker EJ.** 1962. Cyclopian-type malformation in lambs. Archives of environmental health **5:**106-108.

160. **Keeler RF, Binns W.** 1966. Teratogenic compounds of Veratrum californicum (Durand). II. Production of ovine fetal cyclopia by fractions and alkaloid preparations. Canadian journal of biochemistry **44:**829-838.

161. **Keeler RF, Binns W.** 1966. Teratogenic compounds of Veratrum californicum (Durand). I. Preparation and characterization of fractions and alkaloids for biologic testing. Canadian journal of biochemistry **44:**819-828.

162. **Keeler RF, Binns W.** 1968. Teratogenic compounds of Veratrum californicum (Durand). V. Comparison of cyclopian effects of steroidal alkaloids from the plant and structurally related compounds from other sources. Teratology **1:**5-10.

163. **Incardona JP, Gaffield W, Kapur RP, Roelink H.** 1998. The teratogenic Veratrum alkaloid cyclopamine inhibits sonic hedgehog signal transduction. Development **125:**3553-3562.

164. **Herper M.** 2005. The Curious Case of The One-Eyed Sheep. Forbes.

165. **Chen JK, Taipale J, Cooper MK, Beachy PA.** 2002. Inhibition of Hedgehog signaling by direct binding of cyclopamine to Smoothened. Genes Dev **16:**2743-2748.

166. **Rohatgi R, Milenkovic L, Corcoran RB, Scott MP.** 2009. Hedgehog signal transduction by Smoothened: pharmacologic evidence for a 2-step activation process. Proc Natl Acad Sci U S A **106:**3196-3201.

167. **Taipale J, Chen JK, Cooper MK, Wang BL, Mann RK, Milenkovic L, Scott MP, Beachy PA.** 2000. Effects of oncogenic mutations in Smoothened and Patched can be reversed by cyclopamine. Nature **406:**1005-1009.

168. **Watkins DN, Berman DM, Burkholder SG, Wang B, Beachy PA, Baylin SB.** 2003. Hedgehog signalling within airway epithelial progenitors and in small-cell lung cancer. Nature **422:**313-317.

169. **Chen JK, Taipale J, Young KE, Maiti T, Beachy PA.** 2002. Small molecule modulation of Smoothened activity. Proc Natl Acad Sci U S A **99:**14071-14076.

170. **Dyer LA, Makadia FA, Scott A, Pegram K, Hutson MR, Kirby ML.** 2010. BMP signaling modulates hedgehog-induced secondary heart field proliferation. Dev Biol **348:**167-176.

171. **Bragina O, Sergejeva S, Serg M, Zarkovsky T, Maloverjan A, Kogerman P, Zarkovsky A.** 2010. Smoothened agonist augments proliferation and survival of neural cells. Neuroscience letters **482:**81-85.

172. **Tsukui T, Capdevila J, Tamura K, Ruiz-Lozano P, Rodriguez-Esteban C, Yonei-Tamura S, Magallon J, Chandraratna RA, Chien K, Blumberg B, Evans RM, Belmonte JC.** 1999. Multiple left-right asymmetry defects in Shh(-/-) mutant mice unveil a convergence of the shh and retinoic acid pathways in the control of Lefty-1. Proc Natl Acad Sci U S A **96:**11376-11381.

173. **Washington Smoak I, Byrd NA, Abu-Issa R, Goddeeris MM, Anderson R, Morris J, Yamamura K, Klingensmith J, Meyers EN.** 2005. Sonic hedgehog is required for cardiac outflow tract and neural crest cell development. Dev Biol **283:**357-372.

174. **Goddeeris MM, Schwartz R, Klingensmith J, Meyers EN.** 2007. Independent requirements for Hedgehog signaling by both the anterior heart field and neural crest cells for outflow tract development. Development **134:**1593-1604.

175. **Xie L, Hoffmann AD, Burnicka-Turek O, Friedland-Little JM, Zhang K, Moskowitz IP.** 2012. Tbx5-hedgehog molecular networks are essential in the second heart field for atrial septation. Developmental cell **23:**280-291.

176. **Thomas NA, Koudijs M, van Eeden FJ, Joyner AL, Yelon D.** 2008. Hedgehog signaling plays a cell-autonomous role in maximizing cardiac developmental potential. Development **135:**3789-3799.

177. **Choi W-Y, Gemberling M, Wang J, Holdway JE, Shen M-C, Karlstrom RO, Poss KD.** 2013. In vivo monitoring of cardiomyocyte proliferation to identify chemical modifiers of heart regeneration. Development (Cambridge, England) **140:**660-666.

178. **Potthoff MJ, Olson EN.** 2007. MEF2: a central regulator of diverse developmental programs. Development (Cambridge, England) **134:**4131-4140.

179. **Lilly B, Zhao B, Ranganayakulu G, Paterson BM, Schulz RA, Olson EN.** 1995. Requirement of MADS domain transcription factor D-MEF2 for muscle formation in Drosophila. Science **267:**688-693.

180. **Black BL, Cripps RM.** 2010. Myocyte Enhancer Factor 2 Transcription Factors in Heart Development and Disease. In: Nadia Rosenthal and Richard P. Harvey, editors, Heart Development and Regeneration. Oxford: Academic Press **2:**673-699.

181. **Dodou E, Xu S-M, Black BL.** 2003. mef2c is activated directly by myogenic basic helix-loop-helix proteins during skeletal muscle development in vivo. Mechanisms of Development **120:**1021-1032.

182. **Wang DZ, Valdez MR, McAnally J, Richardson J, Olson EN.** 2001. The Mef2c gene is a direct transcriptional target of myogenic bHLH and MEF2 proteins during skeletal muscle development. Development (Cambridge, England) **128:**4623-4633.

183. **De Val S, Anderson JP, Heidt AB, Khiem D, Xu S-M, Black BL.** 2004. Mef2c is activated directly by Ets transcription factors through an evolutionarily conserved endothelial cell-specific enhancer. Developmental biology **275:**424-434.

184. **Agarwal P, Verzi MP, Nguyen T, Hu J, Ehlers ML, McCulley DJ, Xu S-M, Dodou E, Anderson JP, Wei ML, Black BL.** 2011. The MADS box transcription factor MEF2C regulates melanocyte development and is a direct transcriptional target and partner of SOX10. Development (Cambridge, England) **138:**2555-2565.

185. **De Val S, Chi NC, Meadows SM, Minovitsky S, Anderson JP, Harris IS, Ehlers ML, Agarwal P, Visel A, Xu S-M, Pennacchio La, Dubchak I, Krieg Pa, Stainier DYR, Black BL.** 2008. Combinatorial regulation of endothelial gene expression by ets and forkhead transcription factors. Cell **135:**1053-1064.

186. **Hao H, Tummala P, Guzman E, Mali RS, Gregorski J, Swaroop A, Mitton KP.** 2011. The transcription factor neural retina leucine zipper (NRL) controls photoreceptor-specific expression of myocyte enhancer factor Mef2c from an alternative promoter. The Journal of biological chemistry **286:**34893-34902.

187. **Zinzen RP, Girardot C, Gagneur J, Braun M, Furlong EEM.** 2009. Combinatorial binding predicts spatio-temporal cis-regulatory activity. Nature **462:**65-70.

188. **Luo RX, Dean DC.** 1999. Chromatin remodeling and transcriptional regulation. J Natl Cancer Inst **91:**1288-1294.

189. **de la Serna IL, Ohkawa Y, Imbalzano AN.** 2006. Chromatin remodelling in mammalian differentiation: lessons from ATP-dependent remodellers. Nature reviews. Genetics **7:**461-473.

190. **Suzuki MM, Bird A.** 2008. DNA methylation landscapes: provocative insights from epigenomics. Nat Rev Genet **9:**465-476.

191. **Wang Y, Wysocka J, Perlin JR, Leonelli L, Allis CD, Coonrod SA.** 2004. Linking covalent histone modifications to epigenetics: the rigidity and plasticity of the marks. Cold Spring Harb Symp Quant Biol **69:**161-169.

192. **Paranjape SM, Kamakaka RT, Kadonaga JT.** 1994. Role of chromatin structure in the regulation of transcription by RNA polymerase II. Annual review of biochemistry **63:**265-297.

193. **Ho L, Crabtree GR.** 2010. Chromatin remodelling during development. Nature **463:**474-484.

194. **Bowman GD.** 2010. Mechanisms of ATP-dependent nucleosome sliding. Current opinion in structural biology **20:**73-81.

195. **Saha A, Wittmeyer J, Cairns BR.** 2006. Chromatin remodelling: the industrial revolution of DNA around histones. Nat Rev Mol Cell Biol **7:**437-447.

196. **Bultman S, Gebuhr T, Yee D, La Mantia C, Nicholson J, Gilliam a, Randazzo F, Metzger D, Chambon P, Crabtree G, Magnuson T.** 2000. A Brg1 null mutation in the mouse reveals functional differences among mammalian SWI/SNF complexes. Molecular cell **6:**1287-1295.

197. **Reyes J, Barra J, Muchardt C, Camus A.** 1998. Altered control of cellular proliferation in the absence of mammalian brahma (SNF2 α). The EMBO **17:**6979-6991.

198. **Ohkawa Y, Marfella CG, Imbalzano AN.** 2006. Skeletal muscle specification by myogenin and Mef2D via the SWI/SNF ATPase Brg1. EMBO J **25:**490-501.

199. **Lei I, Gao X, Sham MH, Wang Z.** 2012. SWI/SNF protein component BAF250a regulates cardiac progenitor cell differentiation by modulating chromatin accessibility during second heart field development. J Biol Chem **287:**24255-24262.

200. **Takeuchi JK, Lou X, Alexander JM, Sugizaki H, Delgado-Olguín P, Holloway AK, Mori AD, Wylie JN, Munson C, Zhu Y, Zhou Y-Q, Yeh R-F, Henkelman RM, Harvey RP, Metzger D, Chambon P, Stainier DYR, Pollard KS, Scott IC, Bruneau BG.** 2011. Chromatin remodelling complex dosage modulates transcription factor function in heart development. Nature communications **2:**187.

201. **Hang CT, Yang J, Han P, Cheng H-L, Shang C, Ashley E, Zhou B, Chang C-P.** 2010. Chromatin regulation by Brg1 underlies heart muscle development and disease. Nature **466:**62-67.

202. **Stankunas K, Hang CT, Tsun ZY, Chen H, Lee NV, Wu JI, Shang C, Bayle JH, Shou W, Iruela-Arispe ML, Chang CP.** 2008. Endocardial Brg1 represses ADAMTS1 to maintain the microenvironment for myocardial morphogenesis. Developmental cell **14:**298-311.

203. **Wang Z, Zhai W, Richardson JA, Olson EN, Meneses JJ, Firpo MT, Kang C, Skarnes WC, Tjian R.** 2004. Polybromo protein BAF180 functions in mammalian cardiac chamber maturation. Genes Dev **18:**3106-3116.

204. **Huang X, Gao X, Diaz-Trelles R, Ruiz-Lozano P, Wang Z.** 2008. Coronary development is regulated by ATP-dependent SWI/SNF chromatin remodeling component BAF180. Dev Biol **319:**258-266.

205. **Gao X, Tate P, Hu P, Tjian R, Skarnes WC, Wang Z.** 2008. ES cell pluripotency and germ-layer formation require the SWI/SNF chromatin remodeling component BAF250a. Proceedings of the National Academy of Sciences of the United States of America **105:**6656-6661.

206. **Zhan X, Shi X, Zhang Z, Chen Y, Wu JI.** 2011. Dual role of Brg chromatin remodeling factor in Sonic hedgehog signaling during neural development. Proceedings of the National Academy of Sciences of the United States of America **108:**12758-12763.

207. **Ryan T, Shelton M, Lambert JP, Malecova B, Boisvenue S, Ruel M, Figeys D, Puri PL, Skerjanc IS.** 2013. Myosin phosphatase modulates the cardiac cell fate by regulating the subcellular localization of Nkx2.5 in a Wnt/Rho-associated protein kinase-dependent pathway. Circ Res **112:**257-266.

208. **Petropoulos H, Gianakopoulos PJ, Ridgeway AG, Skerjanc IS.** 2004. Disruption of Meox or Gli activity ablates skeletal myogenesis in P19 cells. The Journal of biological chemistry **279:**23874-23881.

209. **Rudnicki MA, and McBurney, M. W. .** 1987. Cell culture methods and induction of differentiation of embryonal carcinoma cell lines. In Robertson, E. J., ed. Teratocarcinomas and embryonic stem cells: a practical approach. IRL Press, Oxford.

210. **Hu MC, Mo R, Bhella S, Wilson CW, Chuang PT, Hui CC, Rosenblum ND.** 2006. GLI3-dependent transcriptional repression of Gli1, Gli2 and kidney patterning genes disrupts renal morphogenesis. Development **133:**569-578.

211. **Abràmoff MD, Magalhães PJ, Ram SJ.** 2004. Image Processing with ImageJ. Biophotonics International **11:**36-42.

212. **Livak KJ, Schmittgen TD.** 2001. Analysis of relative gene expression data using real-time quantitative PCR and the 2(-Delta Delta C(T)) Method. Methods **25:**402-408.

213. **Gianakopoulos PJ, Mehta V, Voronova A, Cao Y, Yao Z, Coutu J, Wang X, Waddington MS, Tapscott SJ, Skerjanc IS.** 2011. MyoD directly up-regulates premyogenic mesoderm factors during induction of skeletal myogenesis in stem cells. The Journal of biological chemistry **286:**2517-2525.

214. **Bader D, Masaki T, Fischman DA.** 1982. Immunochemical analysis of myosin heavy chain during avian myogenesis in vivo and in vitro. J Cell Biol **95:**763-770.

215. **Shevchenko A, Tomas H, Havlis J, Olsen JV, Mann M.** 2006. In-gel digestion for mass spectrometric characterization of proteins and proteomes. Nature protocols **1:**2856-2860.

216. **Eng JK, Searle BC, Clauser KR, Tabb DL.** 2011. A face in the crowd: recognizing peptides through database search. Molecular & cellular proteomics : MCP **10:**R111.009522.

217. **Ho L, Jothi R, Ronan JL, Cui K, Zhao K, Crabtree GR.** 2009. An embryonic stem cell chromatin remodeling complex, esBAF, is an essential component of the core pluripotency transcriptional network. Proceedings of the National Academy of Sciences of the United States of America **106:**5187-5191.

218. **Ovcharenko I, Loots GG, Giardine BM, Hou M, Ma J, Hardison RC, Stubbs L, Miller W.** 2005. Mulan: multiple-sequence local alignment and visualization for studying function and evolution. Genome research **15:**184-194.

219. **Huang da W, Sherman BT, Lempicki RA.** 2009. Bioinformatics enrichment tools: paths toward the comprehensive functional analysis of large gene lists. Nucleic Acids Res **37:**1-13.

220. **Huang da W, Sherman BT, Lempicki RA.** 2009. Systematic and integrative analysis of large gene lists using DAVID bioinformatics resources. Nature protocols **4:**44-57.

221. **Savage J, Conley AJ, Blais A, Skerjanc IS.** 2009. SOX15 and SOX7 differentially regulate the myogenic program in P19 cells. Stem cells (Dayton, Ohio) **27:**1231-1243.

222. **Voronova A, Fischer A, Ryan T, Al Madhoun A, Skerjanc IS.** 2011. Ascl1/Mash1 is a novel target of Gli2 during Gli2-induced neurogenesis in P19 EC cells. PLoS One **6:**e19174.

223. **Hidaka K, Lee JK, Kim HS, Ihm CH, Iio A, Ogawa M, Nishikawa S, Kodama I, Morisaki T.** 2003. Chamber-specific differentiation of Nkx2.5-positive cardiac precursor cells from murine embryonic stem cells. FASEB journal : official publication of the Federation of American Societies for Experimental Biology **17:**740-742.

224. **Williams RL, Hilton DJ, Pease S, Willson TA, Stewart CL, Gearing DP, Wagner EF, Metcalf D, Nicola NA, Gough NM.** 1988. Myeloid leukaemia inhibitory factor maintains the developmental potential of embryonic stem cells. Nature **336:**684-687.

225. **Goulding MD, Chalepakis G, Deutsch U, Erselius JR, Gruss P.** 1991. Pax-3, a novel murine DNA binding protein expressed during early neurogenesis. Embo j **10:**1135-1147.

226. **Ridgeway aG, Skerjanc IS.** 2001. Pax3 is essential for skeletal myogenesis and the expression of Six1 and Eya2. The Journal of biological chemistry **276:**19033-19039.

227. **Goulding M, Lumsden A, Paquette AJ.** 1994. Regulation of Pax-3 expression in the dermomyotome and its role in muscle development. Development **120:**957-971.

228. **Koblar SA, Murphy M, Barrett GL, Underhill A, Gros P, Bartlett PF.** 1999. Pax-3 regulates neurogenesis in neural crest-derived precursor cells. J Neurosci Res **56:**518-530.

229. **Chang H, Yoshimoto M, Umeda K, Iwasa T, Mizuno Y, Fukada S, Yamamoto H, Motohashi N, Miyagoe-Suzuki Y, Takeda S, Heike T, Nakahata T.** 2009. Generation of transplantable, functional satellite-like cells from mouse embryonic stem cells. FASEB journal : official publication of the Federation of American Societies for Experimental Biology **23:**1907-1919.

230. **Guillemot F, Lo LC, Johnson JE, Auerbach A, Anderson DJ, Joyner AL.** 1993. Mammalian achaete-scute homolog 1 is required for the early development of olfactory and autonomic neurons. Cell **75:**463-476.

231. **Nakada Y, Hunsaker TL, Henke RM, Johnson JE.** 2004. Distinct domains within Mash1 and Math1 are required for function in neuronal differentiation versus neuronal cell-type specification. Development **131:**1319-1330.

232. **Pattyn A, Guillemot F, Brunet JF.** 2006. Delays in neuronal differentiation in Mash1/Ascl1 mutants. Dev Biol **295:**67-75.

233. **Vierbuchen T, Ostermeier A, Pang ZP, Kokubu Y, Sudhof TC, Wernig M.** 2010. Direct conversion of fibroblasts to functional neurons by defined factors. Nature **463:**1035-1041.

234. **Wang L, Zhang ZG, Gregg SR, Zhang RL, Jiao Z, LeTourneau Y, Liu X, Feng Y, Gerwien J, Torup L, Leist M, Noguchi CT, Chen ZY, Chopp M.** 2007. The Sonic hedgehog pathway mediates carbamylated erythropoietin-enhanced proliferation and differentiation of adult neural progenitor cells. J Biol Chem **282:**32462-32470.

235. **Rudnicki MA, Jackowski G, Saggin L, McBurney MW.** 1990. Actin and myosin expression during development of cardiac muscle from cultured embryonal carcinoma cells. Dev Biol **138:**348-358.

236. **Machida Y, Murai K, Miyake K, Iijima S.** 2001. Expression of chromatin remodeling factors during neural differentiation. Journal of biochemistry **129:**43-49.

237. **Zheng G, Tao Y, Yu W, Schwartz RJ.** 2013. Brief report: SRF-dependent MiR-210 silences the sonic hedgehog signaling during cardiopoesis. Stem Cells **31:**2279-2285.

238. **Karlstrom RO.** 2003. Genetic analysis of zebrafish gli1 and gli2 reveals divergent requirements for gli genes in vertebrate development. Development **130:**1549-1564.

239. **Li QY, Newbury-Ecob RA, Terrett JA, Wilson DI, Curtis AR, Yi CH, Gebuhr T, Bullen PJ, Robson SC, Strachan T, Bonnet D, Lyonnet S, Young ID, Raeburn JA, Buckler AJ, Law DJ, Brook JD.** 1997. Holt-Oram syndrome is caused by mutations in TBX5, a member of the Brachyury (T) gene family. Nat Genet **15:**21-29.

240. **Bruneau BG, Logan M, Davis N, Levi T, Tabin CJ, Seidman JG, Seidman CE.** 1999. Chamber-specific cardiac expression of Tbx5 and heart defects in Holt-Oram syndrome. Dev Biol **211:**100-108.

241. **Evans MJ, Kaufman MH.** 1981. Establishment in culture of pluripotential cells from mouse embryos. Nature **292:**154-156.

242. **Martin GR.** 1981. Isolation of a pluripotent cell line from early mouse embryos cultured in medium conditioned by teratocarcinoma stem cells. Proc Natl Acad Sci U S A **78:**7634-7638.

243. **Wu SM, Chien KR, Mummery C.** 2008. Origins and fates of cardiovascular progenitor cells. Cell **132:**537-543.

244. **Alsan BH, Schultheiss TM.** 2002. Regulation of avian cardiogenesis by Fgf8 signaling. Development **129:**1935-1943.

245. **Gregoire S, Karra R, Passer D, Deutsch M-A, Krane M, Feistritzer R, Sturzu A, Domian I, Saga Y, Wu SM.** 2013. Essential and unexpected role of Yin Yang 1 to promote mesodermal cardiac differentiation. Circulation research **112:**900-910.

246. **Ueno S, Weidinger G, Osugi T, Kohn AD, Golob JL, Pabon L, Reinecke H, Moon RT, Murry CE.** 2007. Biphasic role for Wnt/beta-catenin signaling in cardiac specification in zebrafish and embryonic stem cells. Proceedings of the National Academy of Sciences of the United States of America **104:**9685-9690.

247. **Lindsley RC, Gill JG, Kyba M, Murphy TL, Murphy KM.** 2006. Canonical Wnt signaling is required for development of embryonic stem cell-derived mesoderm. Development **133:**3787-3796.

248. **Alvarez-Medina R, Le Dreau G, Ros M, Marti E.** 2009. Hedgehog activation is required upstream of Wnt signalling to control neural progenitor proliferation. Development **136:**3301-3309.

249. **Afouda BA, Martin J, Liu F, Ciau-Uitz A, Patient R, Hoppler S.** 2008. GATA transcription factors integrate Wnt signalling during heart development. Development **135:**3185-3190.

Contributions of Collaborators

In addition to her mentorship and training, Dr. Anastassia Voronova performed the exogenous and endogenous GLI2 protein time-course in Figure 4, the FLAG-IP in Figure 9, and prepared the samples that were used for the mass spectrometric analysis in Figure 9. Neven Bosiljcic assisted me with the differentiation of additional mES[GLI2] samples used to make Figure 6.

Appendices

Appendix A - Detailed *Mef2c* Binding Site Information

Protein	*Mef2c* domain	Target Sequence[1]	Location (mm10: Chromosome 13)	Source of Protein	Reference[2]
MEF2C	MADS-box	acctttacagCTAAATTTACtccagagtg	83,504,087 - 83,504,115	Mouse	(182)
MyoD	E-box	gagtgacatgaaCAGGTGcaccctggcct	83,504,111 - 83,504,139	Mouse	(182)
E12	E-box	gagtgacatgaaCAGGTGcaccctggcct	83,504,111 - 83,504,139	Mouse	(182)
GATA-4	GATA-d GATA-p	taagagttcTTATCAgtgtc gtcacccgctatCTATCGgtcagg	83,523,287 - 83,523,306 83,523,351 - 83,523,374	Rat	(44)
ISL-1	ISL-d ISL-p	gtcaggggagcCTAATGcatttgggaa ggtttacttgCTAATGacctggataa	83,523,369 - 83,523,395 83,523,405 - 83,523,430	Hamster	(44)
SOX10	SOX Binding Site	gaatgcactgacTACAAAGtgcatcctgaag ggccatttagctCACAATGaaggtctgtgtt aaatagctctatAACAAAGtaactacagagt	83,565,883 - 83,565,913 83,565,913 – 83,565,943 83,565,947 – 83,565,977	Mouse	(184)
ETS1/C-ETS-1	ETS-A	agttactcTCTTCCTGttatgaca	83,582,754 - 83,582,777	Mammalian	(183), (185)
ETV2/ER71	ETS-A	agttactcTCTTCCTGttatgaca	83,582,754 - 83,582,777	Mammalian	(185)
FOXC1	FOX-NC	ggaagttactctcttccTGTTATGacaggaaagcgtagaca	83,582,752 - 83,582,791	Mouse	(185)
FOXC2/FKHL14	FOX-NC	ggaagttactctcttccTGTTATGacaggaaagcgtagaca	83,582,752 - 83,582,791	Mouse	(185)
FOXO1	FOX-NC	ggaagttactctcttccTGTTATGacaggaaagcgtagaca	83,582,752 - 83,582,791	Mouse	(185)

[1] Uppercase nucleotides in the target sequence represent non-consensus binding domains.
[2] All binding site information for proteins, except SOX10, were compiled with information gathered through TRANSFAC.

Appendix B - Unique Reagent Recipes

B.1 Radioimmunoprecipitation Assay (RIPA) Buffer

50 mM Tris pH 7.5

150 mM NaCl

1% NP-40

0.5% sodium deoxycholate

1x protease inhibitor cocktail (Roche, Canada)

0.5 mM phenylmethanesulfonyl fluoride (PMSF)

B.2 Stockholm's Phosphate Buffered Saline (sPBS)

4.6 g Na_2HPO_4 (anhydrous)

1.04 g NaH_2PO_4-H_2O

32.0 g NaCl

0.8 g KCl

Adjust to pH 7.2, if needed

Dissolve in 4L of ddH_2O

Curriculum Vitae

Awards and Achievements

- Graduate Studies Leadership Award, 2013
- Canadian Institutes of Health Research Master's Award, 2012
- Ontario Graduate Scholarship, 2011
- University of Ottawa Excellence Scholarship, 2011, 2012
- Science Students Association Award for Research Excellence, 2011
- Canadian Institutes of Health Research Undergraduate Grant, Summer 2010 & 2011
- Bruker BioSpin Award, 2010
- University of Ottawa Faculty of Science Co-op Student of the Year, 2009
- Canada Millennium Excellence Laureate - National Award, 2006-2010
- Canadian Merit Scholarship Foundation, Friesens-Lifetouch Provincial Award, 2006
- Ottawa-Carleton District School Board Outstanding Leadership Award, 2006
- Senior Male Athlete of the Year, 2006
- Cairine Wilson Secondary School Valedictorian, Class of 2006

Education

Master of Science September 2011 - July 2014
Biochemistry
University of Ottawa

Bachelor of Science September 2006 - April 2011
Honours with a Specialization in Biochemistry (Co-op);
Minor in Economics
Magna Cum Laude
University of Ottawa

Ontario Secondary School Diploma September 2002 - June 2006
Cairine Wilson Secondary School

Work Experience

Research Assistant May - August 2010 & 2011
Dr. Ilona Skerjanc's Lab
University of Ottawa - Ottawa, Ontario

Investigated heart and skeletal muscle development using mouse embryonic stem cells as a model. This work continued into my honours project and master's degree.

Junior Research Technician January 2009 - December 2009
Dr. Michael Rosu-Myles' Lab
Health Canada - Ottawa, Ontario

Studied the proliferation of human and murine mesenchymal stem cells.

Technical Lab Assistant July 2008 - August 2008
Bwafwano Community Centre and
Acute Care Clinic - Lusaka, Zambia

Organized meetings with pediatric officers from Zambia's Ministry of Health.
Assisted a technician with screening patients for malaria, tuberculosis, and syphilis.

Languages

Bilingual in both written and spoken English and French

Extracurricular Activities

High School Volleyball, Coach — November 2010 - March 2014

- Head coach of the Lisgar Collegiate Institute senior girls volleyball team for four seasons.
- Coached players through weekly practices, games and bi-annual tournaments from November to February, 6-8 hours a week.

Biochemistry, Microbiology and Immunology
Graduate Student Association, Executive Member — May 2012 – May 2013

- Led the planning and organization of 24 events for graduate students in our department as the Vice-President of Social Activities, including a Faculty of Medicine Dodgeball tournament and the council's executive elections.
- Convened with council members at monthly meetings to assist with other faculty initiatives and to address fellow students' concerns.

Ottawa Impact Volleyball, Manager — May 2010 – September 2012

- Founded Impact Volleyball Tournaments for university and community players.
- Spearheaded two ten-team tournaments, raising $950 for Cystic Fibrosis Research.
- Organized drop-in beach volleyball for 10-20 students on a weekly basis between May and August 2010 at Mooney's Bay beach.

Science Students Association, Executive Member — September 2006 - April 2011

- Efficiently directed a thirty-member council that provided academic, mentoring, and extra-curricular services to 3,000+ students as President and Vice-President.
- Pioneered University of Ottawa's annual inter-university Ottawa Science Olympiad.
- Executed a 7-day University of Ottawa Science Orientation Week for 600+ students as Vice-President of Social Activities.

SFUO Board of Administration, Board Member — May 2008 - May 2009

- Elected by peers in the Faculty of Science to represent students at the Student Federation of the University of Ottawa's Board of Administration.

Shared World Initiative, Student — January 2008 - November 2008

- Instilled global citizenship principles in collaboration with scientific and health related practices on a two-month international development placement in Zambia.
- Participated in training before placement and led student workshops after placement.

Publications

Rosu-Myles M., McCully J., Fair J., Mehic J., Menendez P., Roderiguez R., and Westwood C (2013) "The globo-series glycosphingolipid SSEA-4 is a marker of clonal multipotent stromal cells in vitro and in vivo." Stem Cells Dev. 22(9): 1387-97

Voronova A., Coyne E., Al Madhoun A., Fair J., St-Louis C., Li G., Thurig S., Wallace VA., Wiper-Bergeron N., and Skerjanc IS. (2013) "Hedgehog signaling regulates MyoD expression and activity." J Biol Chem. 288(6): 4389-404

Rosu-Myles M., She Y-M., Fair J., Muradia G., Mehic J. (2012) "Identification of a Candidate Proteomic Signature to Discriminate Multipotent and Non-Multipotent Stromal Cells." PLoS ONE 7(6): e38954.

Rosu-Myles M., Fair J., Pearce N. and Mehic J. (2010)."Non-Multipotent Stroma Inhibit The Proliferation and Differentiation of Mesenchymal Stem Cells *In vitro*." *Cytotherapy*. 2(6):818-830